INFORMATION TO USERS

This manuscript has been reproduced from the microfilm master. UMI films the text directly from the original or copy submitted. Thus, some thesis and dissertation copies are in typewriter face, while others may be from any type of computer printer.

The quality of this reproduction is dependent upon the quality of the copy submitted. Broken or indistinct print, colored or poor quality illustrations and photographs, print bleedthrough, substandard margins, and improper alignment can adversely affect reproduction.

In the unlikely event that the author did not send UMI a complete manuscript and there are missing pages, these will be noted. Also, if unauthorized copyright material had to be removed, a note will indicate the deletion.

Oversize materials (e.g., maps, drawings, charts) are reproduced by sectioning the original, beginning at the upper left-hand corner and continuing from left to right in equal sections with small overlaps. Each original is also photographed in one exposure and is included in reduced form at the back of the book.

Photographs included in the original manuscript have been reproduced xerographically in this copy. Higher quality 6" x 9" black and white photographic prints are available for any photographs or illustrations appearing in this copy for an additional charge. Contact UMI directly to order.

UMI®

Bell & Howell Information and Learning
300 North Zeeb Road, Ann Arbor, MI 48106-1346 USA
800-521-0600

A NUMERICAL SIMULATION MODEL FOR A BUILDING WITH TRANSPARENT INSULATION

HAMZEH HUSSEIN RAMADAN

A thesis

in

The School for Building

presented in the fulfillment of the

thesis requirement for the degree of

MASTER OF APPLIED SCIENCES

in

BUILDING ENGINEERING

Concordia University

Montreal, Quebec, Canada, 1998

ABSTRACT

Numerical Simulation Model for a Building with Transparent Insulation Materials

Hamzeh Hussein Ramadan

Utilization of a transparent insulation material (TIM) in a solar collector wall has been proven to have a significant potential to reduce heating load in passive solar buildings. Transparent insulation transmits a high proportion of incident solar radiation onto a layer of thermal mass which subsequently slowly releases heat, thus reduces the requirement for heating throughout the day. Due to the high transmittance and convective suppression properties of the transparent material, the thermal resistance of the wall will be improved extensively with minimum losses of transmitted radiation.

This thesis presents a numerical simulation model for a building with one transparently insulated wall. The explicit finite difference method is employed to study the thermal performance of an outdoor test room as a function of energy consumption and thermal comfort. It involves first a simulation for a one dimensional wall model with honeycomb-structured transparent insulation material (TIM). Then, a methodology is developed to simulate a complete room that has one transparently insulated wall. Different control strategies are employed for the shading device and one new strategy is developed to estimate the thermal performance of the transparently insulated room taking into account the incidence angle-dependent transmittance of TIM, and the non-linear convective-radiative behavior of both, exterior insulation system and the room interior surfaces. Simulation results indicate significant savings in energy consumption as a result of TIM utilization.

TO MY FATHER AND MY MOTHER...

ACKNOWLEDGMENTS

First, I am very grateful to my thesis supervisor, Dr. Andreas Athienitis, for his endless advice, financial support, quick reactions to drafts and a careful reading at the end.

Thanks to Dr. K.G.T. Hollands (University of Waterloo) who sent me many of his valuable published work.

For her encouragement, interest and unbounded support, I owe thanks to my friend Dr. Nada Alaaeddine.

My debt to my brothers Zafer (in Beirut) and Abbas (in Montreal) is difficult to express and will perhaps be understood only by them. Same for my sisters, Souhaila, Jinane, Thouraya, Jouhaina, Amena and Wijdan, I thank them for their emotional support and patience.

Thanks to many graduate students for their useful comments, especially Tingyao Chen and Yang Chen.

Finally, I would like to thank all professors and students at the Centre for Building Studies in Concordia University to whom I am indebted for providing an intellectual and social environment within which it was a pleasure to work and study.

NOMENCLATURE

Nodes numbers signification (Fig 5.1-b)

1 = Glass Protector

2 = Outside surface of honeycomb

3 = Inside surface of honeycomb

4 = Absorber

5,6,7,8,9 = Interior nodes of the concrete layer

10 = Inside surface of the concrete layer

11 = Outside surface of the gypsum board layer

12 = Interior node of the gypsum board layer

13 = Inside node of the gypsum board layer (TI wall inside surface)

14 = Room air

15 = Inside surface of east wall

16 = Interior node of east wall

17 = Inside surface of west wall

18 = Interior node of west wall

19 = Inside surface of north wall

20 = Interior node of north wall

21 = Inside surface of the floor

22 = Interior node of the floor

23 = Inside surface of the ceiling

24 = Interior node of the ceiling

25 = Window

Letters

A = Area (m^2)

a_0 , a_1 , k = Constant depends on climate and altitude (-)

A_{gap} = Aspect ratio of air gap (-)

A_{hc} = Aspect ratio of honeycomb cells (-)

Al = Altitude

ASC = Air change per second

C = Thermal capacitance (joule/°C)

C_{air} = Thermal capacitance of air (joule/°C)

c_p = Specific heat (Joule/kg K)

D_{hc} = Hydraulic diameter of honeycomb cell (m)

Fe = Fraction of effective cross sectional area of honeycomb not occupied by wall material (-)

g = Local acceleration due to gravity (m/s^2)

h_c = Convective heat transfer coefficient ($W/m^2°C$)

h_r = Radiative heat transfer coefficient ($W/ m^2°C$)

i = Node number or time interval (-)

I_{dg} = Intensity of ground diffuse solar radiation (W/m^2)

I_{ds} = Intensity of sky diffuse solar radiation (W/m^2)

j = Nodes connected to node I

K = Thermal conductivity (W/mK)

K_{air} = Thermal conductivity of air (W/mK)

K_{ec} = Extinction coefficient for glass (1/m)

K_p = Proportionality constant (W/°C)

L = Latitude (degree)

L_g = Glass thickness (m)

L_{gap} = Air gap thickness (m)

n_g = Refraction index of glass (-)

Nu = Nusselt number (-)

nw = Number of honeycomb walls intercepted by incident radiation (-)

p = Atmospheric pressure (N/m^2)

q_{aux} = Auxiliary heat (W/m^2)

r_0 ,r_1 r_k = Correction factors due to climate types (-)

Rij = Thermal resistance between node i and j (m^2 °C /W)

example: R1314= Thermal resistance between TI wall inside surface (node 13) and room air temperature (node 14)

Ra = Rayleigh number (-)

t = Time (second)

Ti = Node temperature (°C)

example T17 is the temperature of the inside west wall surface (node 17)

Tair = Air temperature (°C)

τ_b = Beam solar transmittance of honeycomb (-)

T_{cold} = Cold surface temperature (°C)

τ_d = Diffuse solar transmittance of honeycomb (-)

T_{hot} = Hot surface temperature (°C)

Tmean = Mean temperature (°C)

Tmr = Mean radiant temperature (°C)

To = Outside temperature (°C)

T_{op} = Operative temperature (°C)

Tsp = Set point temperature (°C)

U_{inf} = Infiltration heat transfer coefficient (Watt/m^2°C)

V_r = Room volume (m^3)

w = Frequency (rad/sec)

x,y,z = Directions of heat flow

Greek symbols

α = Solar altitude (degree) or diffusivity (m^2/s)

β = Tilt angle (degree)

δ = Declination angle (degree)

δ_{hc} = Honeycomb wall thickness (m)

Δt = Time step (second)

ΔT = Difference between hot surface temperature and cold surface temperature (K)

γ = Surface solar azimuth (degree)

Γ =Volumetric thermal expansion coefficient of the air (K^{-1})

ϕ = Solar azimuth (degree)

θ = Angle of incidence (degree)

ρ = Density (kg/m^3)

ρ_s = Specular solar reflectivity of honeycomb wall (-)

τ = Glazing transmittance (-)

Γ =Volumetric thermal expansion coefficient of the air (K^{-1})

τ_s = Specular solar transmissivity of honeycomb wall (-)

τ_b = Atmosphere beam transmittance (-)

τ_d = Clear sky atmospheric diffuse transmittance (-)

ν = Viscosity of air (Pa s)

ψ = Surface azimuth (degree)

TABLE OF CONTENTS

LIST OF FIGURES

LIST OF TABLES

CHAPTER I

INTRODUCTION

The sun radiates an ample supply of high quality energy throughout the year. The majority of the population on our planet receives more than 200 Watt/m^2, as an average, of solar radiation (Olgyay, 1962). This clean source, if efficiently collected and used, could provide a major part of the world energy needs. Thus, a great deal of research work has been guided to develop an effective collection mechanism of solar radiation.

Increasing attention is being given to the development of new and improved materials particularly suited for enhancing the performance of solar systems. The technology in this field is advancing rapidly. It holds, to some extent, the key to the reduction of existing technical and economic limitations and to the opening of new possibilities for practical solar energy. In the field of thermal energy, transparent insulation (TI) technology has grown notably in recent years. This new technology increases significantly the efficiency of solar thermal conversion systems.

Transparent insulation materials (TIM) combine the properties of good optical transmission (described by the total solar transmittance) and good thermal insulation (described by the heat loss coefficient or U-value). One of the widely known applications of transparent insulation materials is in the cladding of building walls, replacing conventional opaque insulation.

The advantages of the TIM over opaque insulation materials are shown in fig.(1.1). As it is shown, with the solar radiation incident on an opaque insulated wall, the outward transmission heat flow is only insignificantly reduced. However, when the transparent insulation materials is used, the solar radiation contributes significantly to the reduction of heating load.

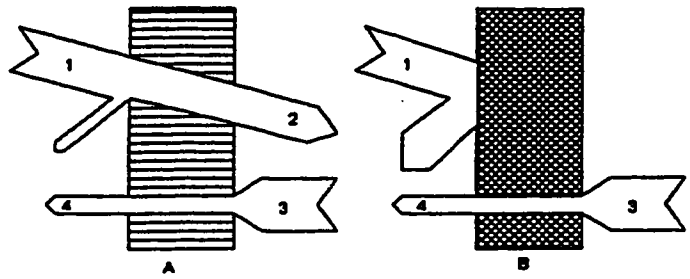

A: Transparent Insulation; B: Opaque Insulation
1: Solar radiation; 2: Solar heat gains; 3: Heat energy
4: Heat losses

Fig.1.1. Thermal behavior of TI versus opaque insulation

1.1 Transparent insulation materials types

Research and development have resulted in a variety of TI materials, a few of which have reached the stage of commercial production. A variety of different materials can be characterized as TIM (Platzer, 1994) and they fall broadly into four categories (Fig.1.2):

Type A: with material structures parallel to the surface plane (multiple glazing, plastic films, IR-reflective glass).

Type B: with material structures perpendicular to the absorber (parallel slats, honeycombs, capillaries).

Type C: scattering structures (duct plates, foams, and bubbles)

Type D: quasi-homogeneous materials (glass fibers, aerogels).

Some of these materials were derived from typical heat or noise insulation applications. The most popular type used today is type B, the honeycomb-structured materials made from plastics like acrylic or polycarbonate (Platzer, 1997). These materials have very high solar transmission with good insulation properties.

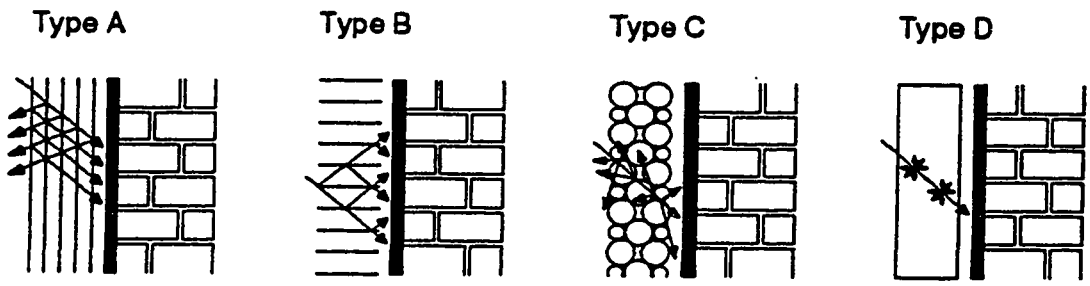

Fig.1.2. Transparent insulation materials types (BINE projekt, 1990)

1.2. Honeycombing

In a passive solar system, the thermal radiative heat losses from the absorber can be reduced by application of selective coatings. Once radiation losses have been restricted, natural convection dominates heat losses. Minimizing this convective heat loss requires the determination of some parameters such as (Hollands, 1978-b &d):

1- The temperature difference between the absorber and the cover.

2- The distance between the absorber and the cover.

3- The angle of inclination of the air layer.

4- The air properties.

5- The geometry of the enclosure.

One of the methods for reducing the convective heat transfer is to divide the enclosure into a large number of cells (Fig.1.3). Due to the reduced dimension of each

cell, in comparison with the enclosure, the viscous forces acting on the air in each cell are increased and the movement of air in the cell is restricted. If the cell were sized correctly to maintain stagnant air (motionless air), the natural convection between the absorber and the cover would be suppressed. This gives the opportunity to increase the distance between the absorber and the cover and therefore to augment the insulating value of the air layer. Thus, honeycombing the air space will improve the thermal resistance of the wall system by means of convection suppression.

The honeycomb cell size must be chosen so as to just suppress the free convective heat transfer at the value of the design temperature difference. Use of smaller cell sizes will result in more of the expensive honeycomb being used than actually necessary and will also cause unnecessary loss in solar transmission of the honeycomb. However, using a cell size larger than needed to suppress convection will result in greater heat loss. These factors underline the importance of properly choosing the cell size.

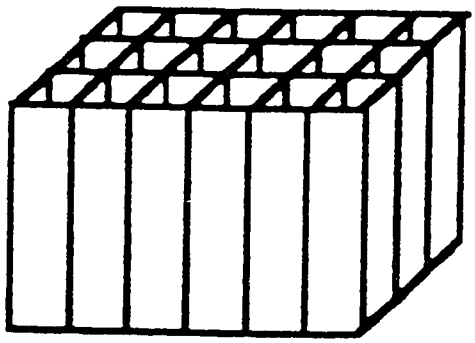

Fig.1.3. Square honeycomb transparent insulation

1.3. Solar transmittance and heat transfer of transparent honeycomb

The advantage of the honeycomb structure is that the solar radiation striking the insulation panel is reflected and re-reflected by the walls in the forward direction and thus reaches the absorber (Fig.1.4). Thus, if reflections are perfectly specular and there is no scattering or absorption in the walls, the solar transmission will be 100 percent (Hollands, 1988). However, the transmittance of the honeycomb insulation is dependent upon the angle of incidence of solar radiation, i.e., it will be affected by the sun's position throughout the year (Symons, 1982).

The high solar transmittance of the transparent honeycomb is matched with a good thermal insulation property. The conditions for having good insulation with low U-value (total heat transfer coefficient) may be described as follow:

1- To prevent heat conduction by air, the structure must be thick enough.

2- To minimize heat conduction through the transparent material, the thickness of honeycomb walls must be low.

3- For reduction of radiative heat transfer, one practical solution is the use of a selective coating on the absorber. However, this should be paired with the introduction of an air gap between the TI unit and the absorber to minimize the coupled radiative and conductive heat transfer induced by the physical contact between TI and the absorber (Hollands et al, 1984).

1.4. Design principle

Transparent insulation is most effective on massive uninsulated walls, constructed of concrete, limestone or brick, with a density of 1200 kg/m^3 or more. When TI is used

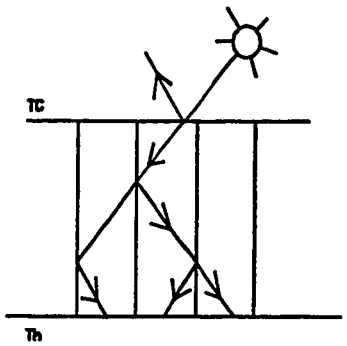

Fig.1.4 Trajectory of incidence radiation through transparent honeycomb material

on solid walls, glass is used in most cases to protect it from the environment. As the use of TI technology has significant implications for the architectural and mechanical systems of a building, employing transparent insulation should be considered early in the design process. Solar gain control, i.e. shading, must also be addressed in the design strategy.

Traditionally, TI has been applied using glass facade systems as curtain walls. Nowadays, however, prefabricated facade elements with integrated absorbers are available.

1.5. TI wall working principles

Typical insulated building facades (using opaque insulation materials) absorb some solar radiation at the outside surface. This part of the radiation is transformed into heat, but is immediately lost to the environment due to the low conductivity of the opaque insulation. Transparent insulation, however, lets solar radiation pass through and reach the massive wall. Again, the radiation is absorbed and transformed to heat, but behind the insulation. For maximum absorption, the wall should have a dark color. Dark reds and

greens absorb nearly as much as energy as black, and may be aesthetically more acceptable than black (Balcomb, 1979). The massive wall stores this heat energy and its temperature rises. Slowly, the heat energy passes through the wall to the inside, so that the inner surface of the wall warms up and contributes to the room heating as a large-area, low-temperature radiator. The insulating properties of TI prevent the generated heat from being transmitted back to the exterior (Fig.1.5).

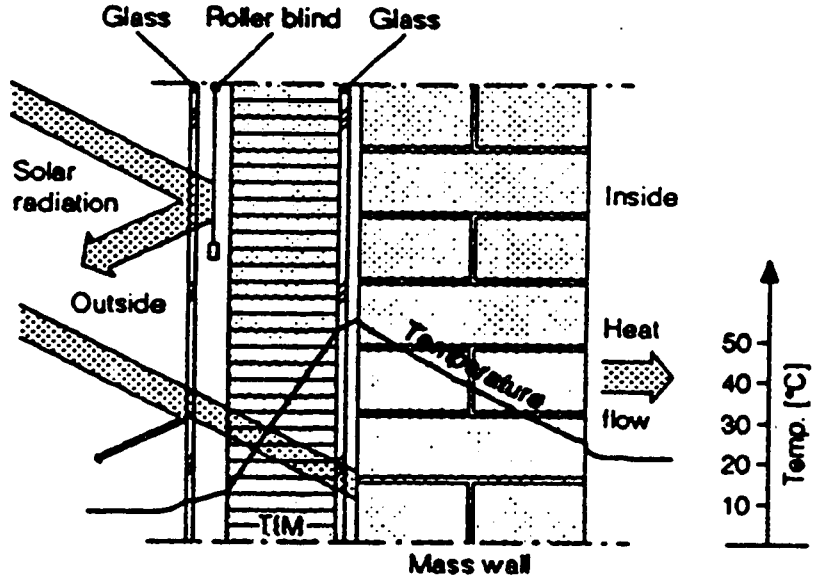

Fig 1.5. Principles of passive heating with TI (BINE Projekt, 1990)

1.6. Mathematical modelling

The prediction of the heat transfer behavior in a given physical configuration is useful in many practical situations. The prediction can be achieved by the generalization and extension of available experimental data or by the solution of a mathematical model describing the physical problem. Because most practical situations are governed by numerous parameters, the acquisition and generalization of the relevant experimental data is often too expensive if not impossible. On the other hand, the solution of an appropriate mathematical model can be accomplished at a much lower cost. One of the most effective tools in the mathematical prediction of practical heat transfer situations is the numerical methods.

1.7. Scope

Solar energy systems exhibit a non-linear dependence upon the weather in both short (instantaneous) and long time (seasonal) scale. As a result, simulations provide the main practical means of optimizing the design of solar energy systems.

A design tool for the evaluation of the heating energy requirements of a building with transparent insulation material needs to be completed by some means of assessing the thermal comfort inside the building during and beyond the heating season.

The main objective of the present work is to develop a numerical simulation model for a room model with transparent insulation materials. A TI wall model is developed first and its thermal behavior is evaluated in term of thermal comfort. Then, a methodology is developed to model a complete room with one transparently insulated wall. The thermal behavior of the TI room model is evaluated in terms of energy

consumption and thermal comfort using different control strategies for the shading device (roller blind).

1.8. Contributions and brief description

A one-zone passive building with one transparently insulated wall is modelled. The dynamic behavior of the building fabric is considered by assuming one dimensional transient heat transfer .The explicit finite difference method is employed to develop a one dimensional transparently insulated wall model and then a detailed room model. Using "Mathcad" (Mathsoft, 1995) as a programming tool makes this model fully interactive. The simulation accounts for the effect of the solar radiation (beam and diffuse) by an instantaneous computing of the solar intensity on the building envelope. Consequently, it accounts for the dependence of the solar transmittance of TIM on incidence angle. The program also models the non-linear thermal behavior of air cavities of the TI wall system and the radiative and convective heat transfer inside the room. The effect of the roller blind on the performance of the transparently insulated room is considered. Different control strategies for controlling the blind are investigated and a new strategy is developed.

A brief description of the work will now be given. After this description some terminology used in this work will be defined.

Chapter II contains a literature survey and concludes with the motivations and objectives of the thesis.

Chapter III presents the calculations of honeycomb cell dimensions and the modelling of its beam and diffuse solar transmittance.

Chapter IV deals with the modelling of the transparently insulated wall. It describes the thermal performance of the TI wall when the room air temperature is assumed constant. The results are reported for different thicknesses of the wall.

Chapter V presents the detailed room model with one transparently insulated wall. The passive response of the room is investigated first. Then a proportionally controlled auxiliary heating system is introduced and the energy consumption and the thermal comfort in the room are evaluated. In this chapter, the effect of the roller blind on the thermal performance of the TI room is investigated under different control strategies and the results are discussed.

Chapter VI presents the conclusions of this thesis.

1.9. Definitions to some terminology used in the thesis

1.9.1. Solar angles

Figure 1.6 shows the geometric relationships between the position of the sun and a plane. These angles can be defined as:

Latitude (L): It is equal to the angle of the location relative to the equator; North is positive.

Declination (δ): It is equal to the angular position of the sun at solar noon with respect to the equatorial plane (varies from -23.45 to 23.45 degrees).

Solar altitude (α): It is equal to the angle between the sun's rays and the horizontal (between 0 and 90 degrees).

Zenith angle (z): It is equal to the angle between the sun's rays and the vertical.

Solar azimuth (ϕ): It is equal to the angle between the horizontal projection of the sun's rays from due south (positive in the afternoon).

Surface solar azimuth (γ): It is equal to the angle between the projections of the sun's rays and of the normal to the surface on the horizontal plane.

Surface azimuth (ψ): It is equal to the angle between the projection of the normal to the surface on a horizontal plane and due south (east is negative).

Tilt angle (β): It is between the surface and the horizontal (0 - 180 degrees).

Angle of incidence (θ): It is the angle between the solar rays and a line normal to the surface.

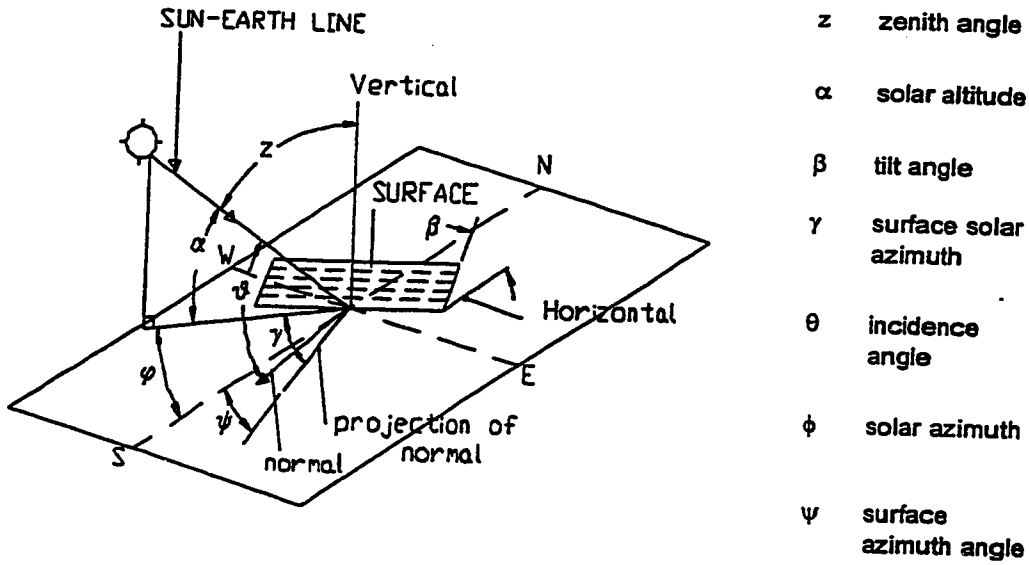

Fig.1.6. Solar angles (Athienitis, 1994)

1.9.1.1.The incidence angle (θ)

The evaluation of the angle of incident has a significant importance (fig 1.7). This angle determines the percentage of the direct sunshine intercepted by any surface. It is calculated as (Duffie and Beckman, 1991):

$$\theta = \text{acos}(\cos(\alpha)\cdot\cos(|\gamma|)\cdot\sin(\beta) + \sin(\alpha)\cdot\cos(\beta)) \quad (1.1)$$

The declination angle can be determined from Cooper (1969). That is,

$$\delta = 23.45\,\text{deg}\cdot\sin\left(360\,\frac{284+n}{365}\cdot\text{deg}\right) \quad (1.2)$$

where n is day number.

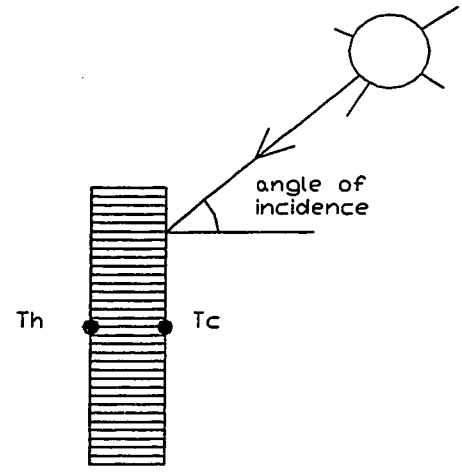

Fig.1.7 Angle of incidence

1.9.2. Aspect ratio (A)

It is a non-dimensional parameter used as a characteristic feature of a cell defined as:

$$A = \frac{L}{D_h} \quad (1.3)$$

where L is the length of the cell, D_h is the hydraulic diameter defined as the diameter of the circle which has the same area as a cross section of the cell.

1.9.3. Nusselt number (Nu)

Nu, in a rectangular enclosure, represents the ratio of heat transfer across the fluid layer in the convecting situation compared to that in purely conducting (Hollands, 1978-b).

1.9.4. Rayleigh number(Ra)

The free convective heat transfer can be characterised by a dimensionless relation namely Rayleigh number. It is defined as:

$$Ra = \frac{c_p \cdot \rho^2 \cdot g \cdot \Gamma \cdot \Delta T \cdot L^3}{\upsilon \cdot k} \qquad (1.4)$$

CHAPTER II

LITERATURE SURVEY

2.1. The development of transparent honeycomb insulation for building

In passive buildings, thermal energy is produced by natural mean with no need to employ any mechanical or hardware equipment. The structural elements of the buildings play the role of storage and collector units and a natural thermal process takes place.

2.1.1 A retrospective

Thermal solar energy components in nearly all cases need two basic elements, the thermal absorber and some transparent cover, which reduces heat losses of the absorber to the environment. Many efforts in the past have been undertaken in order to improve absorbers. Selective coatings are being developed in order to reduce infrared radiation losses without losing their ability to absorb solar radiation. Some work has also been focused on the optical and thermal properties of transparent covers.

Russian engineers introduced in 1929 the concept of using transparent non-conducting, absorbing walls to enhance the thermal resistance between the plate and the cover of a solar flat plate collector (Tabor 1969). However, this idea has been confronted by the availability of a suitable clear transparent material, which provide high opacity for thermal radiation.

Francia (1961) introduced the use of cylindrical glass materials to reduce radiative heat losses through solar collectors. Many other researchers (Hollands 1965, Perrot 1967) followed his work, but the high cost of glass tubes showed the need for development of less expensive transparent material.

Several researchers examined the radiation heat transfer reduction and convection suppression properties of the transparent honeycomb materials. They focused first on the

idea that for large aspect ratio, the cell structure acts as a thermal radiation shield (Hotel 1930, Perrot 1963, 1964). However, as the reduction of thermal radiation heat transfer can be achieved by the selection of the absorber's material and coating, the convective heat transfer will dominate.

Honeycomb structures were used to reduce the convective heat losses between the cover and the absorber (Hollands 1965, Edwards 1969, Charters and Peterson 1971, Guthrie & Charters 1982). Generally, reduction of cell size reduces convection heat transfer. Hollands (1965) demonstrated that a cell size range between 0.4 and 0.6 inch suppresses convection for aspect ratios equal to 1 and 5 respectively. The use of glass has the advantage of better ultra-violet thermal stability than plastics. But the honeycomb wall thickness can be reduced with the use of plastics resulting in less conduction heat losses and material conservation.

Using plastic honeycombs as an alternative to expensive glass solves partially the cost problem but create other difficulties. If the wall covers a big area with a honeycomb cell, the cost of the wall material and manufacturing may become high. Furthermore, a thick wall of honeycomb cell may induce conduction. Therefore, the trend was towards very thin transparent materials (about 50 μm). However, care must be taken during transportation of these very thin materials. Also, their longwave transmittance increases, as they become very thin.

Rectangular-celled extruded polycabonate honeycombs from various plastics have been developed, but only some of them are on the market. Commercial products of small celled honeycomb with improved optical and thermal properties were developed in the

early eighties by companies like "Diveno" and "Okalux Kapillargles GmbH" in Germany for instance. These products use PMMA (polymethylmethacrylate) and PC (polycarbonate) materials, which also provide ultra-violet stability behind a cover glass. The heat transfer in large-celled honeycombs has been treated by a number of researchers as Symon and Peck (1983), Hoogendoorn (1985) and Hollands et al (1984, 1992). This structure guarantees low transmission losses in the solar spectrum and permits easy combination with selective coatings. Meanwhile, different shapes of honeycomb structures have been investigated for heat losses and solar transmission such as sinusoidal (Mc Murrin and Buchberg, 1981), hexagonal (Marshall and Wedel, 1976), and cylindrical shape honeycomb (Buchberg et al 1976). For applications dealing with daylighting and light-guiding, the material is used also in modified forms: The honeycomb cells need not to be perpendicular to the glazing surface, but may be also inclined, usually 45 degrees. Also, honeycombs parallel to the glass sheets are used.

2.1.2. Testing and monitoring of buildings with transparent insulation

The activities in testing and monitoring TI applications have increased significantly starting in the late eighties. P.O. Braum et al (1992) reported 20 projects of transparently insulated walls, most of them honeycomb type, granted by the German Ministry for Research and Technology. In 1986 the European Commission, Directorate General XII for Science, Research and development launched the PASSYS project to develop reliable and affordable procedures for the testing of thermal and solar characteristics of passive solar components in a building system. The TIM component,

honeycomb structured, was tested in five countries including Belgium, Germany, Italy, United Kingdom and the Netherlands (Vandaele and Wouters, 1994).

As retrofitting buildings with honeycomb TIM proved good potentials, many other projects took place (England - Chattha (1989), Germany - Bollin (1989)). So far, the largest demonstration project was the student's residence at Strathclyde University in England (J.W.Twidell 1994) where 1040 m^2 of TIM were applied.

2.1.3. Market Development

From a questionnaire sent to companies active in the field of transparent insulation, Plattzer (1997) estimated that more than 85 buildings in the three countries Germany, Austria and Switzerland, which covers more or less the marketplace today, have been equipped with about 15000 m^2 of TIM. More than two thirds of the installed area was from 1994 onwards. Fig.(2.1) shows the yearly installed areas in the fields of daylighting and solar wall application as reported by Platzer (1997).

This shows that transparent insulation is becoming a commercially viable product. However, this does not imply that a market breakthrough has been achieved. Several obstacles like the building legislation, low energy prices and lack of widespread information keeps sold quantities low up to now.

A yearly international workshop on TIM was launched in 1986 by the European Community (Directorate General for Energy, Belgium), the Fraunhofer Institute for Solar Energy Systems (Germany) and the Franklin Company Consultants Ltd. (U.K). The purpose of these series of meetings is to accelerate the transition of the technology of TI from the development design phase to the market place (L. Jesch 1993). So far, eight

meetings have been taken place in Freiburg, Germany [TI1 (1986), TI2 (1988), TI3 (1989), TI5 (1992)], Birmingham, U.K [TI4 (1991), TI6 (1993)] and the Netherlands [TI7 (1994)].

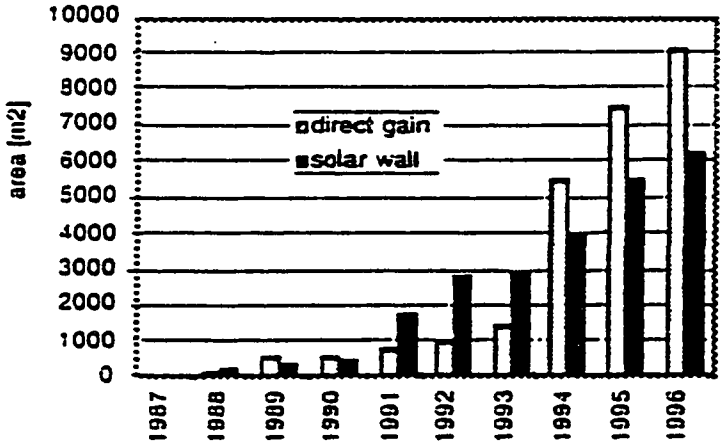

Fig.2.1. Accumulated installed area of transparent insulation (adapted from Platzer, 1997)

2.2. Solar transmittance and thermal properties

The thermal performance of a transparent material can be expressed in terms of its capability to transmit shortwave radiation (solar transmittance) and preserve longwave radiation (thermal conductivity).

Experiments were first performed to evaluate solar transmittance of transparent honeycomb structured materials (Marshall et al 1976-b, Mc Murrin et al 1977, Platzer 1992). Analytical methods for predicting the efficiency of honeycombs prior to testing are useful for optimization and design. The solar collection effectiveness of the device required an accurate determination of its solar transmittance.

Monte-Carlo ray-tracing techniques have been used first to determine, theoretically, solar transmittance of transparent honeycombs (Morris 1976, Feland & Edwards 1978, Platzer 1987). However, the complexity of this technique has impeded its widespread use. Approximate formulations for computing the solar beam transmittance of symmetrical configurations transparent honeycombs has been developed by Hollands et al (1978-a). Shamra & kaushika (1987) investigated the variation of solar transmittance with incidence angle by employing this method. However, Jesch (1987) shows that this approximation deviates from experimental data after 60 degrees. Symons (1982) developed another analytical model, which then used by Chattha (1989) where the scattering and absorption of solar radiation are considered.

On the other hand, numerical techniques have been used recently to estimate solar diffuse radiation transmittance of cellular arrays (Arulanantham & Kaushika 1994). This method expresses the diffuse transmittance of transparent honeycomb materials in terms of polynomial equations.

Regarding heat transfer analysis of transparent materials, initially conduction and radiation through honeycomb was treated using an independent mode analysis. This method assumes that conduction (through air and honeycomb walls), and thermal radiation behave separately without been interlocked. Accordingly, the total heat transfer is taken as the sum of radiation and conduction calculated independently. However, this assumption underestimates the heat transport significantly. While it predicts that the honeycomb will always decrease the radiant heat transfer, collector measurements (Marshal et al 1976-b) and experiments (Hollands et al 1978-c) recorded that if low-emitting bounding plate is employed, radiative heat transfer is increased. Therefore,

coupled heat transfer analysis, which treats the two relevant heat transfer modes simultaneously, has to be considered (Hollands 1984). Nevertheless, in building applications using an approximate constant U-value for the transparent material is common and acceptable (Stahl et al 1984, Braun et al 1992).

2.3. Enhancements to TI wall technology

The thermal performance of the TI wall can be improved by introducing an air gap between the absorber and the TI element and employing a roller blind between the cover and the TI element.

2.3.1 Air gap

The main objective of inserting air gaps in the wall system (with low emissive surface) is to reduce the radiation-conduction coupling between the absorber surface and the transparent material. Edwards et al (1976) tested the effect of an air gap between the honeycomb and the absorber. They concluded that adding an air gap to the honeycomb-absorber system would enhance the performance of the solar collector system. Hollands (1985) through an extensive experimental study demonstrated that having a 2-cm air gap effectively decouples the heat transfer modes and reduces, consequently, the overall heat transfer in the TI wall system.

2.3.2. Shading devices for solar wall systems

Blinds, usually with low emissivity reflective coating, have been used to prevent overheating and degradation of the construct. Moreover, they regulate energy gains

during the transition periods (J.W. Twidell, 1994). When no solar gains are available, blinds play the role of night insulators to reduce the heat losses. Shadings currently in use are: roller blinds, fixed reflective blinds, venetian blinds and reflective venetian blinds. However, few commercial products are available. For a shutter, the main required characteristic, beside low thermal conductance, low cost and durability, is reliability. Therefore, an effective control strategy should be applied. J.W. Twidell (1994) presented a control logic for roller binds used in Stratheclyde University's solar residences. The controller is a real time sampling unit detecting the shaded air temperature and the control strategy is based on the detection of the ambient (outside) Ta*, wall fabric temperature Tw*, and the global vertical luminance on the facade Gv*. The control logic was set to uncover the facade when Ta<15°C and Tw<60°C and Gv>10000 lux (100 watt/m^2) and cover the facade when these conditions could not be met. However, many difficulties appear when the blinds are operated. Hence, another control strategy, which acts with a 10 minutes time sampling period, was used. This would reduce the number of actions of the blinds by a factor of about five.

Nevertheless, using this strategy during very cold winter days may increase the heating bill (Ramadan and Athienitis, 1998-b). For this reason another strategy should be developed to satisfy thermal comfort conditions and to conserve energy during the heating season.

* Symbols used here are identical to those published in the mentioned paper

2.4. Simulations of transparently insulated buildings

Computer models are required to determine the effects of transparently insulated walls on building thermal performance. Many solar building simulation programs have been extended to handle transparent insulation materials (TIM) characteristics like TRNSYS (Sick and Kummer, 1991) and SUNCODE (Boy 1988). Other programs have been developed for solar buildings to model the transparent insulation technology such as PASSPORT (Santamouris, 1994) HAUSSIM (Wilke and Schmid, 1991), HELIOS (Hartwig et al, 1991). However, because of the reasons listed below, it was deemed necessary to develop a dedicated simulation model and program for this study:

1- Some programs are transfer function-based in which the non-linear thermal behavior may not be evaluated (HELIOS, TRNSYS and BID extension for TIM applications).

2- Some of the mentioned programs (SUNCODE, PASSPORT) assume an average constant value of TIM solar transmittance, which is, however, angle of incidence dependent.

3- The sophisticated programs are mostly for different solar applications in building (SUNCODE and TRNSYS for instance) where transparent insulation technology is featured as well as other solar systems. Thus, to experience the transparent insulation features one has to buy the complete expensive program.

4- All the programs do not include the effect of a controlled shading device on the TI wall, a very important requirement as shown in chapter 5.

5- All the programs are input-output based. It is, thus, impossible to modify the core program.

6- All of the above programs assume a constant diffuse solar radiation transmittance for all honeycomb materials. An equivalent value to the beam transmittance at an angle of incidence $\theta = 58°$ was considered. However, as demonstrated by Arulanantham and Kaushika (1994), the diffuse solar radiation transmittance of TIM depends on the tilt angle, aspect ratio and material's characteristics.

2.5. Mathematical modelling of transient conduction

Two approaches dominate the mathematical treatment of transient heat conduction: The response function methods and the numerical methods (Haghighat and Liang, 1992). Both techniques are widely used for passive solar analysis (Athienitis, 1985-a).

2.5.1. Response function methods

It is an analytical approach to solve the governing differential heat equation. The one-dimensional Fourrier equation of heat may be expressed as:

$$\frac{\partial^2 T(x,t)}{\partial x^2} = \frac{1}{\alpha} * \frac{\partial T(x,t)}{\partial t} \qquad (2.1)$$

where T is the temperature, t is time, x is the element thickness and α is the diffusivity. Carslaw and Jaeger (1959), Churchill (1958), Davies (1978) described this methods in detail. Basically, it is a three-stage procedure. First, the given equation in the time domain is transformed into a subsidiary equation in an imaginary space. Then this subsidiary equation is solved by purely algebraic manipulations. The third stage is to use an inverse

transformation to the solution to express the solution in the time domain of the initial problem. The interesting feature of the method is that in many cases ordinary differential equations are transformed into purely algebraic equations and partial differential equations are transformed to ordinary differential equation.

It is convenient to state the solution of the subsidiary equations in matrix notation (Pipes 1957). That is,

$$\begin{pmatrix} T_0 \\ q_0 \end{pmatrix} = \begin{pmatrix} A & C \\ B & D \end{pmatrix} \cdot \begin{pmatrix} T_i \\ q_i \end{pmatrix} \qquad (2.2)$$

where A,B,C,D are called transfer functions and expressed in complex exponential function or hyperbolic function forms. T and q represent the outer (o) and the inner (i) temperature and heat flow respectively.

In the third stage of solution, where the inverse transform is applied, two methods can be used. The time domain method is concerned with the response of multi-layered walls to time series or flux pulses (Kimura 1977, Stephenson and Mitalas 1971) and the other (frequency domain method) with the response to periodic excitations of differing frequencies (Pipes 1957, Muncey 1979).

The former method can usually only be applied to a system of equations, which are both linear and invariable with time. Many building energy simulation programs used this method such as TARP (Walton, 1983) and ENCORE (Konrad and Larsen, 1978).

In the frequency domain method, no time steps are involved in the solution. Instead, the flux transfers are estimated under periodic (cyclic) conditions, where external flux or temperature variations are repeated over a period of time. In this way, the climatic

influence can be represented by a steady state term accompanied by a number of pure sine wave harmonics. However, this method cannot model non-linear heat transfer coefficients. In building energy simulation field, many scientists used the frequency domain methods such as Kirkpatrick and Winn (1984), and Athienitis (1985-b).

2.5.2. Numerical methods

The use of numerical methods for solving heat transfer problems is a result of the complexity of the analytical solutions associated with practical engineering problems. Factors that bring about the use of numerical methods are complex geometry, non-uniform boundary conditions, time-dependent and temperature dependent properties. In some cases, analytical solutions are possible if many implications are made (Lien, 1981).

Although numerical methods must be regarded as representing approximate solutions, their accuracy can, by careful design, be made to satisfy even the most demanding criteria. In the field of building energy analysis, different numerical techniques have been used. The finite difference method is one of the most widely used (Minkowyez et al, 1988). It is conceptually a simple method to implement and is appropriate for most of the problems encountered in building thermal analysis (Holman, 1986). It is a powerful technique for the solution of the partial differential equation that governs the heat transfer problem. It can be used to handle problems of almost any degree of complexity such as transient heat conduction within multi-layered constructions under non-linear boundary conditions or where thermal properties are considered to be temperature and time dependent (Patankar, 1980). Numerical methods are called sometimes discretization methods since the numerical solution is obtained in the form of

the values of the dependent variables at a number of discrete locations in the domain of interest. The discrete locations are often called grids or nodes.

Finite difference methods are concerned with approximating the derivatives of heat equation either directly by a truncated Taylor series expansion, for example, or indirectly by application of the principle of conservation of energy to a small control volume. The former method proves cumbersome and difficult to apply to all but simple problems (Croft and Lilley, 1977).

One effective approach is to refer the spatial discretization to a small control volume. The resulting equation has the significance of satisfying the conservation of energy law. When the model under study is subdivided into a large number of control volumes (with one node within each control volume), the numerical solution approaches the exact solution of the original differential equation (fig.2.2). Here, two finite difference schemes are possible: explicit and implicit.

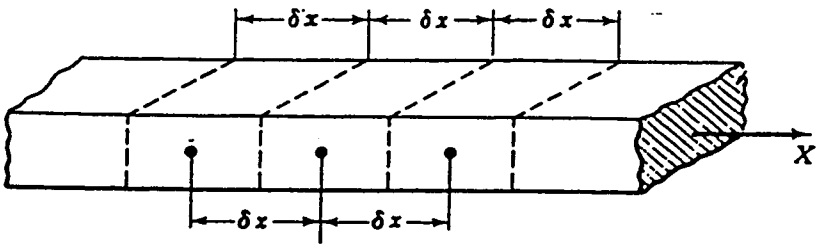

Fig.2.2. Spatial discretization for the finite difference approximation.

2.5.2.1. Explicit versus implicit solution

The three dimensional transient conduction equation is expressed as:

$$k\left(\frac{\partial^2 T}{\partial x^2}+\frac{\partial^2 T}{\partial y^2}+\frac{\partial^2 T}{\partial z^2}\right)=\rho c_p \frac{\partial T}{\partial t} \qquad (2.3)$$

where T is the temperature, c_p is the specific heat, ρ is the density, t is time and x, y and z represent the direction of the heat flow. However, for the plane wall case, which represents our domain of interest, the effect of the second and third-space coordinate may be so small as to justify its neglect, and the multidimensional heat flow problem may be approximated with a one dimensional analysis (Schneider, 1955). So that equation (4.8) may be reduce to a simpler expression. That is,

$$k\frac{\partial^2 T}{\partial x^2}=\rho c_p \frac{\partial T}{\partial t} \qquad (2.4)$$

This equation is substituted by finite difference expressions. It may be represented in explicit (forward) or implicit (backward) formulation. That is,

$$T(i,p+1)=\frac{\Delta t}{C_i}*\left(q_i+\sum_j \frac{T(j,p)-T(i,p)}{R(i,j)}\right)+T(i,p)\text{, (Explicit expression)} \qquad (2.5)$$

$$T(i,p+1)=\frac{\Delta t}{C_i}*\left(q_i+\sum_j \frac{T(j,p+1)-T(i,p+1)}{R(i,j)}\right)+T(i,p)\text{, (Implicit expression)} \qquad (2.6)$$

where (j) represents all nodes connected to node (i), (q_i) represents all heat sources at node (i), (p) is the time interval and (Δt) is the time step, C_i is the thermal capacitance for node (i) and R(i,j) is the conductive, radiative or convective thermal resistance.

The advantage of the explicit finite difference representation is that it gives the future temperature of a single node in term of current temperatures of that node and its neighbors. Thus, if at the end of a certain time period, all the nodal temperatures are

known, then each of nodal temperatures at the end of the next moment, Δt, may be explicitly found, node by node without a matrix inversion or solution of simultaneous equations (Dusinberre, 1961). However, the implicit finite difference form expresses a future nodal temperature in terms of its current value and the future values of its neighbors' temperatures. Thus, to progress from one time step to the next, a system of equations of the form of equation (2.6) must be solved. For this reason, using the direct explicit formulation is preferred, also because non-linearities can be modelled more easily. However, the time increment should be carefully selected in relation to the spatial increment to avoid any numerical instability errors.

2.5.2.2. Errors involved in finite differences

Two types of errors are associated with the finite difference approximation: rounding off and discretization (flower, 1945). The former occurs on each time step of the calculation. However, this error may be reduced significantly by carrying out the numerical calculation in double precision.

Discretization or stability error results from the replacement of the differential equation by the explicit finite difference expression. This could be avoided by reducing the space and time increment. That is, the time step must be chosen as:

$$\Delta t \leq \min\left(\frac{C_i}{\sum_j \frac{1}{R(i,j)}}\right) \qquad (2.7)$$

2.6. Motivation for using the control volume method

The first advantage of this method is its capacity of solving complicated heat engineering problems in a simple procedure. So that, knowing the energy balance on a control volume, we need only to add the boundary conditions and implement a method to solve the resulting system of difference equations. Another advantage is that energy is conserved regardless the size of the control volume. Thus, a problem can be solved quickly on a fairly coarse grid to develop the numerical technique and then on a finer grid to find the final, accurate solution. Finally, the control volume method minimizes complex mathematics and therefore promotes a better physical feel for the problem.

2.7. Objectives of the work

From the literature reviewed above, the need for modelling a room with transparent insulation in detail may be identified. Consequently the objective of this work are conducted as follow:

1. A TI wall will be modelled using the explicit finite difference numerical method. The non-linear behavior of the air gaps and the angle of incidence dependent solar transmittance will be considered.
2. A methodology will be employed to model a room in detail with one transparently insulated wall where the non-linear behavior of the convective and radiative heat transfer between the interior room surfaces is considered.
3. A control strategy for the roller blind will be developed to enhance the thermal performance of the room.

4. The thermal behavior of the TI room will be evaluated in terms of energy consumption and thermal comfort.

CHAPTER III

THEORY BACKGROUND

3.1. Introduction

Honeycomb arrays are parallel transparent sheets that divide the space into compartments or cells. They can create a layer that will transmit solar radiation yet offer good thermal resistance. The added thermal resistance is obtained by reducing infrared radiation and natural convection heat losses without introducing significant wall conduction (Hollands, 1976). After choosing a convenient transparent material, three design parameters must be considered:

1- Cell dimensions.

2- Heat transfer through the cellular array.

3- Solar radiation transmittance.

3.2. Design of honeycomb cell

The main purpose of the honeycomb is to reduce the free convection currents which would otherwise occur in the air layer. Once the value of honeycomb thickness is decided, the cell size must be chosen so as to just suppress the free convective currents at the value of design ΔT (temperature difference between hot and cold faces of honeycomb). The use of smaller cell sizes will result in more of expensive honeycomb being used than actually necessary and will also cause unnecessary loss in solar transmission of the honeycomb. However, as Cane et al (1977) observed, the use of cell sizes larger than needed may induce a convective heat exchange greater than that would take place without the honeycomb. If the aspect ratio is less than 2, very little convection suppression is possible and it is difficult to avoid the region of free convection

augmentation by honeycomb. Consequently, honeycomb with aspect ratio less than 2 should be avoided

The free convection heat transfer across a honeycomb can be characterized by a Nusselt number, Nu, which represents the ratio of the combined conductive and free convective heat transfer through the air to the corresponding heat transfer when the air is stagnant (Holman 1986). Hence, a Nusselt number of unity indicates purely conductive heat transfer and complete suppression of convective motion.

On the other hand, as observed by Charters and Peterson (1972) through flow visualization tests, there is never a complete suppression of convection motion for an inclined cell. Thus, the Nusselt number is never exactly unity even at very small Raleigh number (Ra). However, the Nusselt number increases rather slowly with Ra until it reaches approximately 1.2 after which it rises rather steeply with Ra (Cane, 1977). Consequently, when Nu=1.2 is reached, the effective suppression will be assumed to have taken place where purely conductive heat transfer of still air is augmented by 20%.

3.3. Dimensions of the cell

Cane (1977) reported an extensive experimental study on free convection across inclined square and hexagonal celled plastic honeycomb. He recommends the following for Nusselt number:

$$Nu = 1 + 0.89 \cdot \cos(\beta - 60) \cdot \left(\frac{Ra}{2420 \cdot A_{hc}^{4}} \right)^{2.88 - 1.64 \cdot \sin\beta} \qquad (3.1)$$

where, β is the tilt angle (angle of inclination for honeycomb panel in degrees) and A_{hc} is the aspect ratio of the cell.

This relation is valid when $30° \le \beta \le 90°$ and $\frac{Ra}{A_{hc}^{4}} \le 6000$

Although based on data for $A_{hc} \ge 4$, this relation is approximately valid for $A_{hc}=3$ as well (Cane 1977).

Substituting Nu=1.2 in equation 3.1

$$A_{hc} = f(\beta) \cdot \left(\frac{Ra}{2420}\right)^{\frac{1}{4}} \qquad (3.2)$$

where, $f(\beta) = (4.45 \cdot \cos(\beta - 60))^{\frac{1}{11.52 - 6.56 \cdot \sin\beta}}$, for $30° \le \beta \le 90°$

For air at atmospheric pressure and moderate temperatures equation 3.2 can be expressed dimensionally as:

$$A_{hc} = C(\beta) \cdot (1 + 2 \cdot x)^{\frac{1}{2}} \cdot x \cdot \Delta T^{\frac{1}{4}} \cdot L^{\frac{3}{4}} \qquad (3.3)$$

where, $C(\beta) = 1.03 \cdot f(\beta)$, and $x = \frac{100}{Tm}$

where, Tm is the mean air temperature expressed in degree Kelvin, ΔT is the temperature difference across the honeycomb and L is the depth of the honeycomb expressed in cm.

It can be seen that the cell dimensions depend on mean temperature and temperature difference. However, as shown by Hollands (1978-c), with a good factor of safety, a cell size of the order of 12mm in hydraulic diameter is appropriate for a cell length of 100mm.

3.4. Design selection of honeycomb cells

In choosing the cell size, the honeycomb designer must first make a decision choice concerning the chief function of the honeycomb, and this differentiation on the basis of function leads to a calculation of honeycomb into what may be called "large-celled" and "small-celled" honeycombs. Another classification may be governed by the cell geometry and shape. However, when encountered with the concept of honeycomb, a host of questions arise concerning the best geometry, dimensions and shape of the cell. In fact, the amount of the material that must go into making the transparent insulation is the key factor in answering these questions. Two factors demonstrate the importance of the material content:

1- The amount of absorption and scattering of solar radiation inside the honeycomb wall is proportional to the material content, so is the heat transfer by conduction through the cell.

2- The material cost.

Reducing the amount of material may be achieved by reducing the thickness of the walls and increasing the cell dimensions. However, a decision should be made whether the cell is designed to suppress radiative or convection heat transfer. The long wave radiation suppression needs a small cell and a minimum thickness of wall to establish the required degree of opaqueness. On the other, for convection suppression, a minimum cell size is required below which no added advantage is gained.

As designing to suppress radiant heat transfer is more exigent, an alternative method may be applied. It is the use of a selective surface on the absorber to help the radiant suppression. However, the cost of the coating has to be considered and an air gap should

be added between the absorber and the TI element to decouple the conductive and radiative heat transfer mode.

3.5. Solar transmittance of transparent honeycomb insulation

The successful use of honeycomb transparent insulation for solar energy application depends not only on cost, convection suppression and thermal radiation reduction considerations but also its transmittance to incoming solar radiation over different angles of incidence (Symons, 1982). The solar collection effectiveness of a solar device can be judged by an accurate determination of its solar transmittance. Theoretical studies for such determinations have been made by using methods like Monte-Carlo ray tracing techniques (Morris, 1976 and Feland, 1978). The complexities of this technique have hindered its use. Hollands et al (1978-a) has derived an approximate equation of honeycomb transmittance. However, as shown by Jesch et al (1987), the calculated values by this method deviate from experimental data after 60-degree angle of incidence. Symons (1982), suggested empirical solar transmittance correlation equations based on a simple convection suppression solar transmittance model. The results match the measured data to within 2 percent. Later Chattha and Jesch (1989) used and validated this method.

3.5.1. Beam transmittance of honeycomb transparent insulation

Symons (1982) has reported a simple set of formulations for calculating the solar transmittance of transparent honeycombs. Chattha and Jecsh (1989) have used these formulations for investigating the variation of solar transmittance with incidence angle and included the effect of scattering and absorption of radiation by vertical walls.

Solar radiation falling on the top surface of a honeycomb propagates through the cell as well as through the cell walls. The portion propagating through the cells undergoes reflection (specular as well as diffuse) refraction and absorption by the vertical walls (fig.3.2).

The radiation of the cell walls is propagated downwards through the walls due to total internal reflection and, in the process, is absorbed and scattered inside the material of the walls. Following Symons (1982), Chattha and Jesch (1989), the beam radiation transmittance $T(\theta)$ can be approximated as:

$$T(\theta)=\left(\tau_s+\rho_s\right)^{nw} \qquad (3.4)$$

where nw is the number of walls intercepting incoming rays at angle of incidence θ and azimuth ϕ and is equal to $A_{hc}\cdot\tan(\theta)$ for square celled honeycomb (fig.3.3).

For smooth wall materials, the sum of specularly reflected and transmitted radiation is essentially independent of angle of incidence. For example, Symons (1982) evaluated the value of $\tau_s+\rho_s$ for FEP Teflon honeycomb as approximately equal to 0.983. He measured the variation of this value with the angle of incidence and concluded a reduction of less than one percent when the angle of incidence increases from 0 to 75 degrees. On the other hand, equation (3.4) is only applicable for very thin honeycomb wall materials. It can shown from equation (3.4) that for θ equal 0, $T(\theta)$ is equal to 1.

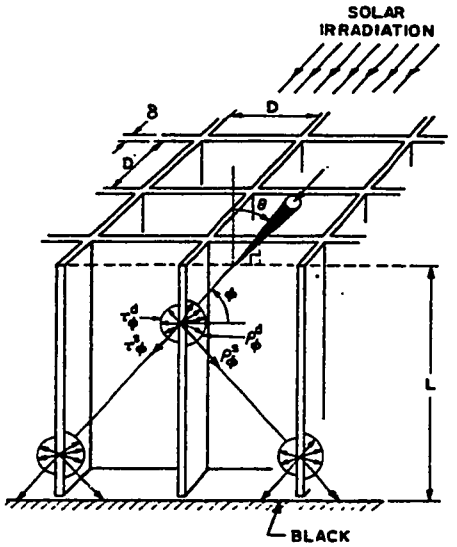

Fig.3.1.Propagation of incident radiation through transparent honeycomb where τ is the transmissivity and ρ is the reflectivity, the superscripts s and d designate for specular and diffuse respectively (Hollands, 1978-a)

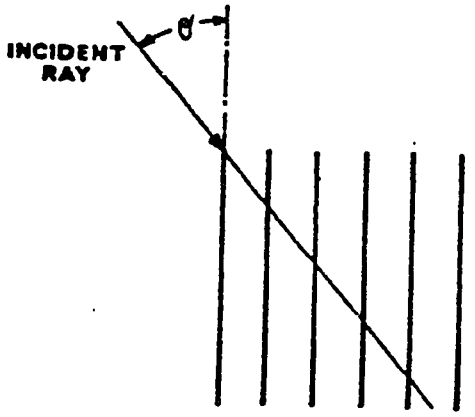

Fig.3.2. Honeycomb walls reached by incident radiation (Symons, 1982)

Therefore, equation (3.4) should be modified to accommodate thicker and wavy honeycomb wall. It may be expressed as:

$$T(\theta)=F_e \cdot F_r^{A_{hc}\cdot\tan(\theta)} \tag{3.5}$$

where, F_e is the fraction of effective cross sectional area of honeycomb not occupied by wall material. That is, (Kaushika and Padma Priya, 1991)

$$F_e=1-\frac{\delta_{hc}\cdot(\delta_{hc}+2\cdot D_{hc})}{D_{hc}^{2}} \tag{3.6}$$

F_r is the fraction of radiation, which is reflected and transmitted specularly at each wall intercept, and it is measured experimentally taking into account the absorption and scattering of solar radiation. Hollands et al (1978-a), Kaushika and Padma Priya (1991) and Chattha and Jesch (1989) reported measured values for different types of honeycomb. These values are summarized in table (3.1)

Table 3.1 F_r and δ_{hc} for different honeycomb materials

	ACRYLIC	POLYCARBONATE	GLASS	LEXAN	FEP-TEFLON
F_r	0.963	0.988	0.955	0.999	0.999
δ_{hc}	1 mm	0.03 mm	1 mm	0.076 mm	0.013 mm

3.5.2. Solar diffuse radiation transmittance of transparent honeycomb

Solar diffuse radiation transmittance for plane glass cover of flat plate collector has been investigated by Brandemuehl and Beckman (1980). Their approach involves the consideration of solar diffuse radiation made up of 2 components (the sky and ground reflected one) to be hemispherical isotropic in nature. For the derivation of transmittance of diffuse radiation the results of beam radiation transmittance are integrated over the appropriate range of the solid angle of incident diffuse radiation. The effective beam incidence angle θ_e, is defined for a given range and transparent system such that

$$T_d = T(\theta_e)$$

The same approach may be applied to the cellular arrays (honeycomb structured) materials. The transmittance for solar diffuse radiation is expressed as:

$$T_d = \frac{\int_{\omega 1}^{\omega 2} T(\theta)\cdot\cos(\theta)\cdot\sin(\theta)\cdot d\phi\, d\theta}{\int_{\omega 1}^{\omega 2} \cos(\theta)\cdot\sin(\theta)\cdot d\phi\, d\theta} \qquad (3.7)$$

where $\omega 1$ and $\omega 2$ represent the angular range of incident diffuse radiation, θ and ϕ are the angle of incidence and azimuth respectively. The angular range has been determined earlier by Brandemuehl and Backman (1980) and the results are adopted in the present work.

For the honeycomb transparent material tilted at an angle β, the diffuse radiation from the ground will have an angle of incidence ranging from $\theta = \frac{\pi}{2} - \beta$ to $\theta = \frac{\pi}{2}$. For a

given value of θ the azimuth angle will range from $\phi = \operatorname{asin}\left(\frac{\cot(\beta)}{\tan(\theta)}\right)$ to $\phi = \pi - \operatorname{asin}\left(\frac{\cot(\beta)}{\tan(\theta)}\right)$.

Using these integration limits and due to axial symmetry, the transmittance for diffuse ground radiation is:

$$T_{dground} = \frac{\int_{\frac{\pi}{2}-\beta}^{\frac{\pi}{2}} \int_{\operatorname{asin}\left(\frac{\cot(\beta)}{\tan(\theta)}\right)}^{\frac{\pi}{2}} T(\theta)\cdot\cos\theta\cdot\sin\theta \, d\phi \, d\theta}{\int_{\frac{\pi}{2}-\beta}^{\frac{\pi}{2}} \int_{\operatorname{asin}\left(\frac{\cot(\beta)}{\tan(\theta)}\right)}^{\frac{\pi}{2}} \cos\theta\cdot\sin\theta \, d\phi \, d\theta} \qquad (3.8)$$

Diffuse radiation from the sky will have angle of incidence ranging from $\theta = 0$ to $\theta = \frac{\pi}{2}$. For the incidence angle $\theta < \frac{\pi}{2} - \beta$, the angle ϕ will vary from 0 to 2π and for the incidence angle $\theta > \frac{\pi}{2} - \beta$ and the angle ϕ will range from $\phi = \pi - \operatorname{asin}\left(\frac{\cot(\beta)}{\tan(\theta)}\right)$ to $\phi = 2\cdot\pi + \operatorname{asin}\left(\frac{\cot(\beta)}{\tan(\theta)}\right)$. By applying these integration limits and due to axial symmetry the sky diffuse transmittance for a transparent honeycomb is expressed as:

$$T_{dsky} = \frac{\int_0^{\frac{\pi}{2}} \int_{-\frac{\pi}{2}}^{\frac{\pi}{2}} T_b(\theta)\cdot\cos\theta\cdot\sin\theta d\phi\, d\theta + \int_{\frac{\pi}{2}-\beta}^{\frac{\pi}{2}} \int_{-\frac{\pi}{2}}^{\operatorname{asin}\left(\frac{\cot(\beta)}{\tan(\theta)}\right)} T_b(\theta)\cdot\cos\theta\cdot\sin\theta d\phi\, d\theta}{\int_0^{\frac{\pi}{2}} \int_{-\frac{\pi}{2}}^{\frac{\pi}{2}} \cos\theta\cdot\sin\theta d\phi\, d\theta + \int_{\frac{\pi}{2}-\beta}^{\frac{\pi}{2}} \int_{-\frac{\pi}{2}}^{\operatorname{asin}\left(\frac{\cot(\beta)}{\tan(\theta)}\right)} \cos\theta\cdot\sin\theta d\phi\, d\theta} \qquad (3.9)$$

Arulanantham and kaushika (1994) used numerical integration techniques to solve the above equations. The results were reduced in terms of equivalent beam angle of incidence and its variation as a function of tilt angle and aspect ratio of the transparent device. The variations are represented as polynomial expressions and summarised in Table (3.2). The polynomial representation is based on the theoretical calculation covering the aspect ratio range from 2 to 40.

Table 3.2. Polynomial expressions for equivalent beam angle of diffuse radiation transmittance for honeycomb. (Arulanantham and Kaushika,1994)

	Ground radiation	Sky radiation
Lexan honeycomb	$\theta_e = 90.0 - 0.6084518*\beta + 3.709793 \times 10^{-4}*\beta*A - 3.0577183 *10^{-5}*\beta*A^2 + 3.0328929*10^{-3}*\beta^2 - 5.0287694*10^{-5}*\beta^2*A + 4.1570456*10^{-7}*\beta^2*A^2$	$\theta_e = 59.69678 - 0.3802643*A + 4.2715073 \times 10^{-3}* A^2 - 0.1429023*\beta - 8.0.555677*10^{-3}*A*\beta+2.1229684*10^{-4}*A^2*\beta + 1.527757*10^{-3}*\beta^2 + 7.0696505*10^{-3}*A*\beta - 2.1496235*10^{-6}*A^2*\beta^2$
Glass honeycomb	$\theta_e = 90.0 - 0.6310797*\beta + 8.3351135*10^{-4}*A*\beta + 6.3467771*10^{-5}*\beta*A^2 + 2.84324*10^{-3}*\beta^2 - 1.2378779*10^{-4}*\beta^2*A + 9.1840957*10^{-7}*\beta^2*A^2$	$\theta_e = 56.03638 - 0.7577057*A + 8.7242126*10^{-3}*A^2 - 0.2273922*\beta + 2.9509664*10^{-3}*A*\beta - 4.4569373*10^{-5}*A^2*\beta + 2.3122095*10^{-3}*\beta^2 - 4.2932341*10^{-5}*A*\beta^2 + 6.1490573*10^{-7}*A^2*\beta^2.$
Acrylic honeycomb	$\theta_e = 90.0 - 0.6182356*\beta - 7.4958801*10^{-4}*A*\beta + 7.8320503*10^{-5} *A^2*\beta + 2.746556*10^{-3}*\beta^2 - 9.1690104*10^{-5}*A*\beta^2 + 4.228286*10^{-7}*A^2*\beta^2.$	$\theta_e = 56.51758 - 0.6809692*A + 7.5445175*10^{-3}*A^2 - 0.215251*\beta + 1.2215376*10^{-3}*A*\beta - 9.6857548*10^{-6}*A^2*\beta + 2.2081658*10^{-3}*\beta^2 - 2.5243033*10^{-5}*A*\beta^2 + 2.5822374*10^{-7}*A^2*\beta^2.$

CHAPTER IV

TRANSPARENTLY INSULATED WALL MODEL

4.1. Introduction

Passive solar design seeks to reduce the house's energy budget by close attention to orientation, insulation, transparent materials placement and design, and the to subtleties of energy transfer properties of building materials. In fact, since solar gains are present in every building, all buildings are passively solar heated to some extent. However, it is when the building has been designed to optimize the use of solar energy and when solar energy contributes substantially to the heating requirements of the building that it is called a solar building.

There are three physical processes that make passive solar heating possible: Solar gain, heat storage and heat distribution (Duffie and Beckman 1991). In passive design the heat gain is accumulated by natural means and the heat storage becomes more essential as the dependence of the building on solar gains increases. The wall heat storage is like a high capacitance solar collector directly coupled to the room. Solar radiation is absorbed and conducted through an outside wall to the inside wall surface and then distributed into the room by convection and radiation. The influence of solar radiation on a particular solar energy system depends on the intensity and the direction from which the solar radiation is received. A thermal storage wall system should be designed with an aspect as close as possible to due south (northern hemispheric). This orientation maximizes the winter heat gain and minimizes the summer heat gains.

4.2. Solar gain and available solar radiation

The sun releases energy in the form of high frequency electromagnetic radiation (Mazria, 1979). The rate of radiation or heat energy reaching the outside of the earth's

atmosphere is designated by the solar constant. The value of the solar constant is approximately 1367 watt per square meter (Duffie and Beckman, 1991).

4.2.1. Intensity of solar radiation on inclined surface

The solar radiation intensity reaching the earth varies from 75% of the solar constant to zero (Angstrom, 1924). The solar radiation from the sun interacts with the atmosphere causing some of it to be reflected by clouds, scattered by dust and absorbed by ozone, carbon dioxide, water vapor and other gases in the earth's atmosphere. The solar radiation reaching the earth is characterized as direct and diffuse. Direct radiation is that solar radiation which reaches us directly from the sun without being scattered or reflected. The diffuse radiation is solar radiation which is scattered or reflected at least once (Duffie and Beckman, 1991).

4.2.2.Clear sky radiation

As mentioned above, sky radiation consists of 2 components: Beam and diffuse.

4.2.2.1. Beam radiation

Hottel (1976) has presented a convenient method for estimating the beam radiation transmitted through clear atmosphere. The atmosphere transmittance for beam radiation is given in the form

$$\tau_b = a_0 + a_1 \cdot \exp\left(\frac{-k}{\cos(z)}\right) \qquad (4.3)$$

where the constant a_0, a_1 and k depends on climate and altitude (Al). That is:

$$a_o = r_0 \cdot \left[0.4237 - 0.00821 \cdot (6 - Al)^2\right]$$
$$a_1 = r_1 \cdot \left[0.5055 + (0.00595 \cdot (6.5 - Al))^2\right]$$
$$k = r_k \cdot \left[0.2711 + (0.01858 \cdot (2.5 - Al))^2\right]$$

The correction factors r_0, r_1 , r_k , are due to the climate type are given in Table.4.1.

Table 4.1 Correction factors for climate types (Duffie and Beckman, 1991)

CLIMATIC TYPE	r_0	r_1	r_2
Tropical	0.95	0.98	1.02
Mid-Latitude Summer	0.97	0.99	1.02
Subarctic Summer	0.99	0.99	1.01
Mid-Latitude Winter	1.03	1.01	1.00

From ASHRAE (1993) the intensity of extraterrestrial normal solar radiation is defined as:

$$I_{on} = I_{sc} \cdot \left(1 + 0.033 \cos\left(360 \frac{n}{365} \cdot \deg\right)\right) \tag{4.4}$$

where I_{sc} is the solar constant.

Consequently, the intensity of beam radiation on an inclined surface is calculated as:

$$I_b = I_{on} \cdot \tau_b \cdot \cos(\theta) \tag{4.5}$$

4.2.2.2. Diffuse radiation

Liu and Jordan (1963) correlated the beam atmospheric transmittance to the diffuse atmospheric transmittance for clear sky. Assuming isotropic distribution of

diffuse radiation Liu and Jordan (1963), considered the diffuse radiation made up of two components: Sky and ground diffuse solar radiation. The intensity of is expressed as:

$$I_{ds}=I_{on}\cdot\sin(\alpha)\cdot\tau_{d}\cdot\frac{1+\cos(\beta)}{2} \tag{4.6}$$

$$I_{dg}=\left[I_{on}\cdot\sin(\alpha)\cdot\left(\tau_{b}+\tau_{d}\right)\right]\cdot\rho_{g}\cdot\frac{1-\cos(\beta)}{2} \tag{4.7}$$

4.3. Mathematical transient model of the transparently insulated wall

A thermal storage wall with honeycomb transparent material is modelled and its thermal behaviour is investigated. The performance of the one-dimensional transient TI wall model is evaluated for different orientations and thickness in terms of thermal comfort. This model will be employed, later, to evaluate the thermal performance of an outdoor room in terms of energy consumption and thermal comfort.

4.3.1. The transient conduction

This is the process by which a fluctuation of heat flux at one boundary of a solid material finds its way to another boundary, being diminished in magnitude due to material storage, and shifted time. Within the building fabric, transient conduction is a function of the temperature and energy excitations at exposed surfaces, the temperature and time dependent thermophysical properties of the individual homogeneous materials, and their relative position. For modelling and simulation purposes it is usual to declare external climatic excitations as known time-series data with the objective to determine internal transient energy flow and hence the dynamic variation of heat flux at internal

surfaces. The thermophysical properties of interest include conductivity, density and specific heat capacity as well as physical dimensions. These properties are themselves time-dependent, but in many applications, such dependencies are ignored and the properties are assumed to be invariant in the time dimensions.

4.4. Modelling of the transparently insulated wall

Figure (4.1) represents the transparently insulated wall model. It consists of

1- Protector.

2- First air gap.

3- Roller blind within the first air gap.

4- Transparent insulation unit.

5- Second air gap.

6- Concrete layer.

7- Third air gap.

8- Gypsum board layer.

4.4.1 Protector

It is a low iron glass used to protect the transparent unit and the roller blind from any environmental damage. It works as a barrier for rain, ice and wind with no significant attenuation of transmitted solar radiation. Parmelee (1945) showed that the effective transmittance of the glazing is:

$$\tau = \frac{(1 - r)^2 \cdot ac}{1 - (r)^2 \cdot (ac)^2} \qquad (4.8)$$

where,
$$r=\frac{1}{2}\cdot\left[\left(\frac{\sin(\theta-\theta'_i)}{\sin(\theta+\theta'_i)}\right)^2+\left(\frac{\tan(\theta-\theta')}{\tan(\theta+\theta')}\right)^2\right] \tag{4.9}$$

and
$$ac=\exp\left[-\frac{k_{ec}\cdot L_g}{\sqrt{1-\left(\frac{\sin(\theta)}{n_g}\right)^2}}\right] \tag{4.10}$$

4.4.2.First air gap:

This gap is located between the protector and the transparent insulation element. It permits the use of a roller blind to prevent overheating during days with excessive solar radiation and to enhance the thermal resistance of the transparently insulated wall system when needed. The unit air gap (cavity) conductance is given for different surface emissivities in several design handbooks (ASHRAE, 1993). It could be calculated as the summation of the convective and radiative heat transfer

4.4.2.1. Convective heat transfer coefficient

From ASHRAE (1993), the convective heat transfer coefficient for a plane layer is calculated as:

$$h_c=\frac{Nu\cdot K_{air}}{L_{gap}} \tag{4.11}$$

where, Nu is the Nusselt number, L_{gap} is the width of the gap and K_{air} is the air conductivity. That is,

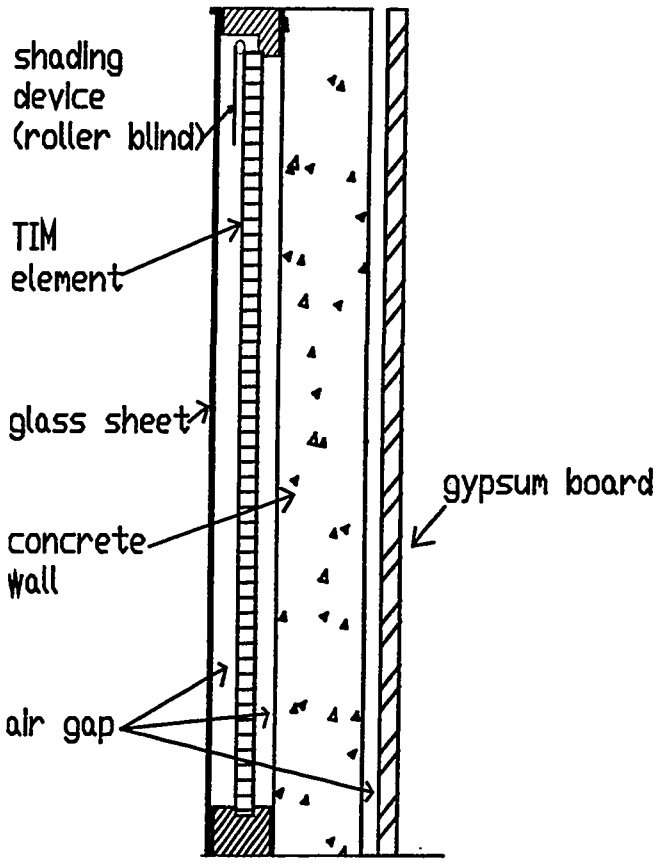

Fig.4.1. TI wall system

$$K_{air}=\frac{0.002528\,Tm^{1.5}}{Tm+200},\ \text{where}\ Tm=\frac{T_{hot}+T_{cold}}{2}$$

After intensive experiments, Elsherbiny et al (1982) suggested that the Nusselt number is the greatest of 3 values:

$$Nu1=0.0605\,Ra^{\frac{1}{3}}$$

$$Nu2=\left[1+\frac{0.104\,Ra^{0.293}}{\left[1+\left(\frac{6310}{Ra}\right)^{1.36}\right]^3}\right]^{\frac{1}{3}}$$

$$Nu3=0.242\left(\frac{Ra}{A_{gap}}\right)^{0.272}$$

and $$Ra=0.737(1+2\cdot a)^2\cdot a^4\cdot\left(T_{hot}-T_{cold}\right)\cdot L_{gap}{}^3\cdot p^2$$

where, Ra is the Rayleigh number, A_{gap} is the aspect ratio of the gap, $a=\frac{100}{Tm}$ and p is the atmospheric pressure.

4.4.2.2. Radiative heat transfer coefficient

The radiative heat transfer coefficient for an air gap may be calculated as (ASHRAE, 1993):

$$h_r=\frac{\sigma\cdot A\cdot(Th^4-Tc^4)}{\left(\frac{1}{\varepsilon 1}+\frac{1}{\varepsilon 2}-1\right)\cdot(Th-Tc)} \qquad (4.12)$$

where σ is the stefan-Boltzman constant, $\sigma=5.67\cdot10^{-8}\cdot\frac{watt}{m^2\cdot K^4}$

4.4.3. Roller blind

The role of an exterior roller blind with low emissivity reflective coating is to improve the thermal performance of the transparently insulated wall. This target may be achieved by controlling the operation of the blind properly. The control strategies are discussed in chapter 5.

4.4.4.Second air gap

The second air gap is introduced between the TI element and the thermal mass (concrete layer). Hollands and Iynkaran (1985) has revealed by an experimental study that radiative and conductive heat transfer are highly coupled through the transparent honeycomb material especially when the absorber is coated by a low selective coating. This coupling occurs at the interface between the absorber and the honeycomb. Since the honeycomb is touching the absorber, heat can be transferred to the honeycomb by conduction. The honeycomb unit radiates then this heat, and a high amount of the energy is lost. Hence, the coupling heat transfer mode bypasses the selective surface advantages. To decouple the two modes of heat transfer Hollands and Iynkaran (1985) suggested moving the honeycomb off the absorber, i.e. introducing an air gap, and thus increasing the resistance between the absorber and the honeycomb element.

The convective and radiative heat transfer coefficient of a cavity is temperature and consequently time dependant as equations (4.11) and (4.12) show. This behaviour is described as non-linear. Figure (4.2) illustrates, for instance, the time dependent heat

transfer of the second air gap (L_{gap} = 13mm) for 7 days simulation starting on January 21st.

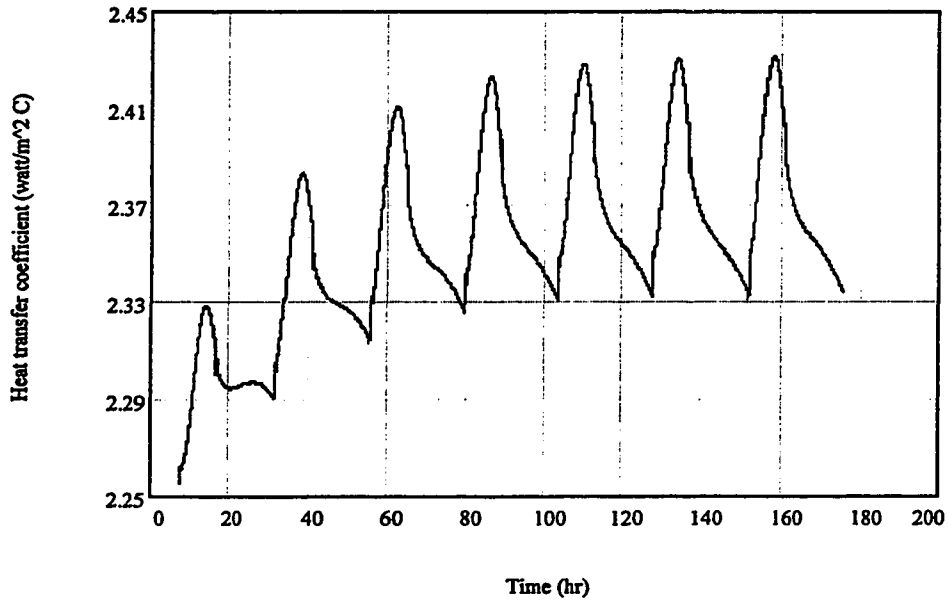

Fig.4.2. Non-linear heat transfer coefficient of the second air gap

4.4.5. Storage wall

The storage wall is a crucial component of the TI wall heating system. Mass is required to store the solar-generated heat energy. Good conductivity allows the heat to pass into the room. The materials for the storage wall must therefore have sufficient heat capacity. Concrete and limestone are best, although brick walls are also suitable (Goetzberger. 1984). To reduce reemission of long wave radiation from the thermal mass (storage wall) to the ambient, the wall absorber may be coated by a low emissivity coating.

4.4.6. Third air gap

Sometimes an air gap is employed between the thermal mass and the interior gypsum board layer, especially in retrofit applications of transparent insulation for exterior opaque walls. In addition to increasing the overall thermal resistance of the TI wall system, this cavity prevents the inside surface temperature from rising too much. The cavity provides space, as well, for electrical wiring and other services.

4.4.7. Gypsum board

The role of the interior gypsum board layer is to improve the thermal resistance of the TI wall and to provide an interior smooth surface that covers electrical wiring. This layer will reduce, meanwhile, the interior wall temperature to prevent it from being overheated.

4.5. Nodal network of TI wall model

Figure (4.3) shows the thermal network of the transparently insulated wall. The significance of each node number is presented in the nomenclature. The thermal resistances between the nodes may be expressed as:

$$R_{i,j}=\frac{\delta x_{i,j}}{k\cdot A_{i,j}}\text{, for conduction.} \tag{4.13}$$

$$R_{i,j}=\frac{1}{h_{r_{i,j}}+h_{c_{i,j}}}\text{, for air gaps.} \tag{4.14}$$

where δx is the thickness of a layer, hc and hr are the convective and radiative heat transfer respectively.

Using the explicit form of the finite difference approximation, an energy balance equation is applied for each node (i), that is,

$$T(i,p+1) = \frac{\Delta t}{C_i} * \left(q_i + \sum_j \frac{T(j,p) - T(i,p)}{R(i,j)} \right) + T(i,p) \qquad (4.15)$$

where (j) represents all nodes connected to node (i), (q_i) represents all heat sources at node (i), (p) is the time interval and (Δt) is the time step, C_i is the thermal capacitance for node (i) and R(i,j) is the conductive, radiative or convective thermal resistance. The time step chosen should satisfy the stability condition of the finite difference equation. That is,

$$\Delta t_{critical} = \min \left(\frac{C_i}{\sum_j \frac{1}{R(i,j)}} \right) \qquad (4.16)$$

and the time step $\Delta t \leq \Delta t_{critical}$

4.6. Simulation

The simulation can be started by setting the initial temperatures of the system and describing the building details. Each temperature is then updated at each time step together with the different heat transfer coefficients, taking into account the instantaneous changes of solar radiation and the ambient temperature which is modelled by discrete Fourier series consisting of daily average (mean term) and one harmonic. It is represented by a sinusoid with maximum value at 3 PM and minimum at 3 AM, such as:

$$T_{out} = Tmean + X\cos(wt + 3\pi/4) \qquad (4.17)$$

where (w) is the frequency (period of one day) and X is the amplitude of the daily temperature profile.

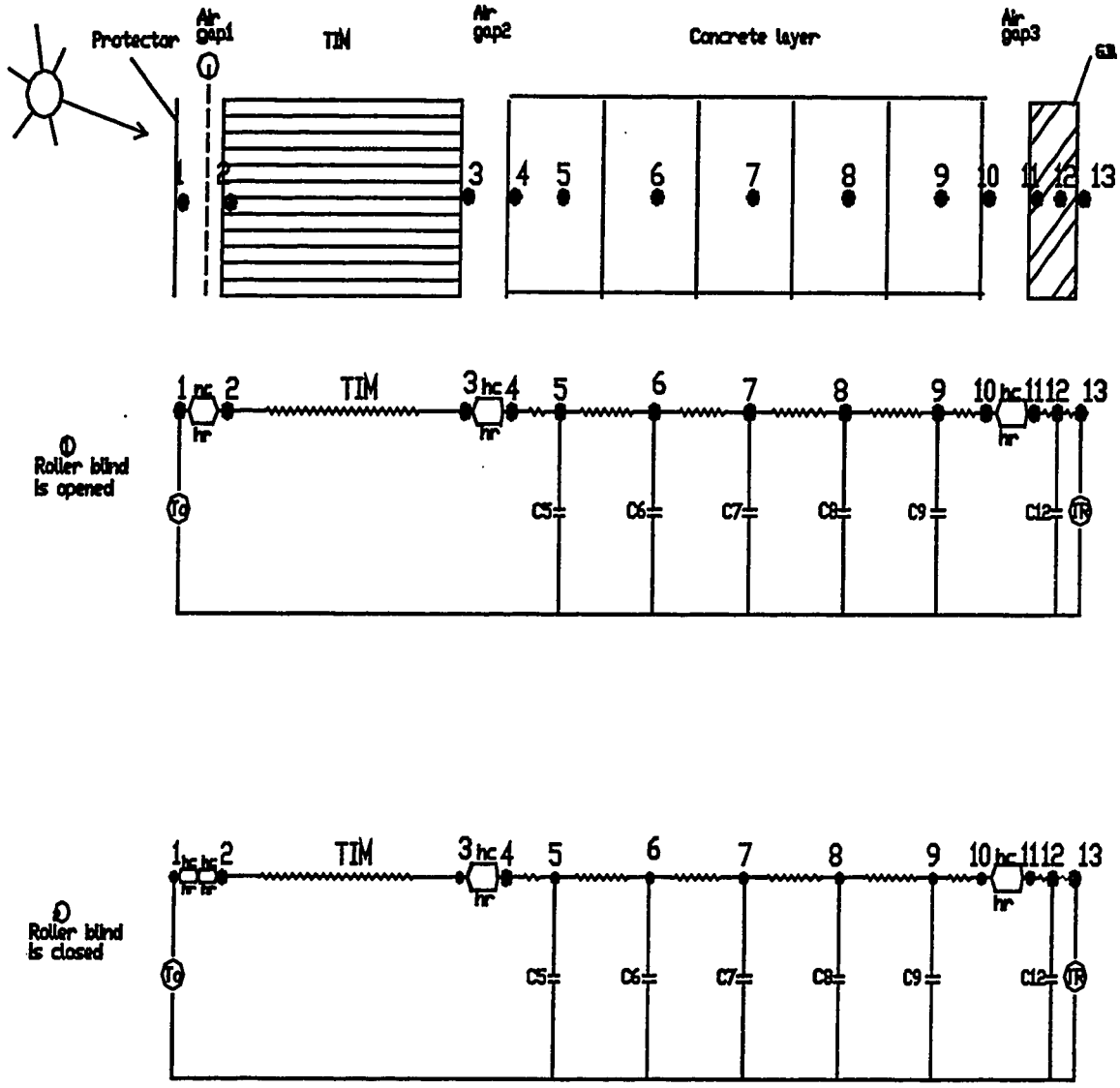

Fig.4.3. Thermal network of TI wall system

4.7. Results for TI wall model

The appendix presents an example of 7 days simulation for a transparently insulated wall model (TIW) located in Montreal. The thermal performance of the wall is studied in terms of thermal comfort and for different thicknesses and orientations. The room air temperature is assumed to be constant at 20°C. Figures 4.4.and 4.5 shows the thermal behavior of a south facing TI wall for different concrete layer thicknesses during a winter day (at 12 A.M) and night (at 8:00 P.M).

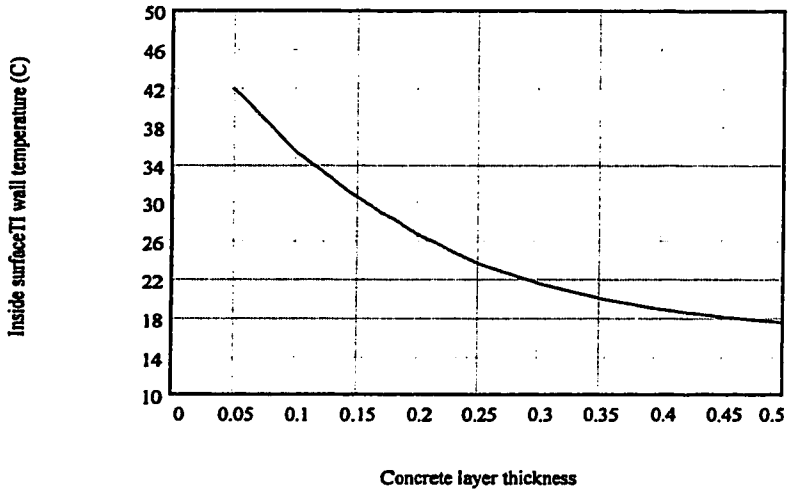

Figure 4.4. The dependence of inside wall temperature on the concrete layer thickness during a winter day (January 21st)

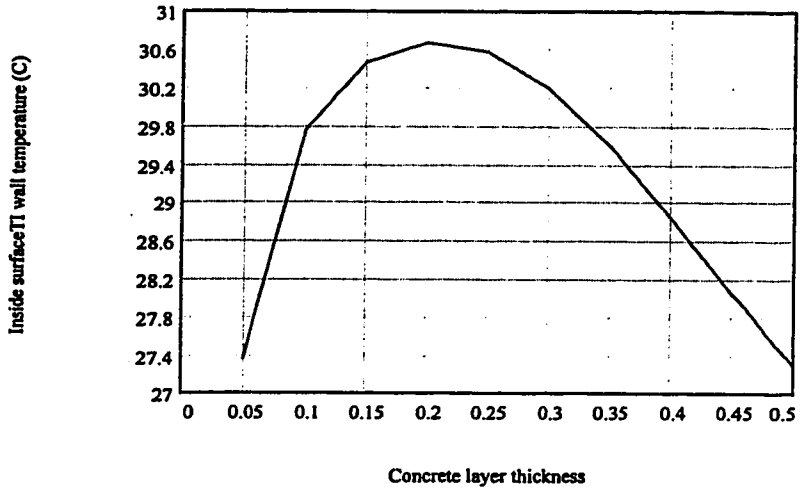

Figure 4.5. The dependence of inside wall temperature on the concrete layer thickness during a winter night (January 21st)

Regarding the orientation of TI wall, a 7 days simulation was repeated under the same conditions for a south (fig.4.6-a&b), east (fig.4.7-a&b) and west wall (fig.4.8-a&b). The best thermal performance is observed for the south wall because of its capability to collect the highest amount of solar radiation during winter and the lowest during summer.

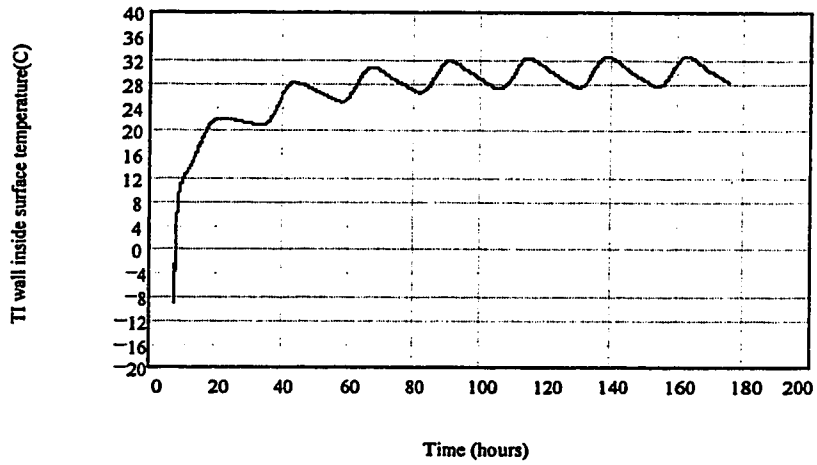

Fig.4.6-a: South facing TI wall inside surface temperature on January 21st

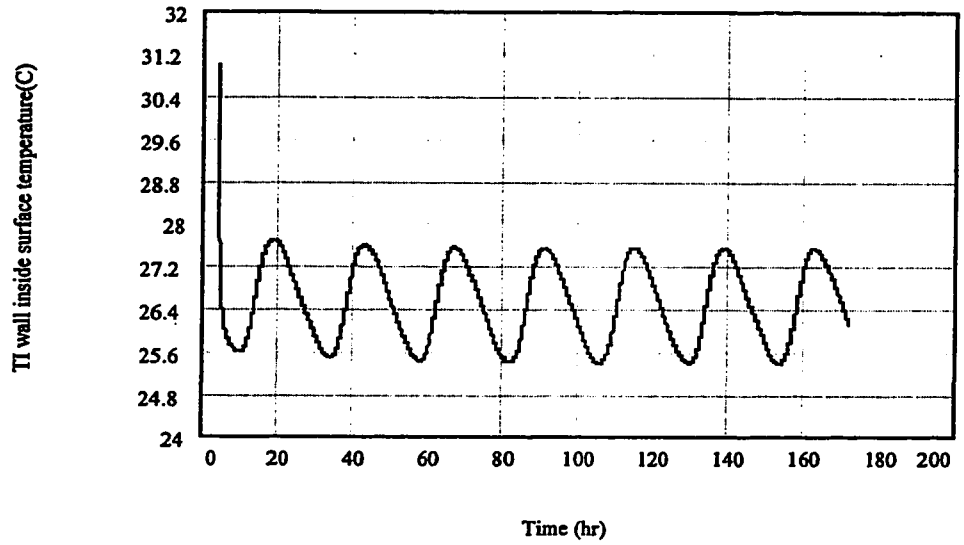

Fig.4.6-b: South facing TI wall inside surface temperature on June 21st

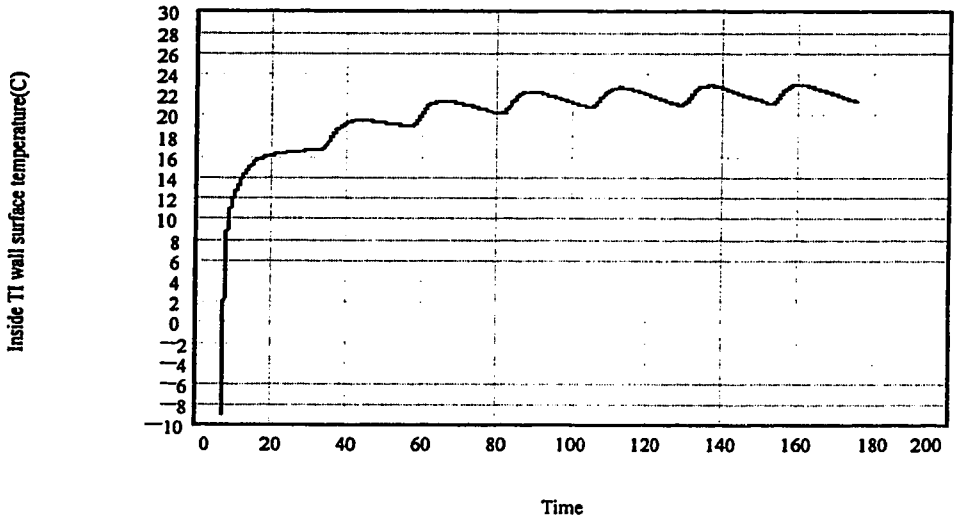

Fig.4.7-a: East facing TI wall inside surface temperature on January 21st

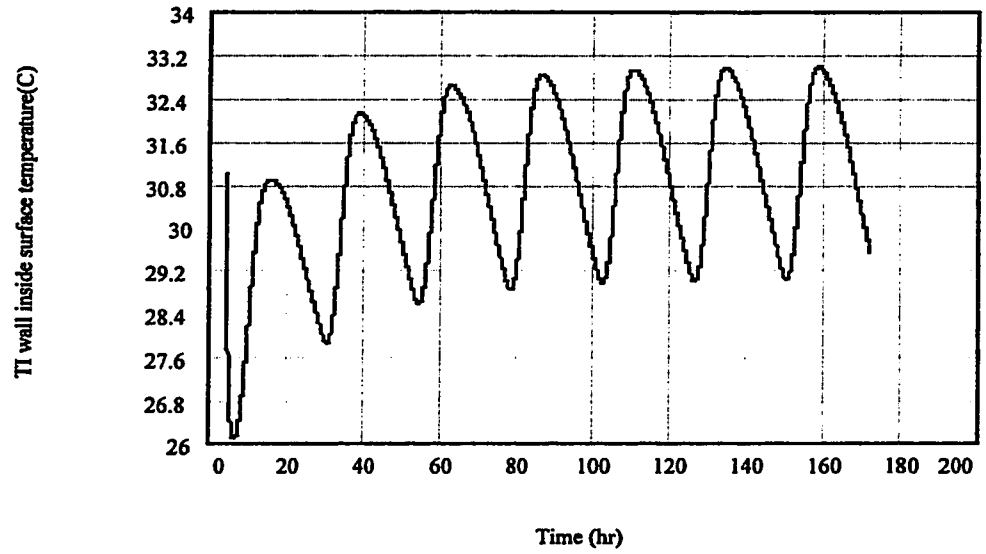

Fig.4.7-b: East facing TI wall inside surface temperature on June 21st

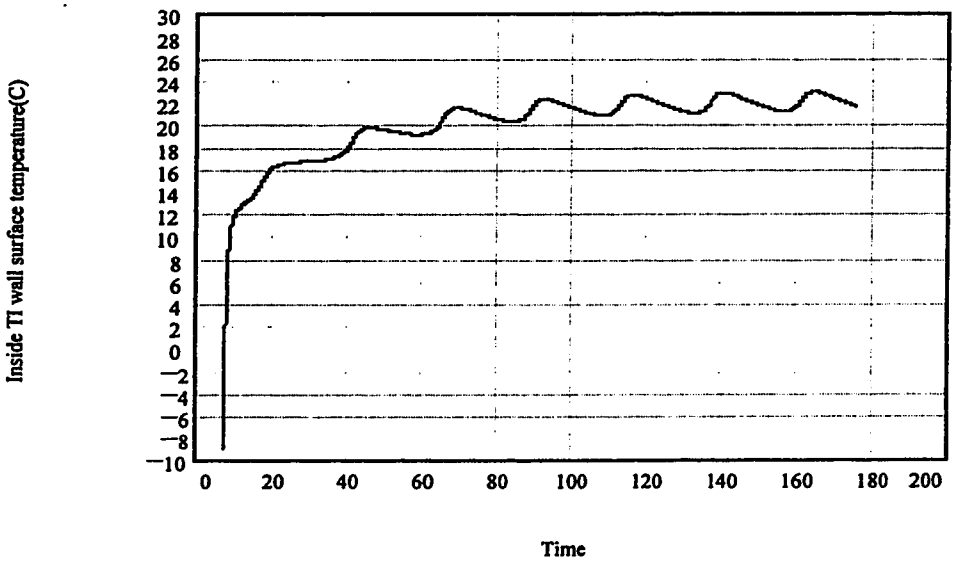

Fig.4.8-a: West facing TI wall inside surface temperature on January 21st

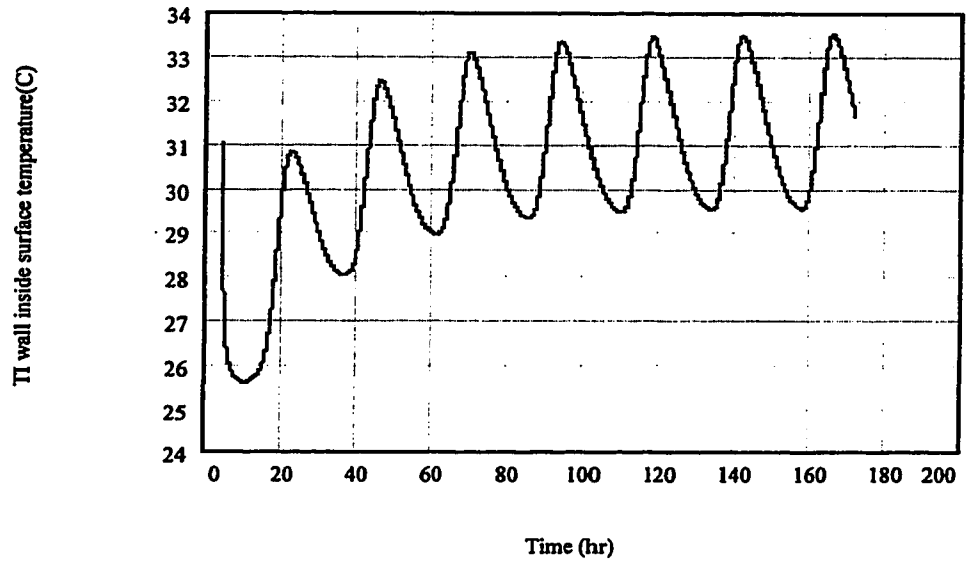

Fig.4.8-b: West facing TI wall inside surface temperature on June 21st

4.8. Sensitivity analysis and numerical validation:

The question of parameter sensitivity particularly arises where numerical models are used for the purposes of dynamical analysis. In order to be able to give a unique formulation of the mathematical problem, the mathematical model is usually assumed to be known exactly. This assumption is, strictly speaking, unrealistic since there is always a certain discrepancy between the actual and its mathematical model. Therefore, it should be part of the solution to a practical problem to know the parameter sensitivity prior to its implementation or to reduce the sensitivity systematically if turns out to be necessary. In numerical optimization techniques spatial and temporal discretization are of high importance for numerical stability and solution accuracy since we have replaced the continuous information contained in the exact solution of the differential equation with

discrete values. For this reason, the sensitivity of the mathematical solution regarding space and time are investigated.

4.8.1. Spatial discretization:

The TI wall interior surface temperature is evaluated for different numbers of control volumes. Table 4.2 shows the sensitivity of the maximum and minimum values of TI wall interior surface temperature to the number of sublayers that divide the concrete layer. The results are represented for a TI wall system consisting of a protector, a 5-cm air gap, the TI element, a second 2-cm air gap and a 25-cm concrete layer. The simulation is for April 1st, with outside temperature varying sinusoidally between 5°C and 15°C, and the interior room temperature is maintained at 20°C.

Table 4.2 Inside TI wall surface temperature (T13) change with number of control volumes

Number of layers	1	2	3	4	5	6	7	8	9	10
T13 maximum	**33.54**	**32.86**	**32.38**	**32.05**	**31.874**	**31.870**	**31.867**	**31.864**	**31.863**	**31.863**
T13 minimum	**27.56**	**27.32**	**27.01**	**26.76**	**26.385**	**26.377**	**26.374**	**26.373**	**26.373**	**26.373**

As can be seen from Table (4.2), selecting more than 5 control volumes does not affect accuracy significantly. Thus, 5 control volumes were deemed to be sufficient.

4.8.2. Temporal discretization:

After choosing to divide the thermal mass into 5 control volumes, the sensitivity of the results is investigated as a function of time step. Table (4.3) shows the changes of the interior surface temperature of TI wall with time step values. It is shown that for any time step lower than $\Delta t_{critical}$ (the maximum time step allowed to satisfy numerical stability) the results do not change significantly. Thus, in order to save computation time, the time step may be chosen just to satisfy numerical stability.

Table 4.3. Maximum and minimum inside TI wall surface temperature change with time step for 5 control volumes.

	$0.9\Delta t_{critical}$	$0.7\Delta t_{critical}$	$0.5\Delta t_{critical}$	$0.3\Delta t_{critical}$	$0.1\Delta t_{critical}$	$0.05\Delta t_{critical}$
T13 max	**31.874**	**31.8729**	**31.8712**	**31.8699**	**31.8694**	**31.8691**
T13 min	**26.385**	**26.382**	**26.380**	**26.3799**	**26.3796**	**26.3793**

4.9. Experimental validation:

Bollin (1992) reported acquired results from the monitoring of a newly built transparently insulated residential house in Freiburg, Germany. Figure (4.9) shows the thermal performance of a transparently insulated (10 cm of polycarbonate honeycomb) south east 24 cm brickwork wall (density 1800 kg/m^3) when the mean room air temperature is between 19 and 21°C. The figure represents inside TI wall temperature, the absorber temperature, indoor room air temperature, the ambient temperature and the heat flow to the internal surface of TI wall for 2 consecutive days on March. The simulated results using the developed TIW model are plotted in the same figure.

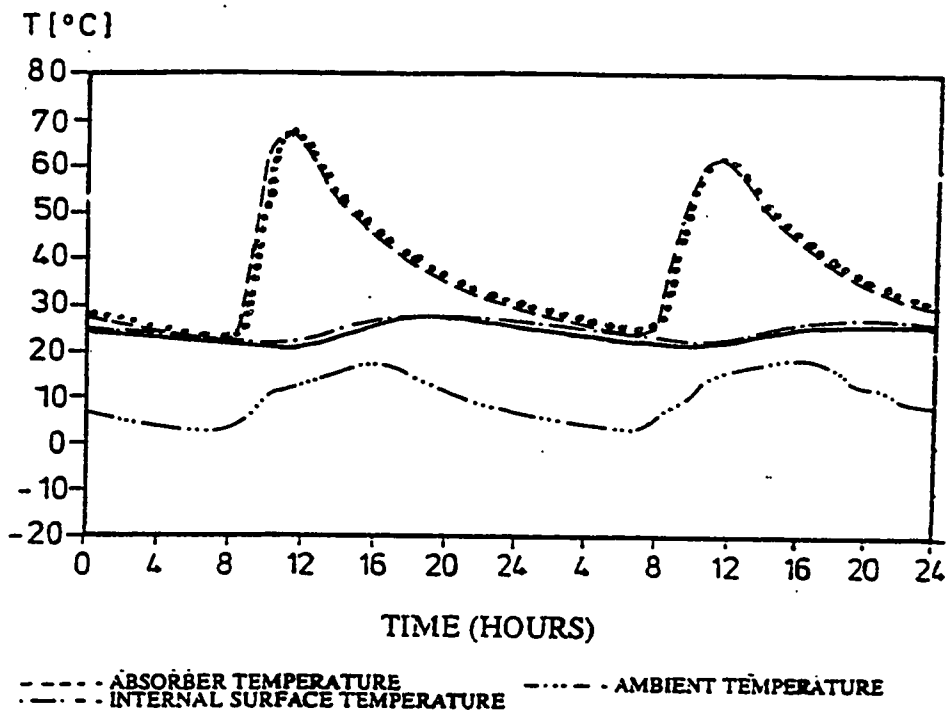

.....simulated absorber temperature

_____ simulated inside TI wall surface temperature

Fig.(4.9) Comparison between experimental measurements (Bollin 1992) and simulation results for a South East TI wall for 2 days on March

Same building details as Bollin (1992) are used and the weather conditions (outside temperature and solar radiation intensity) are simulated. It can be seen from figure (4.9) that the measured data (Bollin 1992) and the simulated results are in very good agreement regarding the maximum and minimum fluctuations of the TI inside and outside surface temperature and the overall thermal behavior of the TI wall system. The slight difference between the simulated results and the measured data is due, mainly, to the difference between the real weather data used in the experimental work and the simulated weather

conditions used in the model. The simulated results are in good agreement, as well, with Boy (1988) Chattha (1989-b) and Gilani (1991).

CHAPTER V

NUMERICAL MODEL FOR A ROOM WITH ONE TRANSPARENTLY INSULATED WALL

5.1. Introduction

An energy analysis program for buildings is used to provide insight during design phase into issues like thermal comfort and energy savings. These aspects are highly coupled and must be studied simultaneously. Modelling the TI wall alone, where the room air temperature is assumed to be constant, does not account, in fact, for the real performance of the system. For this reason, an outdoor test room with one transparently insulated wall is modelled. The purpose, here, is to evaluate the thermal behavior of the room in terms of energy consumption and thermal comfort.

This detailed model must be capable of dynamically handling the following processes:

1- The transient conduction of heat through the enclosure envelope and therefore the associated time lag and thermal storage effect.

2- The effect of shortwave solar radiation impinging on exposed external surfaces.

3- Infiltration losses.

4- The longwave radiation exchange between exposed external surfaces and the surroundings.

5- The longwave radiation exchange between internal surfaces.

6- Time varying convection between the internal surfaces and the room air.

7- Time varying convection between the building envelope and the surroundings

8- Model of a controlled heating system and calculation of the interior temperature change.

9- Linking the consequences of the roller blind operation strategy to the thermal performance of the system.

5.2. Transient conduction

The transient conduction methodology used for the TI wall described in chapter IV. The same approach will be used as well in modelling the transient conduction through the other room components (walls, ceiling, floor and window). Each component is assumed to be composed of an exterior insulation and an interior gypsum board layer except the window, which is assumed double, glazed. Thus, each component is represented by 3 nodes. One node represents the outside surface of the wall, the second node represents the thermal capacitance of the gypsum board and the third nodes is to present the inside wall surface. However, the window is represented by 2 nodes, one for the inside surface and another for the outside surface.

A heat energy balance is applied on each node. Thus, as the inside and outside surface nodes of walls, ceiling, floor and window are modelled as zero capacitance elements, a steady state equation can be applied at these nodes. That is,

$$q_i + \sum_j \frac{T_j - T_i}{R(i,j)} = 0 \qquad (5.1)$$

However, for the node with the thermal capacitance, the transient approach is employed and the explicit finite difference method is used. That is,

$$T(i,p+1) = \frac{\Delta t}{C_i} * \left(q_i + \sum_j \frac{T(j,p) - T(i,p)}{R(i,j)} \right) + T(i,p) \qquad (5.2)$$

where q_i is the auxiliary heat.

5.3. Natural convection in buildings

Natural convection heat flows depend on the surface geometry and inclination, the thermal boundary conditions and the nature of the flow (laminar or turbulent). Some equations for convection heat transfer are developed by numerical analysis, while the majority of the usable expressions have resulted from experimental data. Such correlations hold under the specific conditions of each experiment. (Dascalaki et al 1994) reported an extensive review of the relations used to estimate the convective heat transfer coefficient for building applications.

Generally, natural heat transfer in building enclosure is expressed in terms of vertical and horizontal convective flow.

5.3.1. Convection for vertical surfaces

As natural convection in buildings appears under turbulent flow conditions, ASHRAE (1993) suggests the following correlation for calculating the heat transfer coefficient from vertical walls is:

$$hc_V = 1.31 \cdot \Delta T^{\frac{1}{3}} \tag{5.3}$$

However, as reported by Bauman et al (1983), this value is overpredicted. They suggest the following equation:

$$hc_V = 2.03 \cdot \left(\frac{\Delta T}{x}\right)^{0.22} \tag{5.4}$$

where x is the surface height.

5.3.2. Convection for horizontal surfaces

Two different expressions are recommended by ASHRAE (1993) for horizontal heat transfer convection:

- $hc_u = 1.52 \cdot \Delta T^{\frac{1}{3}}$ (for upwards heat flow) (5.5)

- $hc_d = 0.59 \cdot \left(\frac{\Delta T}{x}\right)^{\frac{1}{4}}$ (for downwards heat flow) (5.6)

5.4. Exterior film coefficient

Heat losses from the building envelope to the ambient is a combination of wind and radiation heat transfer (Duffie and Beckman, 1991). That is,

$$h_{out} = h_{wind} + hr_a \tag{5.7}$$

where h_{out} is the combined exterior film coefficient, h_{wind} is wind heat transfer coefficient which evaluated as:

$$h_{wind} = 8.6 \cdot \left(\frac{V_w^{0.6}}{L_{cha}^{0.4}}\right) \tag{5.8}$$

where V_w is the wind velocity and L_{cha} is the characteristic length. Note that h_{wind} is assumed to have a minimum value of $5 \cdot \frac{watt}{m^2 \cdot degC}$ (Duffie and Beckman, 1991).

The radiative heat transfer coefficient is evaluated as (Holman, 1986):

$$hr_a = \frac{\sigma \cdot \varepsilon \cdot (Ts^4 - Ta^4)}{Ts - Ta} \tag{5.9}$$

where ε is the emissivity of the surface.

5.5. Radiation between interior surfaces

The radiant exchange between the interior surfaces (assumed to be grey) may be expressed as (Holman, 1986):

$$q_{i,j} = A_i \cdot F_{i,j} \cdot \sigma \left[(T_i)^4 - (T_j)^4 \right] \qquad (5.10)$$

where $F_{i,j}$ is the radiation exchange factor. This factor includes the space and surface resistance of thermal radiation flow and it is calculated by using BEEP software developed by Athienitis (1985).

5.6 Infiltration

It is the mechanism of air penetration in the building exterior envelope. Many complex methods can model the air infiltration in buildings such as regression models. However, losses due to infiltration may be calculated by using simple methods as air-change method (ASHRAE, 1993). Thus, the natural infiltration of air to the room is based on an estimated number of air changes per hour. That is:

$$U_{inf} = ACS \cdot V_r \cdot \rho \cdot c_p \qquad (5.11)$$

where U_{inf} is the infiltration conductance, ACS is the air change per second which is evaluated experimentally (Table 5.1), V_r is the volume of the room, ρ and c_p are the density and the specific heat of air, respectively.

5.7. Auxiliary heating model

A convective heat source is assumed to be installed in the room. Thus, the set-point temperature (reference temperature) is connected to the room air temperature.

Table 5.1. Air change per hour for different room types (adapted from ASHRAE 1993)

TYPE OF ROOM	AIR CHANGE PER HOUR
No windows or exterior doors	0.5
Windows or exterior doors in one side	1.0
Windows or exterior doors in two sides	1.5
Windows or exterior doors on three sides	2.0
Entrance halls	2.0

As the heating system is assumed to be proportionally controlled, the auxiliary heat flux may be expressed as:

$$q_{aux} = K_p \cdot (Tsp - Tair) \qquad (5.12)$$

where K_p is the proportionality constant assumed 1000 watt/°C and the maximum capacity of the heating system is 2000 watt, Tsp is the reference temperature and Tair is the room air temperature.

5.8. Description of the room model:

The one zone model is represented graphically (Fig.5.1-a). The outdoor test room is assumed to have a square or rectangular shape. Walls, ceiling and floor consist of an outside insulation and an indoor gypsum board layer.

Figure (5.1-b) represents the thermal network of the test room. The TI wall system has the same characteristics of that discussed in chapter IV and is modelled in the same manner. However, in the present model, heat losses through the room are modelled accurately and the room air temperature is time variant and controlled with a heating system. The resistances between the nodes represent the conductive, convective and radiative heat transfer. Walls are connected to each other by surface nodes through a thermal radiative resistance and to the zone air node by a convective resistance. Both types of resistance are calculated for each time step.

The program models accurately the solar radiation on each face of the building. However, it does not model the actual distribution of the incoming solar radiation through the window to the interior surface of the zone. Instead, this distribution is approximated to be as 70% for the floor and 30% for the other components of the room (Buchberg, 1969). The window is represented by one node supposed to be double-glazed.

The explicit finite difference method is used to calculate the transient temperature variation of each node. However a steady state heat balance equation is employed to calculate the temperature at the interior and exterior surface of the thermal mass and at all other opaque building interior and exterior surfaces. The heat balance equation is applied at each node and solved repeatedly at each time step for the period of simulation. For

instance, the heat balance equation applied on the room air temperature (node 14) is defined as:

$$T14_{i+1} = \frac{\Delta t}{C_{air}} \cdot \left(\frac{T13_i - T14_i}{R1314_i} + \frac{T15_i - T14_i}{R1514_i} + \frac{T17_i - T14_i}{R1714_i} + \frac{T19_i - T14_i}{R1914_i} + \frac{T21_i - T14_i}{R2114_i} + \frac{T23_i - T14_i}{R2314_i} \right) + \ldots$$
$$\ldots \frac{\Delta t}{C_{air}} \cdot \left(\frac{T25_i - T14_i}{R2514_i} + \frac{To_i - T14_i}{R_{inf}} + q_{aux_i} \right) + T14_i \qquad (5.13)$$

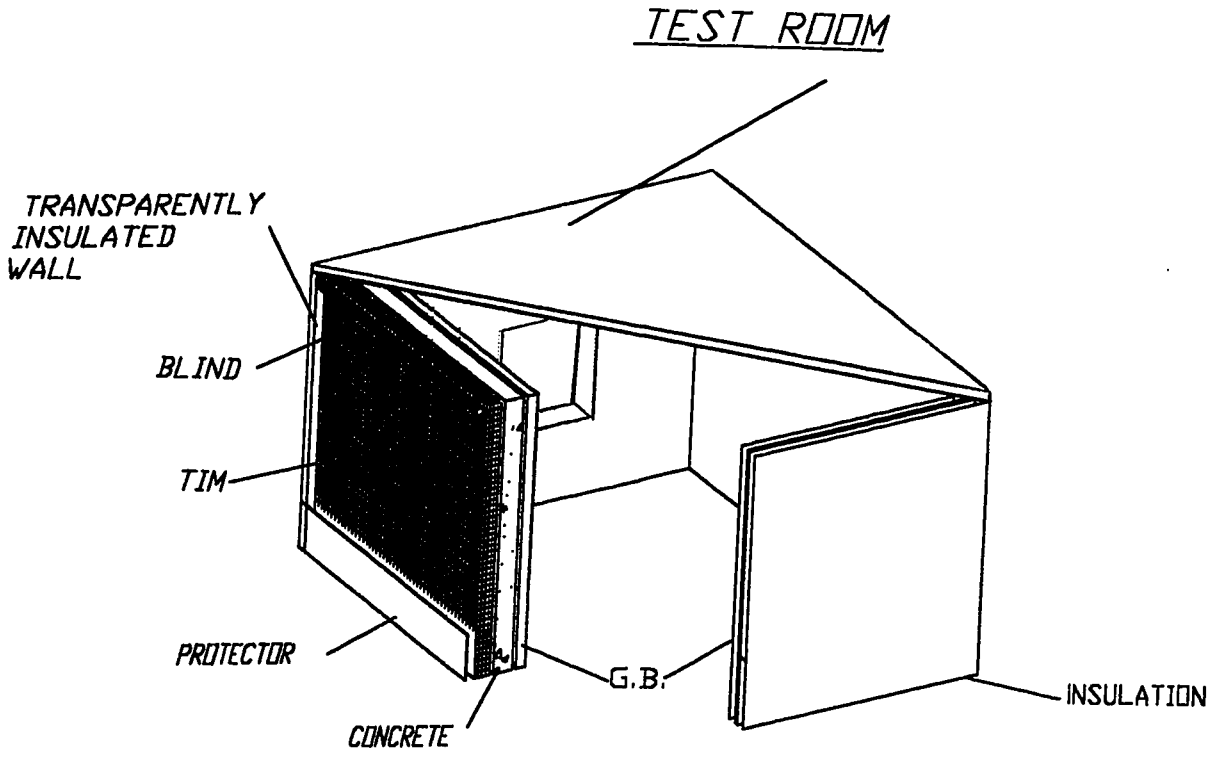

Fig.5.1-a Room model structure

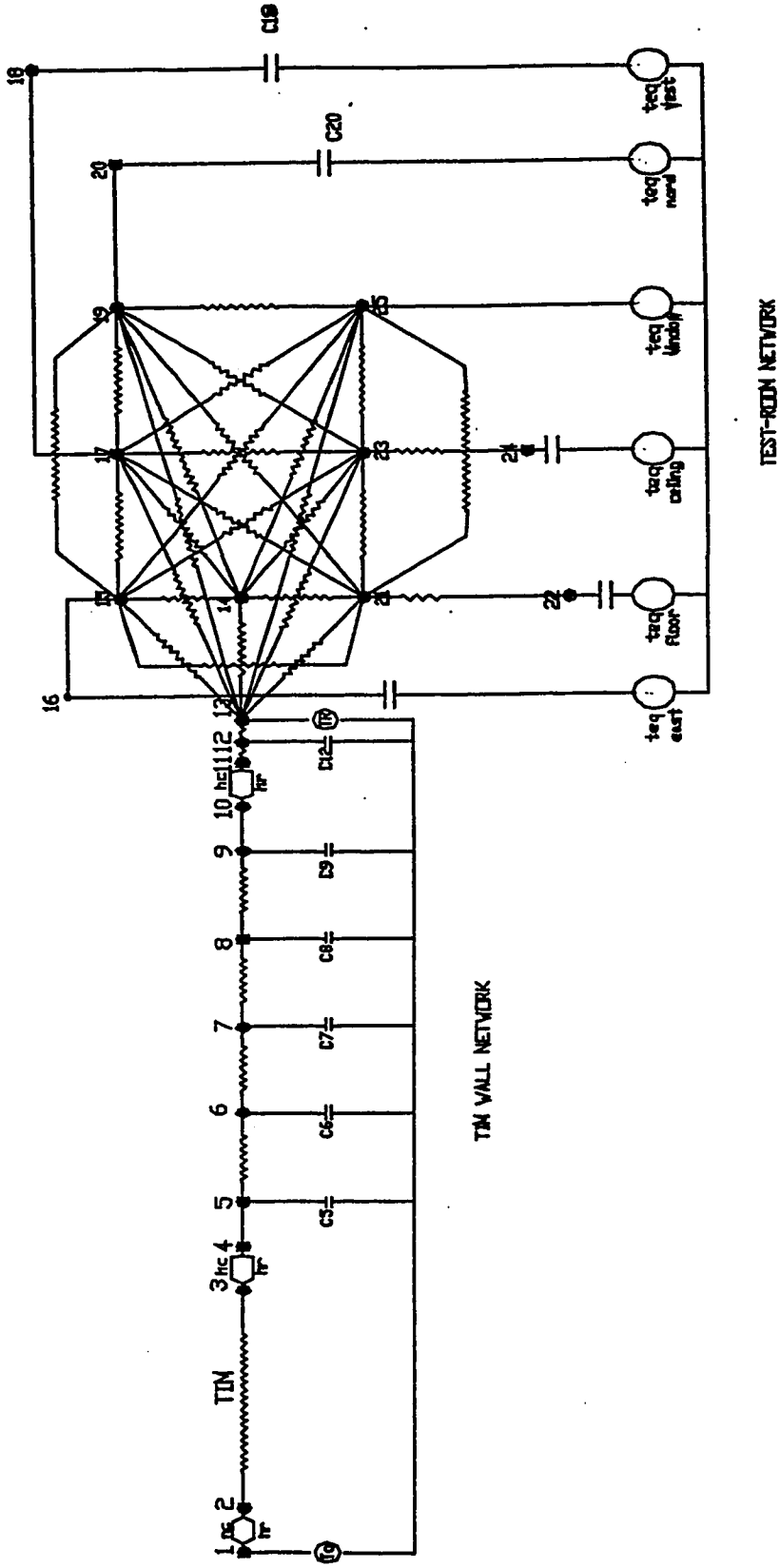

Fig. 5.1-b. Thermal network of a room with one transparently insulated wall

As in modelling the TI wall, the simulation may starts after setting the initial conditions and the building details. Each temperature is then updated at each time step together with the different heat transfer coefficient, taking into account the instantaneous changes of solar radiation and ambient temperature which are simulated or may be red from a weather data file. The results can be obtained from the program for any period of simulation, and the auxiliary heat needed can be integrated for any time period. The simulation methodology is shown in fig. (5.2).

5.9. Opaque room model

A similar test room to that of TI room is modelled with an opaque south facing insulation having the same resistance value of the TI wall. The purpose is to compare the thermal performance of the TI room versus the opaque room in terms of energy consumption and thermal comfort.

5.10. TI room versus Opaque room

Figure (5.3) and (5.4) show the passive thermal response of TI and opaque room respectively. The figures show the benefits of the solar radiation contribution in the transparent insulation case. With the use of the heating system, figures (5.5) and (5.6) presents the savings in the heating energy bill that may provide the TI technology in comparison with opaque insulation systems (Ramadan and Athienitis, 1998-a). However, the performance of the TI wall may be improved more by applying a roller blind between the cover and the TI unit.

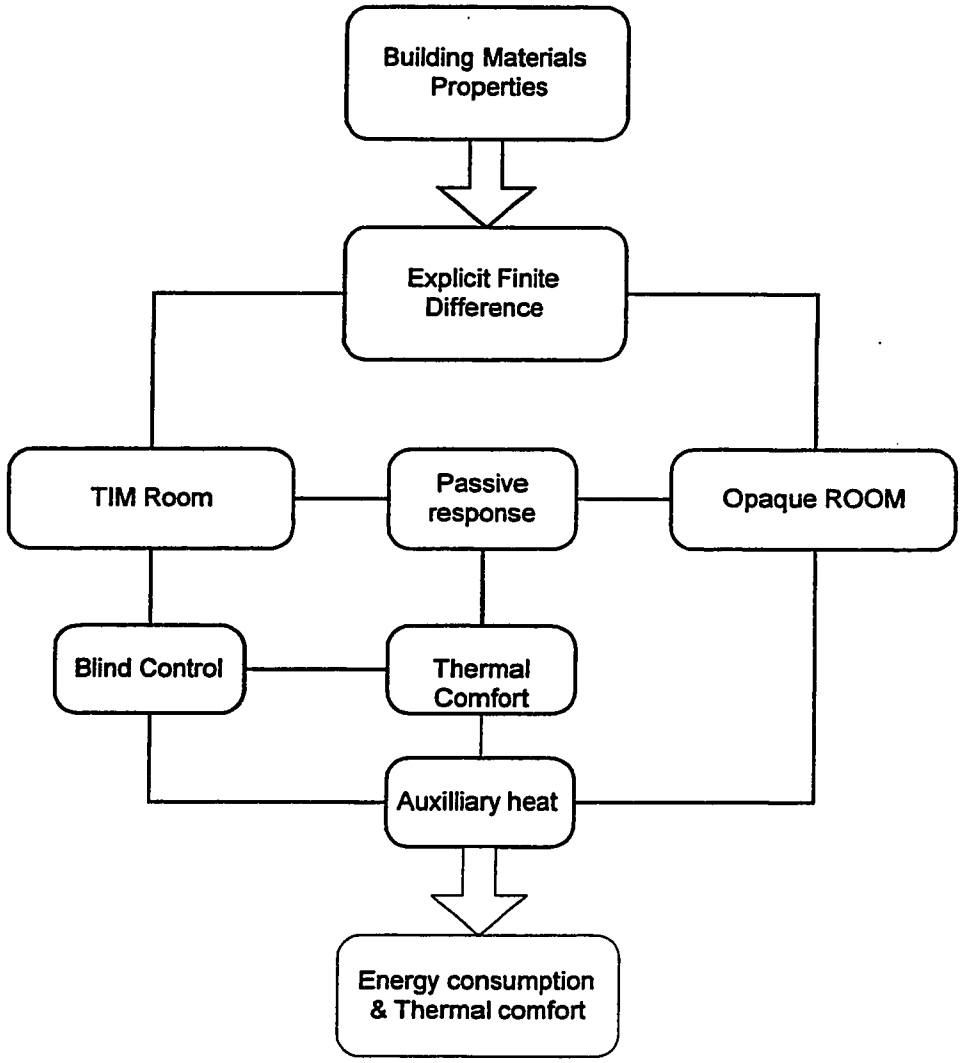

fig.5.2. Simulation methodology

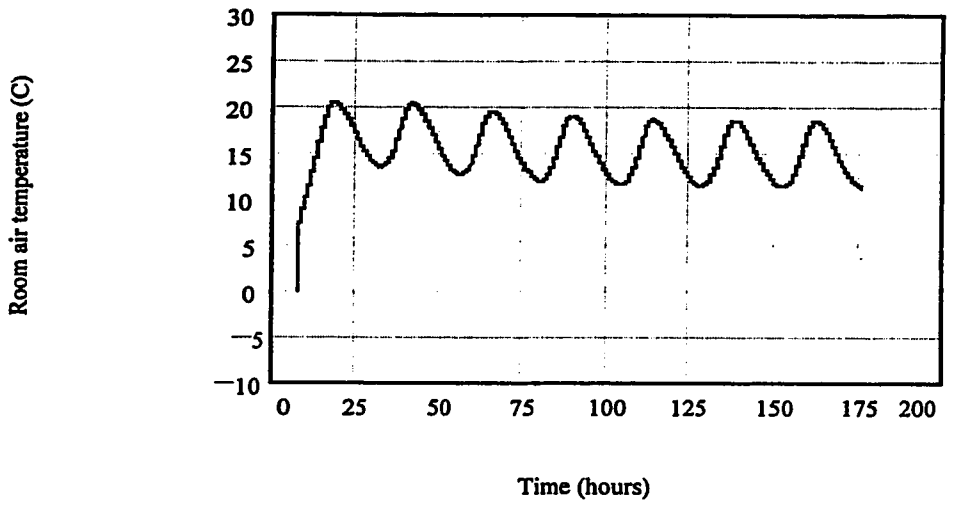

Figure 5.3. Passive response of TI room starting January 21st.

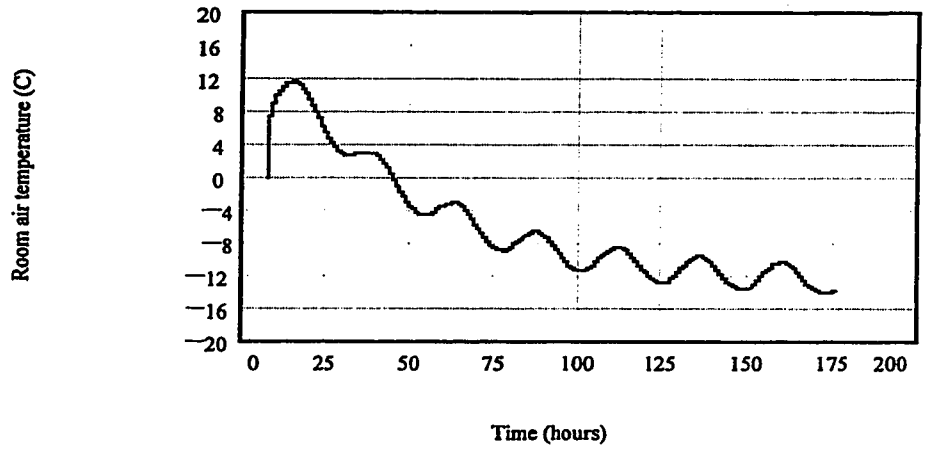

Figure 5.4. Passive response of opaque room starting January 21st.

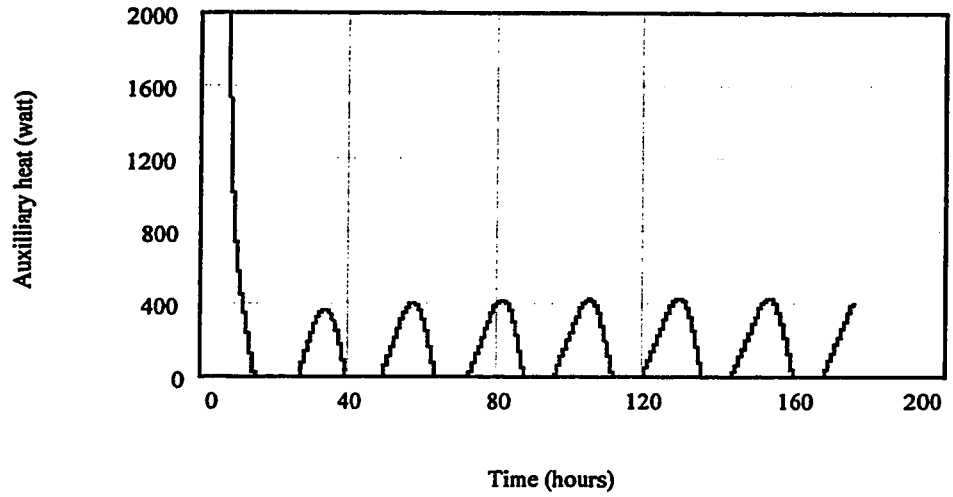

Figure 5.5. Auxiliary heat needed for TI room starting the 21st of January

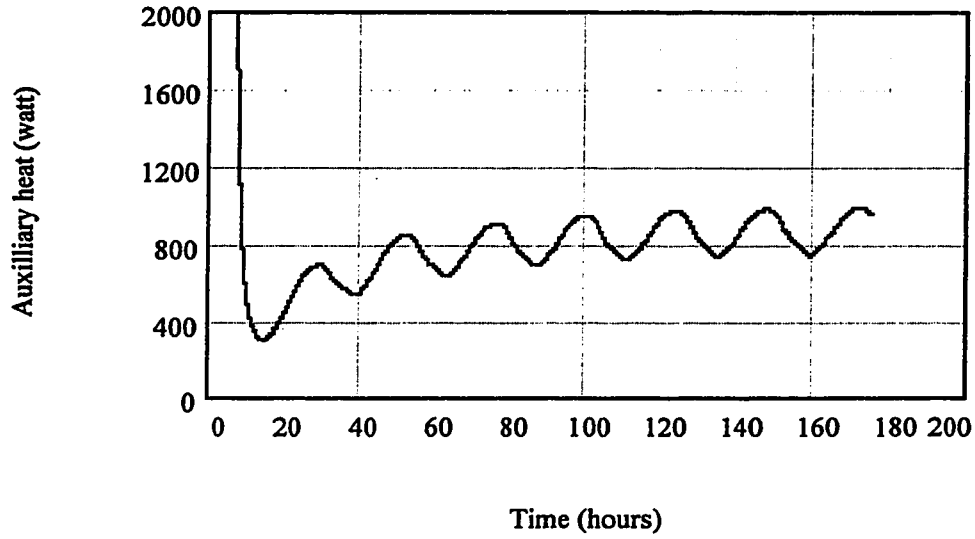

Figure 5.6. Auxiliary heat needed for opaque room starting the 21st of January.

5.11. Operating the roller blind

Using an appropriate control strategy to operate the roller blind may enhance significantly the thermal performance of the TI room. Different control strategies may be applied. In winter season, the blind is opened during days to allow the transmission of solar radiation to the thermal mass and closed during night to reduce heat losses from the heating space. However, in summer, the opposite strategy may be applied. Thus, the blind is closed during summer days to prevent the room from being overheated and open during summer nights to reduce the cooling load. Moreover, covering the TI wall during cloudy winter days will contribute as well in the reduction of heating load. Thus, another control strategy may be applied

5.11.1. Control Strategy -1-

For heating, if $S>100$ watt/m^2 and $T_{ambient}<15°C \Rightarrow$ expose the wall, otherwise cover.

For cooling, if $S<100$ watt/m^2 and $T_{ambient}>15°C \Rightarrow$ expose the wall, otherwise cover.

where S is the total incident radiation and Tambient is the ambient temperature.

5.11.2. Control Strategy -2-

Using the previous control strategy will not prevent overheating during spring and autumn. For this reason, the exterior temperature of the concrete layer should be included as suggested by Twidell et al (1994). That is,

For heating, if $S>100$ watt/m^2 and ($T_{ambient}<15°C$ and $T_{wall}<60°C$) $\Rightarrow$ expose the wall, otherwise cover.

For cooling, if S<100 watt/m^2 and (Tambient>15°C and Twall>60°C) ⇒ expose the wall, otherwise cover.

Nevertheless, using this control strategy has 2 drawbacks (Ramadan, Athienitis, 1998-b):

1- The TI wall will be covered during winter days when the outside concrete layer surface exceeds 60°C. However, during cold winter days this induces a significant decrease in the room air temperature. Consequently, the thermal comfort conditions will not be satisfied and an increase in energy consumption will be recorded. Figure (5.7) shows the energy consumption for the 21st of January using the above control strategy. In comparison with fig. (5.5) where strategy-1- is used, using the second control strategy the energy consumption will increase drastically.

2- Including the outside surface temperature of the concrete layer (Twall) in the strategy during summer is insignificant since the blind is needed to be open during summer nights (Tambient>15°C) regardless the value of Twall.

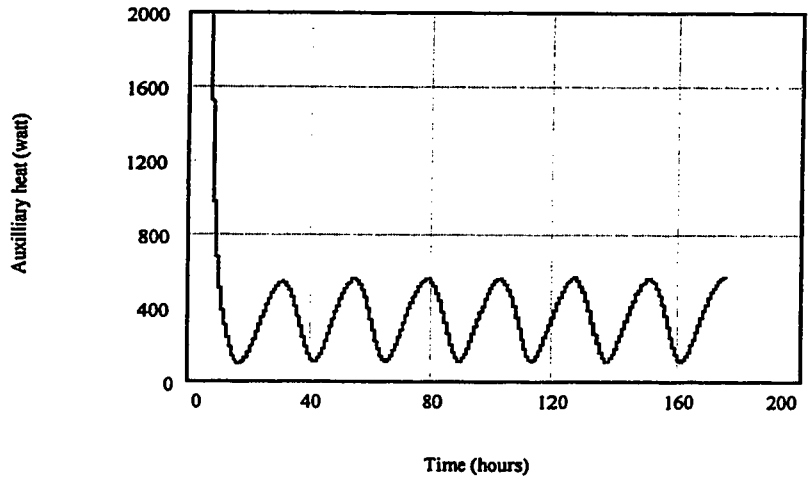

Fig 5.7. Auxiliary heat needed using strategy-2-strarting the 21st of January

5.11.1. Control Strategy -3-

In respect to the previous observations, we suggest another control strategy that categorizes the outside temperature into 3 sets. That is,

1- Tambient >15°C.

2- 5°C ≤ Tambient ≤15°C.

3- Tambient <5°C.

So that, our strategy may be expressed as:

For cooling, if S<100 watt/m^2 and Tambient>15°C ⇒ expose the wall, otherwise cover.

For heating,

if S>100 watt/m^2 and 5°C ≤ Tambient ≤15°C and Twall<50°C,

or if S>100 watt/m^2 and Tambient <5°C⇒ expose the wall, otherwise cover.

This strategy will improve the thermal performance of the transparently insulated room in terms of thermal comfort and energy consumption as it will be shown later.

5.12. Comparative roller effect

Figure (5.8) shows the passive response of the TI room using the control strategy-3-. Comparing with figure (5.3) where strategy-1- is used, an augmentation of more than of 2°C is realised in the room temperature when this strategy is applied in winter. Moreover, in April where the mean ambient temperature is 10°C (Fig.5.9), the room seems to overheat using control strategy-1-. Figure (5.10) shows a decrease of about 5°C in the room interior temperature due to the use of strategy-3-.

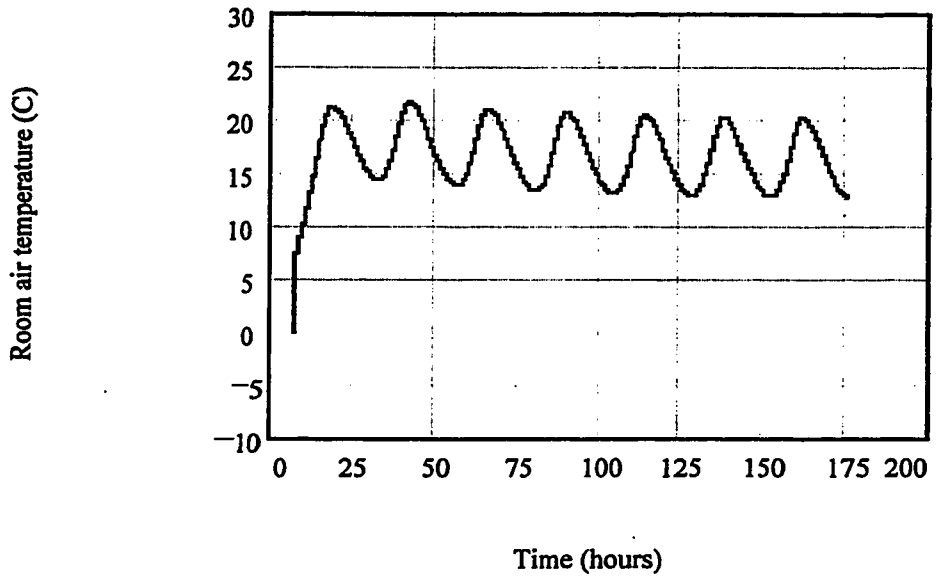

Fig.(5.8) Passive response of TI room using control strategy-3-starting January 21st

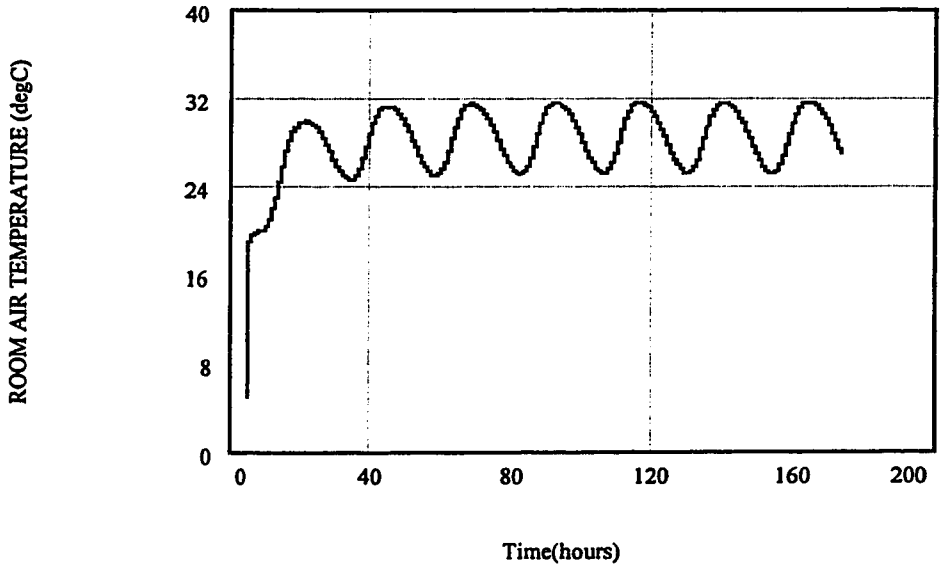

Fig.5.9. The passive response of TI room using strategy-1-starting April 1st

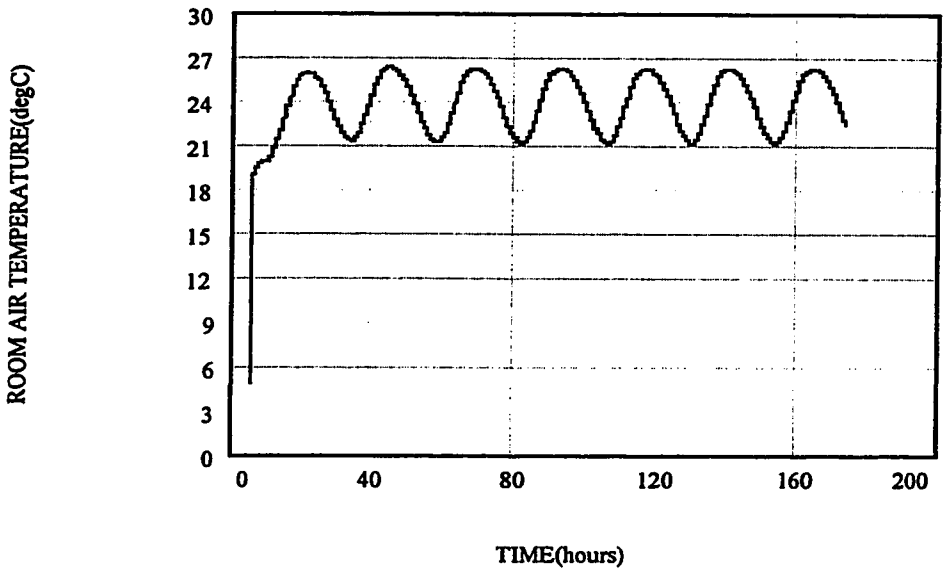

Fig.5.10. The passive response of TI room using strategy-3-starting April 1st

5.13. Thermal comfort

Comfort may be defined as the sensation of complete physical and mental well being. Thus defined, it is only to a limited extent within the control of the designer. The occupants' cultural, biological, emotional and physical characteristics also come into play. Hence, if a group of people is subjected to the same climate, the individual members are unlikely to be satisfied simultaneously. So that, the designer must aim to create optimal thermal comfort for the group as a whole.

The operative temperature is common a parameter to verify thermal comfort level. It is calculated as:

$$T_{op} = \frac{Tmr + Tair}{2} \qquad (5.13)$$

where Tmr is the mean radiant temperature Tair is the room air temperature.

Some laboratory-based studies (Knudsen et al, 1989) recommend an optimal operative temperature in winter for a person undergoes a sedentary activities (1.2 met) and has a clothing level of 1 clo (typical indoor winter ensemble) as 22°C±2°C. During summer warm condition with light clothing (0.5 clo) they recommend an operative temperature equal to 24.5°C±1.5°C. However, in a field based research, Griffiths (1990) shows that generally, the temperatures required for thermal comfort are significantly lower in all building types than those predicted from models established through laboratory-based researches. He gave, for instance, the following operative temperature for optimal conditions:

21°C for office workers in Germany and France; 19°C for schoolteachers in France; 19°C for hospital occupants in the UK; and still lower temperatures for houses in the UK and France.

The operative temperature of the TI room model is calculated to verify thermal comfort level. Figure (5.11) shows the operative temperature due to the passive response of the room for 7 days simulation starting January 21st where the mean outside temperature is assumed to be -15°C. It can be observed that the operative temperature of the TI room is near the comfort region with no heating on a clear sunny winter day.

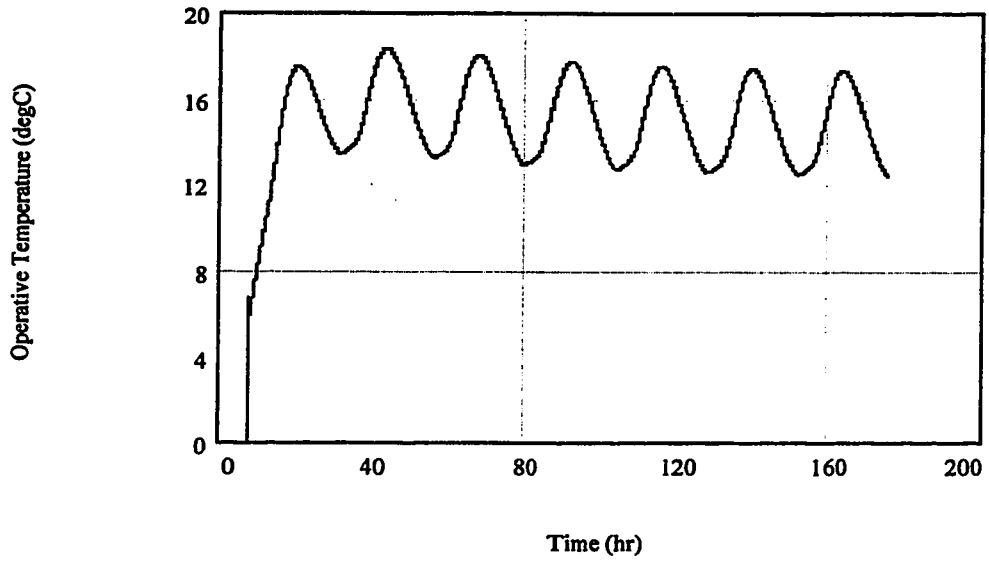

Fig. 5.11. Operative temperature for TI room starting January 21st.

CHAPTER VI

CONCLUSION

This thesis presented an explicit finite difference model for a room with one transparently insulated wall. The thermal performance of the room was investigated in terms of thermal comfort and energy consumption with and without transparent insulation (but the same thermal resistance). The passive response of the room with transparent insulation shows that the indoor temperature is near the comfort region with no heating on a clear winter sunny day. The energy consumption of the room with TIM is reduced significantly as compared to that of the standard room. Another improvement in the thermal performance of the room is observed with the use of a controlled roller blind. In addition to the significant savings that provide the TIM, using a blind with an appropriate control strategy may reduce more the energy bill and enhance the indoor thermal comfort. Following this work, other conclusions may be drawn as follow:

1- Honeycomb transparent insulation provides high solar gains with good thermal insulation features. It has the ability to suppress convective heat transfer, reduce radiative losses and maintain high solar transmissivity.

2- Operating the roller blind with an appropriate control strategy will increase gains and conserve energy in cold periods and decrease overheating during hot periods. The strategy should detect the changes in outside temperature, solar radiation intensity and the absorber temperature before moving the roller upward or downward.

3- Mathcad software was used as a programming tool. This program proves to be simple to manipulate and able to handle complicated mathematical modelling. It is interactive features made the model easy to be modified and ready to be used for pedagogical purposes. However, with complex programs, computing process is relatively slow.

4- The developed model should be complemented by an experimental study to validate the model on one hand, and to study the practical features of this technology under Canadian weather conditions on the other hand.

5- This work may be extended to handle the followings:

- The non-linear thermal behavior of the transparent materials.
- The ability to deal with different types of transparent materials.
- Modelling the room with more than one transparently insulated wall.
- Modelling a multi-zone building with transparent insulation system.

REFERENCES

1. Angstrom A.K., "Solar and Terrestrial radiation", *Quart. J. Roy. Meterol. Soc.* Vol.50, pp.121-125.
2. Arulanantham M. and Kauskika N.D, "Global Radiation Transmittance of Transparent Insulation Material", *Solar Energy*, Vol.53, No.4,pp. 323-328, (1994).
3. ASHRAE *Handbook. Fundamentals*, Atlanta, (1993).
4. Athienitis A.K., *Application of Network Methods to Thermal Analysis of Passive Solar Buildings in the Frequency Domain*, Ph.D Thesis, University of Waterloo, Canada, (1985-a).
5. Athienitis A.K., Chandrashekar M. and Sullivan H.F., "Modelling and Analysis of Thermal Networks Through Subnetworks for Multizone Passive Solar Buildings", *Journal of Applied Mathematical Modelling*, Vol.9, No.2, pp.109-116, (1985-b).
6. Athienitis, A.K., "Numerical Model of Floor Heating System". ASHRAE Transactions, Vol. 100, No.1, pp. 1024-1030.
7. Athienitis,A.K., *Building Thermal Analysis*, An Electronic Mathcad Book, (1994).
8. Balcomb, J.D., "Passive Solar Heating for Buildings", *Proceedings for The Passive Collection of Solar Energy in Buildings*, UK-ISES, London, pp.75-85, (1979).
9. BINE Projekt Info-Service, Leaflet No.3, BINE, Mechenstrasse 57, 5300 Bonn 1, F.R.G., (1990)
10. Bollin E., "One Year Experience With a Solar House with transparent Insulation", *Proceedings of the Second European Conference on Architecture*, Paris, pp.618-620, (1989).

11. Bollin E., "Monitoring and evaluation of a residential house with transparently insulated walls", *Proceedings of the fifth International Meeting on Transparent Insulation Technology*, Freiburg, Germany, pp.49-52, 1992.

12. Boy.E, "Comparison of Measurements on Transparent Thermal Insulation Systems With Numerical Simulation of Building Envelopes", Proceedings of the 2nd International Workshop on Transparent Insulation, Freiburg, F.R.G., pp.46-49, (1988).

13. Brandemuehl M.J and Beckman W.A, "Transmission of Diffuse Radiation Through CPC and Flat Plate Collectors Glazing", *Solar Energy* Vol.24, pp. 511-513, (1980).

14. Braun P.O., Goetzberger A., Schmid J. and Stahl W., " Transparent Insulation of Building Facades- Steps From Research to Commercial Applications", Solar Energy, Vol. 49, No. 5, pp.413-427, (1992).

15. Buchberg H., "Sensitivity of Room Thermal Response of Buildings to Perturbations in the Climate", *Building Science*, Vol.4, pp.43-61, (1969)

16. Buchberg H., Lalude O.A. and Edwards D.K.," Design Considerations for Solar Collectors with Cylindrical Glass Honeycombs", Solar Energy, Vol.18, pp.193-203, (1976).

17. Cane R.L.D., Hollands K.G.T., Raithy G.D and Unny T.E., "Free Convection Heat Transfer across Inclined Honeycombs Panels", *ASME Transactions*, pp.86-91, Feb. (1977)

18. Carslaw H.S. and Jaeger S.G., *Conduction of Heat in Solids*, Second Edition, Oxford University Press, Oxford, (1959).

19. Charters W.W.S. and Peterson L.F., "Free Convection Suppressing Using Honeycomb Cellular Materials", Solar Energy, Vol.13, pp.353-361, (1972)

20. Chattha J.A., Jesch L.F., " Solar Transmission Potential of Transparent of Transparent Honeycomb Insulation", *Proceeding of the ISES World Congress*, Japan, (1989-a)

21. Chattha J.A., "Heat Flow Through a Transparently Insulated Brick Wall: Evaluation of Monitored Results", Proceedings of the 3rd International Workshop on Transparent Insulation, Freiburg, F.R.G., pp.82-85, (1989-b).

22. Churchill R.V., *Operational Mathematics*, McGraw-Hill, New York, (1958).

23. Croft D.R and Lilley D.G., Heat Transfer Calculations Using Finite Difference Equations, Applied Science Ltd., (1977).

24. Dascalaki E., Santamouris M., Balaras C.A. and Asimakopoulos D.N., "Natural Convection Heat Transfer Coefficients from Vertical and Horizontal Surfaces for Buildings Applications", *Energy and Buildings*, Vol.20, pp.243-249, (1994).

25. Davis B., *Integral Transforms and Their Applications*, Springer-Verlag, New York, (1978).

26. Duffie J.A., Beckman W.A., *Solar Engineering of Thermal Process*, A Wiley-Interscience Publication, (1991).

27. Dusinberre G.M., *Heat Transfer Calculations by Finite Differences*, International Textbook Comp., (1961)

28. Edwards D.K.,"Suppression of Cellular Convection by Lateral Walls", *J.Heat Transfer*, Vol.91, pp.145-158, (1969).

29. Edwards D.J., Arnold J.R. and Catton I.," End Clearance Effects on Rectangular-Honeycomb Solar Collectors", Solar Energy, Vol.18, pp.253-257, (1976).

30. Elsherbiny S.M, Raithby G.D, Hollands K.G.T, "Heat Transfer by Natural Convection Across Vertical and Inclined Air Layers", *Transactions of the ASME*, Vol. 104, pp. 96-102, (Feb, 1982)

31. Fellands J.R., and Edwards D.K., "Solar and Infrared Radiation Properties of Parallel Plate Glass Honeycomb", *J.Energy*, Vol.2, No.5, pp.253-257,(1978).

32. Fowler C.M., "Analysis of Numerical Solutions of Transient Heat Flow Problems", *Quart. Appl. Math.*, Vol.3, pp.361, (1945).

33. Francia G., "Un Nouveau Collecteur de l'Energie Rayonnante Solaire, Théorie et Vérifications Expérimentales", *Conférence des Nation Unies sur les Sources Nouvelles d'Energie*, E/conf.35/S/71,pp. 554-558, (1961).

34. Gilani S.I., "Comparison of a Transparently Insulated Building with a Conventional One- Experimental Results", *Proceedings of the fourth International Meeting on Transparent Insulation Technology*, Birmingham, UK, pp.103-106, 1991.

35. Goetzbeger A., Schmid J., Wittwer V., "Transparent Insulation System for Passive Solar Energy Utilization in Buildings", *Int. J. Solar Energy*, Vol.2, pp. 289-308, (1984).

36. Griffiths J., "Thermal Comfort in Buildings with Passive Solar Features-Field Study", *Final Report to CEC*, University of Surrey, (1990).

37. Guthrie K.I. and Charters W.W.S., "An Evaluation of a Transverse Slatted Flat Plate Collectors", *Solar Energy*, Vol.28 No.2, pp.89-97, (1982).

38. Haghighat F. and Liang H., "Determination of Transient Heat Conduction Through Building Envelopes-A Review, *ASHRAE Transaction*, Vol. 98 part I, pp.284-290, (1992).

39. Hartwig H., Wellinger K. and Schneiter P., "Simulation of building with Transparent Insulated Walls (HELIOS)", *Proceedings of the fourth International Workshop on Transparent Insulation Technology*, Birmingham, (1991).

40. Hollands K.G.T., "Honeycomb Devices in Flat-Plate Collectors", *Solar Energy*, Vol. 9, pp. 159, (1965).

41. Hollands K.G.T, Raithby G.D and Unny T.E, "Studies on Methods of Reducing Heat Losses from Flat Plate Solar Collectors", *Phase I Report*, Prepared for the United States Energy Research and Development Administration Division of Solar Energy under the Contract No. E(11-1)-2597, University of Waterloo, (1976).

42. Hollands K.G.T, Marshall K.N and Wedel R.K, "An Approximate Equation for Predicting the Solar Transmittance of Transparent Honeycomb", *Solar Energy* 21,pp. 231-236, (1978-a).

43. Hollands K.G.T., "Free Convection in Solar Collectors", *Solar Energy Conversion*, An Introductory Course, Selected Lectures from the 5th Course on Solar Energy Conversion., Dixon A.E., Leslie J.D (ed), Pergamon Press (1978-b).

44. Hollands K.G.T, Raithby G.D and Konicek L., "Methods for Reducing Heat Losses from Flat Plate Solar Collectors", *Phase II Report*, Prepared for the United States Energy Research and Development Administration Division of Solar Energy under the Contract No. Y-76-C-02-2597, University of Waterloo, (1978-c).

45. Hollands K.G.T., "Dimensional Relations for Free Convective Heat Transfer in Flat-Plate Collectors", *Proceedings of the 1978 Annual Meeting of the American Section of the International Solar Energy Society*, Boer K.W. and Franta G.E.(eds), Denver, August (1978-d).

46. Hollands, K.G.T., Raithby G.D., Russel F.B. and Wilkinson R.G., "Coupled Radiative and Conductive Heat Transfer across Honeycomb Panels and Through Single Cells". *Int. J. Heat and Mass Transfer*, Vol. 27/11, pp.2119-2131, (1984).

47. Hollands K.G.T and Iyankaran K, "Proposal for a Compound Honeycomb Collector", *Solar Energy*, 34, No.4/5, pp. 309-316, (1985).

48. Hollands, K.G.T., "Designing Honeycombs for Minimum Materials and Maximum Transmission", *Proceedings of the 2nd International Workshop on Transparent Insulation*, Freiburg, F.R.G., pp.40-43, March (1988).

49. Hollands K.G.T, Iynkaran K., Ford C., Platzer W.J., "Manufacture, Solar transmission, and heat transfer characteristics of a large-celled honeycomb transparent insulation:, *Solar Energy*, 49, 5, pp.381-386, (1992).

50. Holman J.P, *Heat Transfer*, McGraw-Hill, sixth edition, (1986).

51. Hoogendoorn C.J., *Natural Convection*, Hemisphere Publ. Corp., (1985)

52. Hottel H.C., "A Simple Model for Estimating the Transmittance of Direct Solar Radiation Through Clear Atmospheres", *Solar Energy*, Vol.18, pp.129, (1976).

53. Jesch L.F., Chattha J.A., Jankovic L., "Transparent Insulation for Retrofit Applications", *Proceedings of ISES World Solar Congress*, Hamburg, F.R.G., (1987).

54. Jesch L.F., "Introduction", *Proceedings of the Sixth International Meeting on Transparent Insulation Technology*, Birmingham, UK, pp.5, (1993).

55. Kaushika N.D and Padma Priya R, "Solar Transmittance of Honeycomb and Parallel Slat Arrays", *Energy Conversion Management*, Vol. 32, No.4, pp. 345-351, (1991).

56. Kimura K., *Scientific Basis of Air Conditioning*, Applied Science Ltd., London, (1977).

57. Kirkpatrick A.T. and Winn C.B., "Spectral Analysis of the Effective Temperature in Passive Solar Buildings", *J. Solar Energy Engineering*, Vol.106, pp.112-119, (1984).

58. Klein S.A., *TRNSYS, A Transient Simulation Program*, Engineering Experiment Station Report 38, Solar Energy Laboratory, University of Wisconsin, Madison, (1977).

59. Knudsen H.N., deDear R.J., Li T.L., Puntner T.W. and Fanger P.O, "Thermal Comfort in Passive Solar Buildings", *Final Report*, CEC Research Project EN3S-0035-DK(B), Laboratory of Heating and Air Conditioning, Technical University Of Denmark, May, (1989).

60. Konrad A. and Larsen B.T., "ENCORE-Canada a Computer Program for the Study of Energy Consumption of Residential Buildings in Canada", *Proceedings of the 3rd International Symposium on the Use of Computers for Environmental Engineering Related to Buildings*, Banff Alberta, May, (1978).

61. Lien H., John H, A *Heat Transfer Textbook*, Prentice-Hall, N.J. (1981).

62. Liu B., and Jordan R., "The Interrelationship and Characteristic Distribution of Direct, Diffuse, and Total Solar Radiation", *Solar Energy*, Vol.4, pp.1-19, (1960).

63. Marshall K.N. and Wedel R.K.," Use of Lexan and Kepton Honeycombs to Increase solar Collector Efficiency", *Proceedings of National Heat Transfer Conference*, D4-D10, (1976-a).

64. Marchal K.N., Wedel R.K. and Dammann R.E., "Development of Plastic Honeycomb Flat-Plate Solar Collectors", *Report*, Lockheed Missiles and Space Company Inc, Palo Alto, California, USA, Contract No. SAN/1081-76/1,(1976-b)

65. Mathsoft, *Mathcad user's guide*, Mathsoft Inc., Cambridge, USA,(1995)

66. Mazria E., *The Passive Solar Book*, Rodale Press, (1979).

67. McMurrin J.C, Djordjevic N.A., Buchberg H., "Performance Measurements of a Cylindrical Glass Honeycomb Solar Collector Compared With Predictions", *J. Heat Transfer*, Vol.99, No.2, pp.169-173,(1977).

68. McMurrin J.C. and Buchberg H.B., Design Optimization of Sinusoidal Glass Honeycomb for Flat Plate Solar Collectors, *J. of Solar Engineering*, Vol.103, pp.268-274, (1981).

69. Minkowyez W.J., Sparrow E.M, Schneider G.E. and Pletcher R.H., *Handbook of Numerical Heat Transfer*, John Wiley and Sons, Somerset, N.J., (1988).

70. Morris P.A., Radiative Transfer Through Thin Walled Glass Honeycomb", *ASME* paper No. 76-HT-48, (1976).

71. Muncey R.W.R., *Heat Transfer Calculation For Buildings*, Applied Science Ltd., (1979).

72. Oglay V., *Design With The Climate*, Princeton, (1962)

73. Olsen L, "Transparent Insulation for Thermal Storage Walls", *Solar Energy R & D in the European Community Series A*, Vol. 2, pp. 127, D. Reidel Publishing Company, Dordrecht, (1982)

74. Parmelee G.V., "Transmission of Solar Radiation Through Flat Glass", *ASVE transactions*, Vol.51, pp.317-350, (1945).

75. Patankar S.V., *Numerical Heat Transfer and Fluid Flow*, Hemisphere Publishing Corp., Washington, D.C., (1980).

76. Perrot M., "Les Structures Cellulaires Antirayonament et Leurs Applications Indistruelles", *Solar Energy*, Vol.101, pp. 34-40, (1967)

77. Pipes L.A.," Matrix Analysis of Heat Transfer Problems", *J. Franklin Inst.*, Vol.263, pp.195, (1957).

78. Platzer,W.J.,"Solar Transmission of Transparent Insulation Material", *Solar Energy Materials*, Vol.16, pp.255-265, (1987).

79. Platzer W.J, "Total Heat Transport Data for Plastic Honeycomb-Type Structures", *Solar Energy*, Vol. 49, N=5, pp. 351-358, (1992).

80. Platzer,W. J., "Transparent Insulation Materials: A Review", *SPIE Conf. Proc.* 2255, *Optical Materials Technologies for Energy Efficiency and Solar Energy XIII*, pp. 616-627, (1994).

81. Platzer,W. J., "Advances in Transparent Insulation Technology", *Proceeding of the International Conference on Building Envelope Systems and Technology*, Bath, U.K., April, (1997).

82. Ramadan H.H, Athienitis A.K., "Numerical simulation for a building with transparent insulation", *Proceedings of the Renewable Energy Technologies in Cold Climates Conference*, Montreal, Canada, May (1998-a).

83. Ramadan H.H., Athenitis A.K., "Numerical Simulation for a Building with One Transparently Insulated Wall", to be presented In *World Renewable Energy Congress-V,* Florence, Italy, September, (1998-b).

84. Santamouris M., Sgalas Y., PASSPORT User Manual. Simplified Tool for Calculation of Heating Demand of Building including the CEN Method-Version II, Protechna Ltd., Athens, (1994).

85. Schneider P.J., *Conduction Heat Transfer*, Addision-Wesley Publishing Company, (1955).

86. Sick F. and Kummer J.P, "An Extension of the TRNSYS Multizone Component for Transparent Insulation Applications", Proceedings of the Biennial Congress of ISES. Denver, Vol.3, Part 1, pp. 3167-3172, Prgamon Press, (1991).

87. Stahl W., Wittwer V. and Pfluger, "Transparent Insulation", Solar Energy materials, Vol.11, pp.199-208, (1984)

88. Stephenson D.G. and Mitalas G.P., "Calculation of Heat Conduction Transfer Functions for Multilayer Slabs" ASHRAE Transactions Vol.2, pp.117-126 (1971).

89. Symons, J.G., "The Solar Transmittance of Some Convection Suppression Devices for Solar Energy Applications: An Experimental Study". *J. Solar Energy Engineering*, Vol. 104, pp. 251-256, (1982).

90. Symons, J.G and Peck M.K.," An Overview of the CSIRO Project on Advanced Flat Solar Collectors". *Proceedings of the ISES Solar World Congress*, Perth, August, (1983), pp.748-752.

91. Tabor H. (1969), "Cellular Insulation (Honeycombs)", *Solar Energy*, 12, pp.549-552.

92. Trombe F, Robert J.F, Cabonot M. and Sesolis B, "Concrete Walls to Collect and Hold Heat". *Solar Age* 2, pp. 13, (1977).

93. Twidell J.W, Johnstone C., Zuhdy B., Scott A., "Strathclyde University's Passive Solar, Low Energy Residences With Transparent Insulation", *Solar Energy*, Vol. 52, N=1, pp. 85-109, (1994).

94. Vandaele L. and Wouters P. *The PASSYS Services*, Summary report, European Commission, Directorate General XII for Science, Reasearch and Development, Belgium, (1994).

95. Walton G.N., *Thermal Analysis Research Program (TRAP)*, Research Manual, Dept. of Commerce N.B.S., March, (1983).

96. Wilke W.S. and Schmid J., "Modeling and Simulation of Elements for Solar Heating and Daylighting", *Solar Energy*, Vol.46, No.5, pp.295-304, (1991)

APPENDIX

TIW

TRANSPARENTLY INSULATED WALL MODEL

AN ILLUSTRATIVE EXAMPLE

1-Dimensions and properties of building materials :

degC := 1

K := 1

Area of the walls:

$A13 := 9 \cdot m^2$ ....Transparent insulation wall area (south face)

$A15 := 7 \cdot m^2$ ...East wall area

$A17 := 9 \cdot m^2$ ...West wall area

$A19 := 9 \cdot m^2$ ...Back wall area (north face)

$A21 := 9 \cdot m^2$ ...Floor Area

$A23 := 9 \cdot m^2$ ...Ceiling Area

$A25 := 2 \cdot m^2$ ...Window Area

1.1-The TI wall

Concrete properties:

$c := 800 \cdot \frac{joule}{kg \cdot degC}$ ... specific heat

$k := 1.4 \cdot \frac{watt}{m \cdot degC}$ ... conductivity

$\rho := 2200 \cdot \frac{kg}{m^3}$ ... density

$L := 0.2 \cdot m$ ...Concrete thickness

Gypsum board properties:

$c_{gb} := 840 \cdot \frac{joule}{kg \cdot degC}$ ... specific heat

$K_{gb} := 0.28 \cdot \frac{watt}{m \cdot degC}$ ... conductivity

$\rho_{gb} := 1440 \cdot \frac{kg}{m^3}$ ... density

$L_{gb} := 0.013 \cdot m$ ..Gypsum board thicknes

Concrete wall resistances and capacitances:

$R_c := \frac{L}{k \cdot A13}$ ..Thermal resistance of the concrete layer

$R_b := \frac{R_c}{10}$ $R_{c1} := \frac{R_c}{5}$

$R_{c2} := R_{c1}$ $R_{c4} := R_{c1}$

$R_{c3} := R_{c1}$ $R_{c5} := R_{c1}$

$C5 := \rho \cdot c \cdot \frac{L}{5} \cdot A13$ . . . thermal capacitance

$C6 := C5$

$C7 := C5$

$C8 := C5$

$C9 := C5$

Gypsum board resistances and capacitances:

$R_{gb} := \frac{L_{gb}}{K_{gb} \cdot A13}$ $R_{gb1} := \frac{R_{gb}}{2}$ $R_{gb1} = 2.579 \cdot 10^{-3} \cdot \frac{degC}{watt}$

$C12 := \rho_{gb} \cdot c_{gb} \cdot L_{gb} \cdot A13$ $C12 = 1.415 \cdot 10^{5} \cdot \frac{joule}{degC}$

The transparent honeycomb material:

$h_{ins} := 1.2 \cdot \frac{watt}{m^2 \cdot degC}$

$h_{ins} := 1.2 \cdot \frac{watt}{m^2 \cdot degC}$ ..honeycomb conductance

$R_{ins} := \frac{1}{A13 \cdot h_{ins}}$ ...honeycomb thermal resistance

Air gaps

$Ro_0 := 0.005 \cdot \frac{degC}{watt}$ ....initial exterior film resistance

$R_{cav2_0} := 0.024 \cdot \frac{degC}{watt}$

$R_{cav1_0} := 0.024 \cdot \frac{degC}{watt}$ ...initial first cavity thermal resistance

$R_{cav3_0} := 0.024 \cdot \frac{degC}{watt}$ ...initial third cavity thermal resistance

Emissivity and absorptance

$\varepsilon 1 := 0.9$ ...emissivity of glass

$\varepsilon 2 := 0.5$ ...emissivity of TIM

$\varepsilon 3 := 0.1$ ...emissivity of the absorber

$\varepsilon 4 := 0.9$ ...emissivity of concrete

$\alpha_{wall} := 0.9$ ...concrete wall absorptance

$\varepsilon 5 := 0.9$ ..emissivity of gupsum board

Total thermal resistance of the exterior TI wall system (excluding concret layer, the 3 rd air gapand the gypsum board layer:

$R_{exterior_0} := R_{cav1_0} + R_{cav2_0} + R_{ins} + Ro_0$

$R_{exterior_0} := R_{cav1_0} + R_{cav2_0} + R_{ins} + Ro_0$

1.2-Room walls

conductive thermal resistances for other room walls:

$X_{east} := 0.013 \cdot m$ ....East wall thickness

$X_{west} := 0.013 \cdot m$ ....West wall thickness

$X_{north} := 0.013 \cdot m$ ....North walls thickness

$X_{floor} := 0.013 \cdot m$ ...Floor thickness

$X_{ceiling} := 0.013 \cdot m$ ...Ceiling thickness

$K_{east} := 0.28 \cdot \frac{watt}{m \cdot degC}$ ...East wall conductivity

$K_{west} := 0.28 \cdot \frac{watt}{m \cdot degC}$ ...West wall conductivity

$K_{north} := 0.28 \cdot \frac{watt}{m \cdot degC}$ ...North wall conductivity

$K_{floor} := 0.28 \cdot \frac{watt}{m \cdot degC}$ ...floor conductivity

$K_{ceiling} := 0.28 \cdot \frac{watt}{m \cdot degC}$ ...Ceiling conductivity

Thermal conductive resistances for room walls:

$R1516 := \frac{X_{east}}{2 \cdot A15 \cdot K_{east}}$ ....conductive resistance for the half of east wall

$R1615 := R1516$

$R160 := R1516$ ....conductive resistance for the other half of east wall

$R1718 := \frac{X_{west}}{2 \cdot A17 \cdot K_{west}}$ ....conductive resistance for the half of west wall

$R1817 := R1718$

$R180 := R1718$ ....conductive resistance for the other half of west wall

$R1920 := \frac{X_{north}}{2 \cdot A19 \cdot K_{north}}$ ....conductive resistance for the half of north wall

$R200 := R1920$ ....conductive resistance for the other half of north wall

$R2019 := R1920$

$R2122 := \frac{X_{floor}}{2 \cdot A21 \cdot K_{floor}}$ ....conductive resistance for the half of the floor

$R220 := R2122$ ....conductive resistance for the other half of the floor

$R2221 := R2122$

$R2324 := \frac{X_{ceiling}}{2 \cdot A23 \cdot K_{ceiling}}$ ....conductive resistance for the half of the ceiling

$R240 := R2324$ ....conductive resistance for the other half of the ceiling

$R2423 := R2324$

Exterior insulation for walls: fiber glass

$X_{fiberglass} := 0.09 \cdot m$ $K_{fiberglass} := 0.035 \cdot \frac{watt}{m \cdot K}$ $R_{xi} := \frac{X_{fiberglass}}{K_{fiberglass}}$

$U_{xi} := \frac{1}{R_{xi}}$

For east wall: $R_{eastxi} := \frac{1}{A15 \cdot U_{xi}}$

For west wall: $R_{westxi} := \frac{1}{A17 \cdot U_{xi}}$

For north wall: $R_{northxi} := \frac{1}{A19 \cdot U_{xi}}$

For the floor: $R_{floorxi} := \frac{1}{A21 \cdot U_{xi}}$

For the ceiling: $R_{ceilingxi} := \frac{1}{A23 \cdot U_{xi}}$

Properties of walls

$\rho_{east} := 1440 \cdot \frac{kg}{m^3}$ $c_{east} := 840 \cdot \frac{joule}{kg \cdot degC}$ $V_{east} := A15 \cdot X_{east}$

...density of east wall ...specific heat of east wall ...wall volume

$C16 := \rho_{east} \cdot c_{east} \cdot V_{east}$

...thermal capacity of east wall

$\rho_{west} := 1440 \cdot \frac{kg}{m^3}$ $c_{west} := 840 \cdot \frac{joule}{kg \cdot degC}$ $V_{west} := A17 \cdot X_{west}$

...density of west wall ...specific heat of west wall ...wall volume

$C18 := \rho_{west} \cdot c_{west} \cdot V_{west}$

...thermal capacity of west wall

$\rho_{north} := 1440 \cdot \frac{kg}{m^3}$ $c_{north} := 840 \cdot \frac{joule}{kg \cdot degC}$ $V_{north} := A19 \cdot X_{north}$

...density of north wall ...specific heat of north wall ...wall volume

$C20 := \rho_{north} \cdot c_{north} \cdot V_{north}$

...thermal capacity of north wall

$\rho_{floor} := 1440 \cdot \frac{kg}{m^3}$ $c_{floor} := 840 \cdot \frac{joule}{kg \cdot degC}$ $V_{floor} := A21 \cdot X_{floor}$

...density of the floor ...specific heat of the floor ...wall volume

$C22 := \rho_{floor} \cdot c_{floor} \cdot V_{floor}$

...thermal capacity of the floor

$\rho_{ceiling} := 1440 \cdot \frac{kg}{m^3}$ $c_{ceiling} := 840 \cdot \frac{joule}{kg \cdot degC}$ $V_{ceiling} := A23 \cdot X_{ceiling}$

...density of the ceiling ...specific heat of the ceiling ...wall volume

$C24 := \rho_{ceiling} \cdot c_{ceiling} \cdot V_{ceiling}$

...thermal capacity of the ceiling

2-Initial Conditions

$To_0 := -15 \cdot degC$ ...mean outside temperature

$$\begin{bmatrix} T1_0 \\ T2_0 \\ T3_0 \\ T4_0 \end{bmatrix} := \begin{bmatrix} To_0 \\ To_0 + 2 \cdot degC \\ To_0 + 12 \cdot degC \\ To_0 + 15 \end{bmatrix}$$

...

T1 is the protector temperature.
T2, T3, are the TIM modelled as 2 nodes
T4 is the absorber temperature(concrete wall)

$$\begin{bmatrix} T5_0 \\ T6_0 \\ T7_0 \\ T8_0 \\ T9_0 \\ T10_0 \\ T11_0 \\ T12_0 \end{bmatrix} := \begin{bmatrix} To_0 + 14 \\ To_0 + 13 \\ To_0 + 12 \\ To_0 + 11 \\ To_0 + 10 \\ To_0 + 9 \\ To_0 + 8 \\ To_0 + 7 \end{bmatrix}$$

...internal node temperature of the thermal mass and gypsum board

$TR := 20 \cdot degC$ ..room air temperature when assumed constant

$T13_0 := To_0 + 6 \cdot degC$ ..TI wall inside surface temperature

$T14_0 := To_0 + 5 \cdot degC$ ..room air temperature

$T15_0 := To_0 + 4 \cdot degC$ ..east wall inside surface temperature

$T16_0 := To_0 + 2 \cdot degC$ ..east wall interor node temperature

$T17_0 := To_0 + 4.5 \cdot degC$ ..west wall inside surface temperature

$T18_0 := To_0 + 2.1 \cdot degC$ ..west wall interor node temperature

$T19_0 := To_0 + 4 \cdot degC$ ..north wall inside surface temperature

$T20_0 := To_0 + 2.2 \cdot degC$ ..north wall interor node temperature

$T21_0 := To_0 + 3.5 \cdot degC$ ..floor inside surface temperature

$T22_0 := To_0 + 2.3 \cdot degC$ ...floor interor node temperature

$T23_0 := To_0 + 3.5 \cdot degC$ ..ceiling inside surface temperature

$T24_0 := To_0 + 3 \cdot degC$ ...ceiling interor node temperature

$T25_0 := To_0 + 1 \cdot degC$ ...window temperature

$h_{i_0} := 10 \cdot \frac{watt}{m^2 \cdot degC}$ ...intitial internal film conductance

$R_{i_0} := \frac{1}{A13 \cdot h_{i_0}}$ ...initial interior film resistance

<u>3-Stability Test</u>

$$TS1_0 := \frac{C5}{\left(\frac{1}{R_{exterior_0} + R_b} + \frac{1}{R_{c1}}\right)} \qquad TS2 := \frac{C6}{\left(\frac{1}{R_{c1}} + \frac{1}{R_{c2}}\right)} \qquad TS3 := \frac{C7}{\left(\frac{1}{R_{c2}} + \frac{1}{R_{c3}}\right)}$$

$$TS4 := \frac{C8}{\left(\frac{1}{R_{c3}} + \frac{1}{R_{c4}}\right)} \qquad TS5 := \frac{C9}{\left(\frac{1}{R_{c4}} + \frac{1}{R_b}\right)} \qquad TS6 := \frac{C12}{\left(\frac{1}{R_{gb1}} + \frac{1}{R_{gb1}}\right)}$$

$$TS7 := \frac{C16}{\left(\frac{1}{R1516} + \frac{1}{R_{eastxi} + R160}\right)}$$

$$TS8 := \frac{C18}{\left(\frac{1}{R1718} + \frac{1}{R_{westxi} + R180}\right)}$$

$$TS9 := \frac{C20}{\left(\frac{1}{R1920} + \frac{1}{R_{northxi} + R200}\right)}$$

$$TS10 := \frac{C22}{\left(\frac{1}{R2122} + \frac{1}{R_{floorxi} + R220}\right)}$$

$$TS11 := \frac{C24}{\left(\frac{1}{R2324} + \frac{1}{R_{ceilingxi} + R240}\right)}$$

The time step Δt should be lower than the minimum of the values in the vector TS.

$$TS := \left(TS1_0 \quad TS2 \quad TS3 \quad TS4 \quad TS5 \quad TS6 \quad TS7 \quad TS8 \quad TS9 \quad TS10 \quad TS11\right)$$

$$\Delta t_{critical} := \min(TS) \qquad \Delta t_{critical} = 182.52 \cdot sec$$

$$\Delta t := floor\left(\Delta t_{critical} \cdot 0.7\right) \qquad \Delta t = 127 \cdot sec$$

4. Solar radiation simulation:

Consider a location with the following data:

$La := 45 \cdot deg$ ... latitude

$j := 0, 1 .. 3$ surface azimuth array

$\psi_j :=$

0·deg
-90·deg
90·deg
180·deg

... surface azimuth angle

$n := 21$ ... day number

$\beta := 90 \cdot deg$ ... tilt angle

$\rho_g := 0.2$ ... ground reflectance

4.1- solar geometry calculations:

Declination angle:

$$\delta := 23.45 \cdot deg \cdot \sin\left(360 \cdot \frac{284 + n}{365} \cdot deg\right) \qquad \delta = -20.138 \cdot deg$$

Sunset time:

$$t_s := (\operatorname{acos}(-\tan(La) \cdot \tan(\delta))) \cdot \frac{hr}{15 \cdot deg} \qquad t_s = 4.566 \cdot hr$$

$SRT := 12 \cdot hr - t_s$ ....sunrise solar time $SRT = 7.434 \cdot hr$

$SST := 12 \cdot hr + t_s$ ...sunset solar time $SST = 16.566 \cdot hr$

4.2-Time steps:

$$N := \left(\frac{2 \cdot t_s}{\Delta t} \right)$$

Time array from sunrise to sunset and hour angle h:

$i := 0, 1 .. N$ $\quad t_i := i \cdot (\Delta t) - t_s$ $\quad h_i := 15 \cdot \frac{deg}{hr} \cdot t_i$ $\quad N := ceil(N)$

$Time_i := \frac{i \cdot \Delta t}{hr} + \frac{SRT}{hr}$ ..timing

4.3-solar angles:

Solar altitude: $\alpha_i := asin\left(cos(La) \cdot cos(\delta) \cdot cos\left(h_i\right) + sin(La) \cdot sin(\delta)\right)$

Solar azimuth: $\phi_i := acos\left(\frac{sin\left(\alpha_i\right) \cdot sin(La) - sin(\delta)}{cos\left(\alpha_i\right) \cdot cos(La)} \right) \cdot \frac{h_i}{|h_i|}$

Angle of incidence: $cos\theta_{i,j} := cos\left(\alpha_i\right) \cdot cos\left(\left|\phi_i - \psi_j\right|\right) \cdot sin(\beta) + sin\left(\alpha_i\right) \cdot cos(\beta)$

$$\theta_{i,j} := acos\left(\frac{cos\theta_{i,j} + |cos\theta_{i,j}|}{2} \right)$$

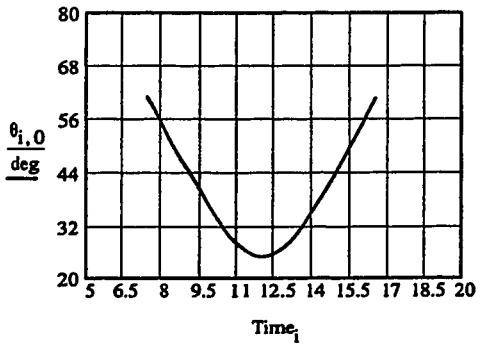

Incident angle change in one day

4.4-Calculation of the transmittance of atmosphere and the protector:

Beam atmospheric transmittance calculations:

Correction factors due to climate type:

CT=1 ...Tropical

CT=2 ...Midlatitude summer

CT=3 ...Subarctic summer

CT=4 ...Midlatude winter

$CT := 4$

$$r_0 := \begin{cases} 0.95 & \text{if } CT=1 \\ 0.97 & \text{if } CT=2 \\ 0.99 & \text{if } CT=3 \\ 1.03 & \text{if } CT=4 \end{cases} \qquad r_1 := \begin{cases} 0.98 & \text{if } CT=1 \\ 0.99 & \text{if } CT=2 \\ 0.99 & \text{if } CT=3 \\ 1.01 & \text{if } CT=4 \end{cases} \qquad r_k := \begin{cases} 1.02 & \text{if } CT=1 \\ 1.02 & \text{if } CT=2 \\ 1.01 & \text{if } CT=3 \\ 1.00 & \text{if } CT=4 \end{cases}$$

$Al := 0.5$ Altitude (km)

$a_o := r_0 \cdot \left[0.4237 - 0.00821 \cdot (6 - Al)^2\right]$

$a_1 := r_1 \cdot \left[0.5055 + (0.00595 \cdot (6.5 - Al))^2\right]$

$k := r_k \cdot \left[0.2711 + (0.01858 \cdot (2.5 - Al))^2\right]$

$$\tau_{b_i} := a_o + a_1 \cdot \exp\left(\frac{-k}{\sin(\alpha_i + 0.0001)}\right)$$

$\tau_{b_N} := 0.0$

Determine the glazing properties as a function of time interval i:

Glass properties: $7.76 \cdot 0.003 = 0.023$

$k_{ec} := \frac{7.76}{m}$ ... extinction coeff.

$L_g := 0.003 \cdot m$ ... glazing thickness

$n_g := 1.53$ ... refractive index

Angle of refraction and component reflectivity:

$$\theta'_i := \operatorname{asin}\left(\frac{\sin(\theta_{i,0})}{n_g}\right)$$

$$r_i := \frac{1}{2}\cdot\left[\left(\frac{\sin(\theta_{i,0}-\theta'_i)}{\sin(\theta_{i,0}+\theta'_i)}\right)^2+\left(\frac{\tan(\theta_{i,0}-\theta'_i)}{\tan(\theta_{i,0}+\theta'_i)}\right)^2\right]$$

Beam transmittance, τ, reflectance, ρ, and absorptance, α, of glazing:

$$ac_i := \exp\left[-\frac{k_{ec}\cdot L_g}{\sqrt{1-\left(\frac{\sin(\theta_{i,0})}{n_g}\right)^2}}\right] \qquad \tau_i := \frac{(1-r_i)^2\cdot ac_i}{1-(r_i)^2\cdot(ac_i)^2}$$

$$\rho_i := r_i + \frac{r_i\cdot(1-r_i)^2\cdot(ac_i)^2}{1-(r_i)^2\cdot(ac_i)^2} \qquad \alpha_{pro_i} := 1-\rho_i-\tau_i$$

Solar properties of single glazing:

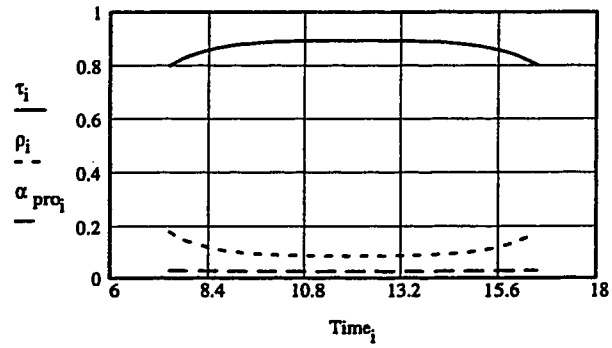

Extraterrestrial normal solar radiation:

$$I_{on_n} := 1367 \cdot \frac{watt}{m^2} \cdot \left(1 + 0.033 \cdot \cos\left(360 \cdot \frac{n}{365} \cdot deg\right)\right)$$

$$I_{b_{i,j}} := \left(I_{on_n} \cdot \tau_{b_i} \cdot \cos\left(\theta_{i,j}\right)\right)$$

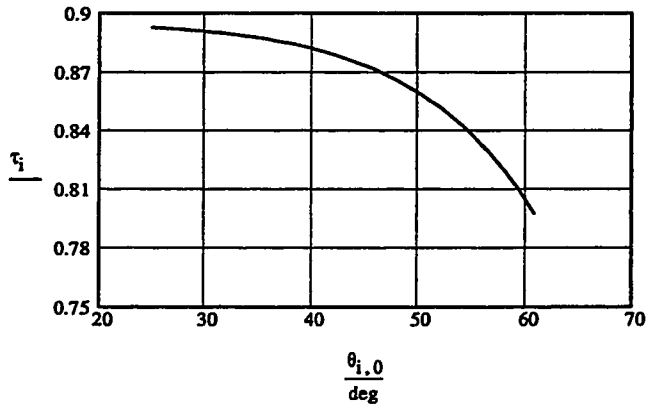

Atmosphere beam transmittance change

$G_{bt_i} := I_{b_{i,0}} \cdot \tau_i$ ...beam transmitted solar radiation through the protector

$G_{ba_i} := I_{b_{i,0}} \cdot \alpha_{pro_i}$ ...beam absorbed solar radiation by the protector

For the calculation of transmitted diffuse solar radiation, it is assumed that the protector diffuse transmittance is equal to the beam transmittance at an angle of incidence equal to 60 degrees (1.04 radiant). Therefore, in this case:

$$\theta_{60} := \operatorname{asin}\left(\frac{\sin(1.04)}{n_g}\right)$$

$$r_{60} := \frac{1}{2}\cdot\left[\left(\frac{\sin(1.04-\theta_{60})}{\sin(1.04+\theta_{60})}\right)^2 + \left(\frac{\tan(1.04-\theta_{60})}{\tan(1.04+\theta_{60})}\right)^2\right]$$

Diffuse transmittance, τ, reflectance, ρ, and absorptance, α, of glazing:

$$a_{60} := \exp\left[-\frac{k_{ec}\cdot L_g}{\sqrt{1-\left(\frac{\sin(1.04)}{n_g}\right)^2}}\right] \qquad \tau_{60} := \frac{(1-r_{60})^2\cdot a_{60}}{1-(r_{60})^2\cdot(a_{60})^2}$$

$$\rho_{60} := r_{60} + \frac{r_{60}\cdot(1-r_{60})^2\cdot(a_{60})^2}{1-(r_{60})^2\cdot(a_{60})^2} \qquad \alpha_{60} := 1-\rho_{60}-\tau_{60}$$

$$\tau_d := \tau_{60}$$

$$\alpha_d := \alpha_{60}$$

$$I_{ds_i} := I_{on_n}\cdot\sin(\alpha_i)\cdot(0.2710-0.2939\cdot\tau_{b_i})\cdot\frac{1+\cos(\beta)}{2} \quad \ldots \text{instantaneous sky diffuse radiation}$$

$$I_{dg_i} := \left[I_{on_n}\cdot\sin(\alpha_i)\cdot(0.2710-0.2939\cdot\tau_{b_i}+\tau_{b_i})\right]\cdot\rho_g\cdot\frac{1-\cos(\beta)}{2} \quad \ldots \text{ground reflected}$$

$$I_{t_{i,j}} := I_{b_{i,j}} + I_{ds_{i,0}} + I_{dg_{i,0}} \quad \ldots \text{Total incident radiation}$$

$G_{dt_i} := \tau_d \cdot \left(I_{ds_i} + I_{dg_i}\right)$ . . . transmitted diffuse irradiation (instantaneous)

$G_{da_i} := \alpha_d \cdot \left(I_{ds_i} + I_{dg_i}\right)$ ...Absorbed diffuse radiation

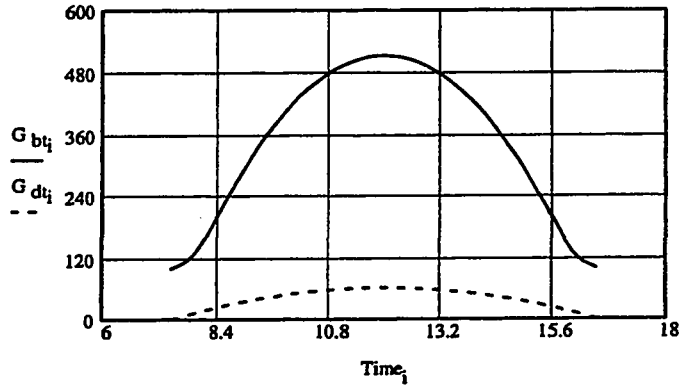

Trasmitted radiation (protector)

Instantaneous beam and
diffuse
transmitted solar radiation
for single-glazing:

$G_{total_i} := \left(G_{bt_i} + G_{dt_i}\right)$

...This quantity represents the total solar radiations transmitted through the single glazing used in the TI wall system as a protector.

$G_{absorbed_i} := \left(G_{ba_i} + G_{da_i}\right)$ ...Total absorbed solar radiation by the protector

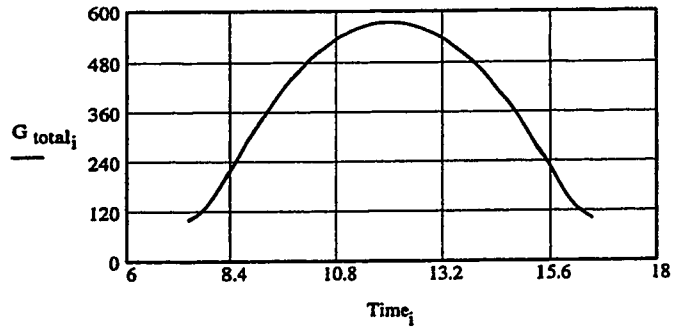

Total transmitted radiation (protector)

5-Calculation of the transmitted solar radiations through the TIM system:

5.1.Beam transmittance:

The general formula could be expressed as:

$$T(\theta)=F_e \cdot F_r^{A_{hc}\cdot\tan(\theta)}$$

Transparent honeycomb dimensions to suppress convection:

$L_{hc} := 10\cdot cm$ ... Honeycomb thickness

$$f_{hc} := \left(4.45\cdot\cos\left(\frac{\beta}{deg}-\frac{60}{deg}\right)\right)^{\frac{1}{11.52-6.56\cdot\sin(\beta)}}$$ ... Dimensionless variable

$T1_{hc} := 280\cdot K$ ... Design value of Cold surface of honeycomb

$T2_{hc} := 350\cdot K$ ... Design value of Hot surface of honeycomb

$$T_{mhc} := \frac{T1_{hc}+T2_{hc}}{2}$$ ... Design value of mean temperature of honeycomb

$C_{hc} := 1.13\cdot f_{hc}$

$$x_{hc} := \frac{100}{T_{mhc}}$$

$\Delta T_{hc} := T2_{hc} - T1_{hc}$ ... Temperature difference across the honeycomb

$$A_{hc} := C_{hc}\cdot\left(1+2\cdot x_{hc}\right)^{\frac{1}{2}}\cdot x_{hc}\cdot\Delta T_{hc}^{\frac{1}{4}}\cdot\left(\frac{L_{hc}}{cm}\right)^{\frac{3}{4}}$$ ... Honeycomb aspect ratio

$$D_{hco} := \frac{L_{hc}}{A_{hc}}$$ ...Honeycomb hydraulic diameter

For square cells

$A_{cell} := \frac{\pi \cdot D_{hco}^{2}}{4}$ ... Honeycomb cell area

$D_{hc} := \sqrt{A_{cell}}$ ... Width of honeycomb cell

$D_{hc} = 0.011 \cdot m$ ... Minimum width required for honeycomb cell to suppress convection heat transfer

Properties of the Transparent material used(Lexan squared cell honeycomb):

$L_{hc} := 100 \cdot mm$ ...Honeycomb depth(height)

$\delta_{hc} := 0.076 \cdot mm$ ...Honeycomb's wall thickness

$D_{hc} := 10 \cdot mm$ ...Honeycomb's wall spacing

$E := \frac{\delta_{hc} \cdot (\delta_{hc} + 2 \cdot D_{hc})}{D_{hc}^{2}}$ ... Fraction of cellular cross-section area occupied by wall material (for a square cell).

$A_{hc} := \frac{L_{hc}}{D_{hc}}$ .....Aspect ratio of honeycomb

$\rho_{se} := 0.97$ ...Equivalent specular reflectivity of honeycomb wall

$\rho_{de} := 0.02$ ...Equivalent diffuse reflectivity of honeycomb wall

$F_r := \rho_{se} + \rho_{de}$ $F_e := 1 - E$

$T_{beam_i} := F_e \cdot F_r^{A_{hc} \cdot \tan(\theta_{i,0})}$ ..beam transmittance of honeycomb transparent material

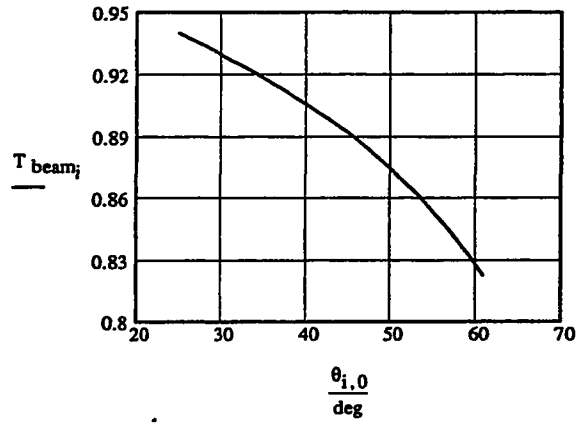

Figure-1-

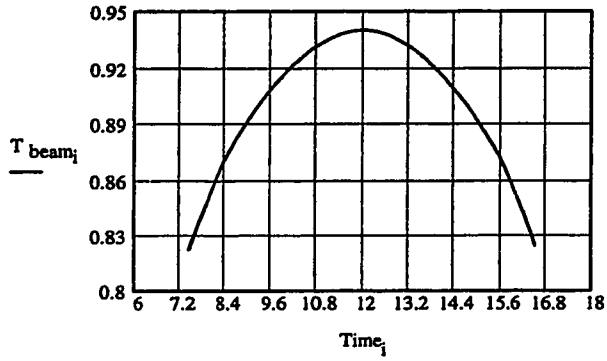

Figure-2-

Fig1- Honeycomb transmittance change with the angle of incidence.
Fig2- Honeycomb transmittance change through the day.

$S_{b_i} := G_{bt_i} \cdot T_{beam_i}$ ...beam transmitted radiation through transparent honeycomb

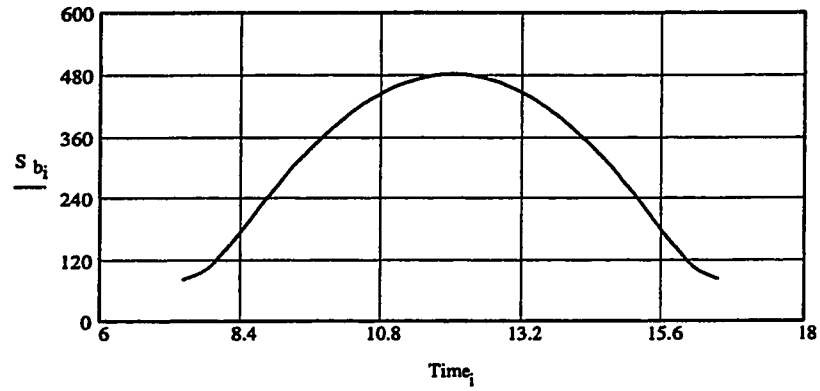

Transmiited radiation through honeycomb

5.2.Diffuse transmittance:

$$\beta 1 := \frac{\beta}{deg}$$

The equivalent beam angle of diffuse radiation transmittance for Lexan honeycomb can be expressed as:

$$\theta_{e1} := 90 - 0.6084518 \cdot \beta 1 + 3.709793 \cdot 10^{-4} \cdot \beta 1 \cdot A_{hc} - 3.0577183 \cdot 10^{-5} \cdot \beta 1 \cdot A_{hc}^{2} + 3.0328929 \cdot 10^{-3} \cdot (\beta 1)^{2}$$

$$\theta_{e2} := -5.0287694 \cdot 10^{-5} \cdot (\beta 1)^{2} \cdot A_{hc} + 4.1570456 \cdot 10^{-7} \cdot (\beta 1)^{2} \cdot A_{hc}^{2}$$

$$\theta_{e3} := 59.69678 - \left(0.3802643 \cdot A_{hc}\right) + \left(4.2715073 \cdot 10^{-3} \cdot A_{hc}^{2}\right) - 0.1429023 \cdot \beta 1$$

$$\theta_{e4} := -8.0555677 \cdot 10^{-3} \cdot A_{hc} \cdot \beta 1 + 2.1229684 \cdot 10^{-4} \cdot A_{hc}^{2} \cdot \beta 1 + 1.527757 \cdot 10^{-3} \cdot (\beta 1)^{2}$$

$$\theta_{e5} := 7.0696505 \cdot 10^{-3} \cdot A_{hc} \cdot \beta 1 - 2.1496235 \cdot 10^{-6} \cdot A_{hc}^{2} \cdot (\beta 1)^{2}$$

The equivalent beam angle of diffuse ground radiation is :

$$\theta_{eg} := \theta_{e1} + \theta_{e2} \qquad \theta_{egradiant} := \frac{\theta_{eg} \cdot \pi}{180}$$

$$\theta_{eg} = 56.128 \qquad \theta_{egradiant} = 0.98$$

The equivalent beam angle of diffuse sky radiation is:

$\theta_{es} := \theta_{e3} + \theta_{e4} + \theta_{e5}$

$\theta_{es} = 55.117$

$\theta_{esradiant} := \frac{\theta_{es} \cdot \pi}{180}$

$\theta_{esradiant} = 0.962$

Equivalent ground diffuse transmittance for honeycomb:

$T_{eg} := F_e \cdot F_r^{A_{hc} \cdot \tan(\theta_{egradiant})}$

$T_{eg} = 0.848$

Equivalent sky diffuse transmittance for honeycomb

$T_{es} := F_e \cdot F_r^{A_{hc} \cdot \tan(\theta_{esradiant})}$

$T_{es} = 0.853$

$S_{dg_i} := \tau_d \cdot I_{dg_i} \cdot T_{eg}$ ...Transmitted ground diffuse solar radiation

$S_{ds_i} := \tau_d \cdot I_{ds_i} \cdot T_{es}$ ...Transmitted sky diffuse solar radiation

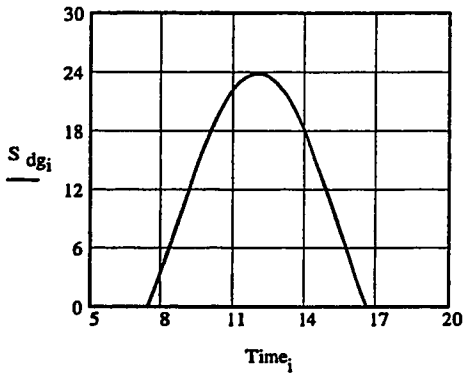

Transmitted ground diffuse radiation

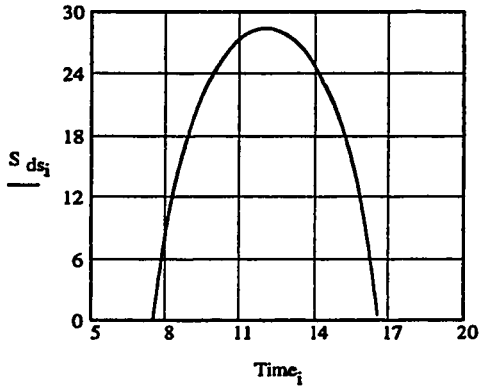

Transmitted sky diffuse radiation

$S_{total_i} := \left(S_{b_i} + S_{ds_i} + S_{dg_i}\right)$ ...beam and diffuse transmitted radiation through the Transparent Insulation Material

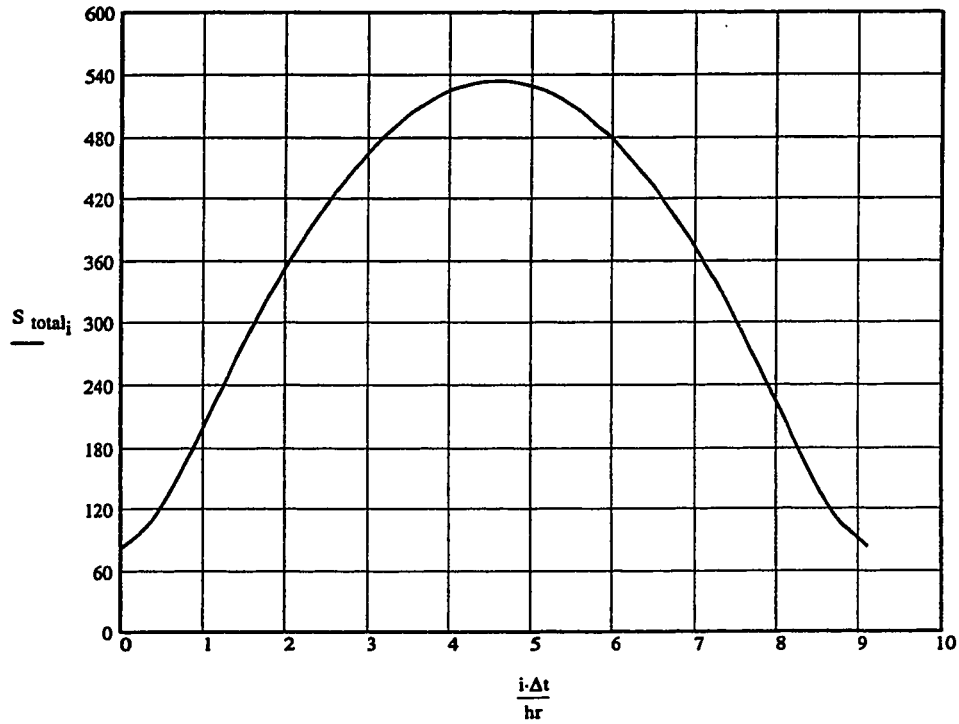

Total transmitted radiation through TIM

6-Simulation for "l" days:

Time steps for one day

$$NSD := \frac{24 \cdot 3600 \cdot sec}{\Delta t}$$ ....number of steps per day

round(NSD) := if(NSD − floor(NSD) < 0.5, floor(NSD), ceil(NSD))

NSD := round(NSD)

Time steps for "l" days

days := 7

l := 1, 2 .. days

t := 0, Δt .. days·NSD·Δt

i := 0, 1 .. days·NSD

Transmitted radiation for "l" days

$S_{total_{i+NSD \cdot l}} := S_{total_i}$ ...Transmitted radiation through TIM

$\tau_{i+NSD \cdot l} := \tau_i$ ...Glass transmittance

$G_{total_{i+NSD \cdot l}} := G_{total_i}$ ... Transmitted solar radiation through the glass cover

$G_{absorbed_{i+NSD \cdot l}} := G_{absorbed_i}$ ...Absorbed solar radiation through the protector

$I_{t_{i+NSD \cdot l, j}} := I_{t_{i,j}}$ ...Total incidence for different orientations

$I_{b_{i+NSD \cdot l, j}} := I_{b_{i,j}}$ ...Beam incident radiation

$I_{ds_{i+NSD\cdot l}} := I_{ds_i}$ ..Sky diffuse incident radiation

$I_{dg_{i+NSD\cdot l}} := I_{dg_i}$ ...Ground diffuse incident radiation

$Time_i := \frac{i \cdot \Delta t}{hr} + \frac{SRT}{hr}$ ...Timing for "l" days

7-One dimensional transparently insulated wall

The general form of the explicit finite difference formulation corresponding to node i and time interval p is

$$T(i,p+1) = \left(\frac{\Delta t}{C_i}\right) \cdot \left(q_i + \sum_j \frac{T(j,p) - T(i,p)}{R(i,j)}\right) + T(i,p)$$

Critical time step:

$$\Delta t_{critical} = \min\left[\frac{C_i}{\sum_j \frac{1}{R_{i,j}}}\right]$$ for all nodes i.

A wall employs the concept of transparent insulation. It consists of a transparent exterior layer, an air gap with a blind and a concrete thermal storage and one gypsum board layer. The latter is consider as one layer while the concrete is devided into five sublayers.

The exterior insulation consists of a glass protector, an air gap for the roller blind, a transparent honeycomb material, and another air gap to the absorber. This exterior system will be modelled under the non-linear behavior of the exterior film and both air gaps.

7.1 The outside temperature

$w := 2 \cdot \frac{\pi}{86400 \cdot sec}$ ... frequency based on period of one day

$To_i := \left[5 \cdot \cos\left[w \cdot \left(i + \frac{SRT}{hr} \cdot \frac{3600 \cdot sec}{\Delta t} \right) \cdot \Delta t + 3 \cdot \frac{\pi}{4} \right] - 15 \right] \cdot degC$ ... Outside temperature

7.2 The outside film coefficient

1-The exterior film is a function of the wind velocity and is a time dependent.

2-The convective heat transfer coefficient is taken as a minimum of 5 W/(m^2·degC) (still air conditions). When forced convection is applied, this value should be greater.

$kph := 20$ ... wind speed (kilometers per hour)

$V_w := kph \cdot \frac{1000}{3600}$ ... wind speed (m/sec)

$L_{cha} := 2$ ... characteristic length

$hc_w := 8.6 \cdot \frac{V_w^{0.6}}{L_{cha}^{0.4}} \cdot \frac{watt}{m^2 \cdot degC}$

$h_{wind} := if\left(hc_w > 5 \cdot \frac{watt}{m^2 \cdot degC}, hc_w, 5 \cdot \frac{watt}{m^2 \cdot degC} \right)$

$\sigma := 5.67 \cdot 10^{-8} \cdot \frac{watt}{m^2 \cdot K^4}$ ... (Stefan-Boltzmann constant)

$Tmean1_0 := \left(273 + \frac{T2_0 + T1_0}{2} \right)$ ... initial mean temperature

$hr_{p_0} := \varepsilon 1 \cdot \sigma \cdot 4 \cdot (Tmean1_0)^3$

$ho_{p_0} := h_{wind} + hr_{p_0}$ ... combined exterior film coefficient

$Ro_0 := \frac{1}{ho_{p_0} \cdot A13}$

7.3 Heat transfer coefficients for the first exterior cavity the TIM) due to the initial conditions:

$p := 1$ ...Atmospheric pressure

$L_{cav1} := 30 \cdot mm$ ...first cavity lenght(mm)

$Tmcav1_0 := \frac{T1_0 + T2_0}{2} + 273$ ...mean temperature of the first cavity

$acav1_0 := \frac{100 \cdot degC}{Tmcav1_0}$

$K_{cav1air_0} := \frac{0.002528 \cdot (Tmcav1_0)^{1.5}}{Tmcav1_0 + 200} \cdot \frac{watt}{m \cdot degC}$

$Ra_{cav1_0} := 2.737 \cdot (1 + 2 \cdot acav1_0)^2 \cdot (acav1_0)^4 \cdot |T1_0 - T2_0| \cdot \left(\frac{L_{cav1}}{mm}\right)^3 \cdot p^2$ ...Rayleigh number

$Nu1_{cav1_0} := 0.0605 \cdot \left(|Ra_{cav1_0}|\right)^{\frac{1}{3}}$ ...Nusselt number

$$Nu2_{cav1_0} := \left[1 + \frac{0.104 \cdot \left(Ra_{cav1_0}\right)^{0.293}}{\left[1 + \left(\frac{6310}{Ra_{cav1_0}}\right)^{1.36}\right]^3}\right]^{\frac{1}{3}}$$

$$h_{ccav1_0} := \frac{K_{cav1air_0} \cdot A13}{L_{gb}} \cdot if\left(Nu1_{cav1_0} > Nu2_{cav1_0}, Nu1_{cav1_0}, Nu2_{cav1_0}\right)$$

...convective heat transfer coefficient for the first cavity

$$h_{rcav1_0} := \frac{4 \cdot A13 \cdot \sigma \cdot (Tmcav1_0)^3}{\left(\frac{1}{\varepsilon 1} + \frac{1}{\varepsilon 2} - 1\right)}$$ ...radiative heat transfer coefficient of the first cavity

$$R_{cav1_0} := \frac{1}{h_{ccav1_0} + h_{rcav1_0}}$$ ....thermal resistance of the first cavity

7.4 Calculation of heat transfer coefficients for the second (between the TIM and the absorber) due to the initial condit

$L_{cav2} := 13 \cdot mm$ ...second cavity lenght

$$Tmcav2_0 := \frac{T3_0 + T4_0}{2} + 273$$ ...mean temperature of the second cavity

$$acav2_0 := \frac{100 \cdot degC}{Tmcav2_0}$$

$$K_{cav2air_0} := \frac{0.002528 \cdot (Tmcav2_0)^{1.5}}{Tmcav2_0 + 200} \cdot \frac{watt}{m \cdot degC}$$

$$Ra_{cav2_0} := 2.737 \cdot (1 + 2 \cdot acav2_0)^2 \cdot (acav2_0)^4 \cdot |T3_0 - T4_0| \cdot \left(\frac{L_{cav2}}{mm}\right)^3 \cdot p^2$$ ...Rayleigh number

$$Nu1_{cav2_0} := 0.0605 \cdot \left(\left|Ra_{cav2_0}\right|\right)^{\frac{1}{3}}$$ ...Nusselt number

$$Nu2_{cav2_0} := \left[1 + \frac{0.104 \cdot (Ra_{cav2_0})^{0.293}}{\left[1 + \left(\frac{6310}{Ra_{cav2_0}}\right)^{1.36}\right]^3}\right]^{\frac{1}{3}}$$

$$h_{ccav2_0} := \frac{K_{cav2air_0} \cdot A13}{L_{cav2}} \cdot if(Nu1_{cav2_0} > Nu2_{cav2_0}, Nu1_{cav2_0}, Nu2_{cav2_0})$$

...Convective heat transfer coefficient for the second cavity

$$h_{rcav2_0} := \frac{4 \cdot A13 \cdot \sigma \cdot (Tmcav2_0)^3}{\left(\frac{1}{\varepsilon 2} + \frac{1}{\varepsilon 3} - 1\right)}$$ ...Radiative heat transfer coefficient of the second cavity

$$R_{cav2_0} := \frac{1}{h_{ccav2_0} + h_{rcav2_0}}$$ ....thermal resistance of the first cavity

7.5.Calculation of heat transfer coefficients for cavity and conditions:

$$Tm_0 := \frac{T13_0 + TR}{2} + 273$$ ..mean temperature of interior film

$$Tmcav3_0 := \frac{T10_0 + T11_0}{2} + 273$$

...mean temperature of third cavity

$$L_{cav3} := 13 \cdot mm$$ ..third cavity thickness

$$a_0 := \frac{100 \cdot degC}{Tmcav3_0}$$

$$K_{air_0} := \frac{0.002528 \cdot (Tmcav3_0)^{1.5}}{Tmcav3_0 + 200} \cdot \frac{watt}{m \cdot degC}$$

$$Ra_0 := 2.737 \cdot (1 + 2 \cdot a_0)^2 \cdot (a_0)^4 \cdot |T10_0 - T11_0| \cdot \left(\frac{L_{cav3}}{mm}\right)^3 \cdot p^2$$ ...Rayleigh number

$$Nu1_0 := 0.0605 \cdot (|Ra_0|)^{\frac{1}{3}}$$ ...Nusselt number

$$Nu2_0 := \left[1 + \frac{0.104 \cdot (Ra_0)^{0.293}}{\left[1 + \left(\frac{6310}{Ra_0}\right)^{1.36}\right]^3}\right]^{\frac{1}{3}}$$

$$h_{cc_0} := \frac{K_{air_0} \cdot A13}{L_{cav3}} \cdot if\left(Nu1_0 > Nu2_0, Nu1_0, Nu2_0\right)$$ ...Convective heat transfer coefficient for cavity

$$h_{rc_0} := \frac{4 \cdot A13 \cdot \sigma \cdot \left(Tmcav3_0\right)^3}{\left(\frac{1}{\varepsilon 4} + \frac{1}{\varepsilon 5} - 1\right)}$$ ...Radiative heat transfer coefficient for the third cavity

$$R_{g_0} := \frac{1}{\left(h_{cc_0} + h_{rc_0}\right)}$$ ..third cavity resistance

$$h_{r_0} := 4 \cdot \varepsilon 5 \cdot A13 \cdot \sigma \cdot \left(Tm_0\right)^3$$ ...Radiative heat transfer coefficient for interior film

$$Cte1 := 1.31 \cdot \frac{watt}{m^2}$$

$$Cte2 := 1.52 \cdot \frac{watt}{m^2} \qquad Cte3 := 0.59 \cdot \frac{watt}{m^2}$$

$$h_{c_0} := Cte1 \cdot A13 \cdot \left(\left|T13_0 - TR\right|\right)^{\frac{1}{3}}$$ ...Convective heat transfer coefficient for interior film

8. Node temperatures:

Node 1: The protector:

$$\frac{T2 - T1}{R_{cav1}} + \frac{To - T1}{Ro} = 0$$

Solve for T1 $$\frac{-\left[\frac{1}{R_{cav1}} \cdot T2 + \frac{1}{(Ro)} \cdot To\right]}{\left[\frac{-1}{R_{cav1}} - \frac{1}{(Ro)}\right]}$$

Node 2: The outside face of TIM

$$\frac{T1 - T2}{R_{cav1}} + \frac{T3 - T2}{R_{ins}} = 0$$

Solve for T2

$$\frac{-\left(\frac{1}{R_{cav1}} \cdot T1 - \frac{1}{R_{ins}} \cdot T3\right)}{\left(\frac{-1}{R_{cav1}} + \frac{1}{R_{ins}}\right)}$$

Node 3: The inside face of TIM

$$\frac{T4 - T3}{R_{cav2}} + \frac{T2 - T3}{R_{ins}} = 0$$

Solve for T3:

$$\frac{-\left(\frac{1}{R_{cav2}} \cdot T4 + \frac{1}{R_{ins}} \cdot T2\right)}{\left(\frac{-1}{R_{cav2}} - \frac{1}{R_{ins}}\right)}$$

Node 4: The exterior face of the concrete wall

$$\frac{T3 - T4}{R_{cav2}} + \left(S_{total} \cdot \alpha_{wall}\right) + \frac{T5 - T4}{R_b}$$

Solve for T4:

$$\frac{-\left(\frac{1}{R_{cav2}} \cdot T3 + S_{total} \cdot \alpha_{wall} + \frac{1}{R_b} \cdot T5\right)}{\left(\frac{-1}{R_{cav2}} - \frac{1}{R_b}\right)}$$

Calculations

$$\begin{bmatrix} \left(273+\frac{To_i+T1_i}{2}\right) \\ if\left(I_{t_{i,0}}>100\cdot\frac{watt}{m^2},S_{total_i},0\cdot\frac{watt}{m^2}\right) \\ \varepsilon 1\cdot\sigma\cdot 4\cdot\left(Tmean1_i\right)^3 \\ h_{wind}+hr_{p_i} \\ \frac{1}{ho_{p_i}\cdot A13} \\ \frac{T1_i+T2_i}{2}+273 \\ \frac{100\cdot degC}{Tmcav1_i} \\ \frac{0.002528\cdot\left(Tmcav1_i\right)^{1.5}}{Tmcav1_i+200}\cdot\frac{watt}{m\cdot degC} \\ 2.737\cdot\left(1+2\cdot acav1_i\right)^2\cdot\left(acav1_i\right)^4\cdot\left|T1_i-T2_i\right|\cdot\left(\frac{L_{cav1}}{mm}\right)^3\cdot p^2 \\ 0.0605\cdot\left(\left|Ra_{cav1_i}\right|\right)^{\frac{1}{3}} \\ \left[1+\frac{0.104\cdot\left(Ra_{cav1_i}\right)^{0.293}}{\left[1+\left(\frac{6310}{Ra_{cav1_i}}\right)^{1.36}\right]^3}\right] \\ \frac{K_{cav1air_i}\cdot A13}{L_{cav1}}\cdot if\left(Nu1_{cav1_i}>Nu2_{cav1_i},Nu1_{cav1_i},Nu2_{cav1_i}\right) \\ \frac{A13\cdot\sigma\cdot\left[\left(T2_i+273\right)^4-\left(T1_i+273\right)^4\right]}{\left(\frac{1}{\varepsilon 1}+\frac{1}{\varepsilon 2}-1\right)\cdot\left[\left(T2_i+273\right)-\left(T1_i+273\right)\right]} \\ if\left(I_{t_{i,0}}>100\cdot\frac{watt}{m^2},\frac{1}{h_{ccav1_i}+h_{rcav1_i}},\frac{2}{h_{ccav1_i}+h_{rcav1_i}}\right) \\ \frac{T3_i+T4_i}{2}+273 \end{bmatrix}$$

$$\left[\ Tmean1_{i+1}\ \right]$$

$$
\begin{vmatrix}
S_{total_i} \\
hr_{p_{i+1}} \\
ho_{p_{i+1}} \\
Ro_{i+1} \\
Tmcav1_{i+1} \\
acav1_{i+1} \\
K_{cav1air_{i+1}} \\
Ra_{cav1_{i+1}} \\
Nu1_{cav1_{i+1}} \\
Nu2_{cav1_{i+1}} \\
h_{ccav1_{i+1}} \\
h_{rcav1_{i+1}} \\
R_{cav1_{i+1}} \\
Tmcav2_{i+1} \\
acav2_{i+1} \\
K_{cav2air_{i+1}} \\
Ra_{cav2_{i+1}} \\
Nu1_{cav2_{i+1}} \\
Nu2_{cav2_{i+1}} \\
h_{ccav2_{i+1}} \\
h_{rcav2_{i+1}} \\
R_{cav2_{i+1}} \\
T1_{i+1} \\
T2_{i+1} \\
T3_{i+1} \\
T4_{i+1} \\
Tm_{i+1} \\
Tmcav3_{i+1}
\end{vmatrix}
:=
\begin{vmatrix}
\frac{100 \cdot degC}{Tmcav2_i} \\
\frac{0.002528 \cdot (Tmcav2_0)^{1.5}}{Tmcav2_i + 200} \cdot \frac{watt}{m \cdot degC} \\
2.737 \cdot (1 + 2 \cdot acav2_i)^2 \cdot (acav2_i)^4 \cdot |T3_i - T4_i| \cdot \left(\frac{L_{cav2}}{mm}\right)^3 \cdot p^2 \\
0.0605 \cdot \left(\left|Ra_{cav2_i}\right|\right)^{\frac{1}{3}} \\
\left[1 + \frac{0.104 \cdot (Ra_{cav2_i})^{0.293}}{\left[1 + \left(\frac{6310}{Ra_{cav2_i}}\right)^{1.36}\right]^3}\right] \\
\frac{K_{cav2air_i} \cdot A13}{L_{cav2}} \cdot if(Nu1_{cav2_i} > Nu2_{cav2_i}, Nu1_{cav2_i}, Nu2_{cav2_i}) \\
\frac{4 \cdot A13 \cdot \sigma \cdot (Tmcav2_i)^3}{\left(\frac{1}{\varepsilon 2} + \frac{1}{\varepsilon 3} - 1\right)} \\
\frac{1}{h_{ccav2_i} + h_{rcav2_i}} \\
\frac{-\left[\frac{1}{R_{cav1_i}} \cdot T2_i + \frac{1}{(Ro_i)} \cdot To_i\right]}{\left[\frac{-1}{R_{cav1_i}} - \frac{1}{(Ro_i)}\right]} \\
\frac{-\left[\frac{1}{(R_{cav1_i})} \cdot T1_i + \frac{1}{R_{ins}} \cdot T3_i\right]}{\left[\frac{-1}{(R_{cav1_i})} - \frac{1}{R_{ins}}\right]} \\
\frac{-\left(\frac{1}{R_{cav2_i}} \cdot T4_i + \frac{1}{R_{ins}} \cdot T2_i\right)}{\left(\frac{-1}{R_{cav2_i}} - \frac{1}{R_{ins}}\right)} \\
\frac{-\left(\frac{1}{R_{cav2_i}} \cdot T3_i + S_{total_i} \cdot A13 \cdot \alpha_{wall} + \frac{1}{R_b} \cdot T5_i\right)}{\left(\frac{-1}{R_{cav2_i}} - \frac{1}{R_b}\right)}
\end{vmatrix}
$$

$$
\begin{bmatrix}
a_{i+1} \\
K_{air_{i+1}} \\
Ra_{i+1} \\
Nu1_{i+1} \\
Nu2_{i+1} \\
h_{cc_{i+1}} \\
h_{rc_{i+1}} \\
R_{cav3_{i+1}} \\
h_{c_{i+1}} \\
h_{r_{i+1}} \\
R_{i_{i+1}} \\
T5_{i+1} \\
T6_{i+1} \\
T7_{i+1} \\
T8_{i+1} \\
T9_{i+1} \\
T10_{i+1} \\
T11_{i+1} \\
T12_{i+1} \\
T13_{i+1}
\end{bmatrix}
:=
\begin{bmatrix}
\frac{T13_i + TR}{2} + 273 \\
\frac{T10_i + T11_i}{2} + 273 \\
\frac{100 \cdot degC}{Tmcav3_i} \\
\frac{0.002528 \cdot (Tmcav3_i)^{1.5}}{Tmcav3_i + 200} \cdot \frac{watt}{m \cdot degC} \\
2.737 \cdot (1 + 2 \cdot a_i)^2 \cdot (a_i)^4 \cdot |T10_i - T11_i| \cdot \left(\frac{L_{cav3}}{mm}\right)^3 \cdot p^2 \\
0.0605 \cdot (|Ra_i|)^{\frac{1}{3}} \left[1 + \frac{0.104 \cdot (Ra_i)^{0.293}}{\left[1 + \left(\frac{6310}{Ra_i}\right)^{1.36}\right]^3}\right] \\
\frac{K_{air_i} \cdot A13}{L_{cav3}} \cdot if(Nu1_i > Nu2_i, Nu1_i, Nu2_i) \\
\frac{4 \cdot A13 \cdot \sigma \cdot (Tmcav3_i)^3}{\left(\frac{1}{\varepsilon 4} + \frac{1}{\varepsilon 5} - 1\right)} \\
\frac{1}{h_{cc_i} + h_{rc_i}} \\
Cte1 \cdot A13 \cdot (|T13_i - TR|)^{\frac{1}{3}} \\
4 \cdot \varepsilon 5 \cdot A13 \cdot \sigma \cdot (Tm_i)^3 \\
\frac{1}{h_{c_i} + h_{r_i}} \\
\frac{\Delta t}{C5} \cdot \left(\frac{T4_i - T5_i}{R_b} + \frac{T6_i - T5_i}{R_{c1}}\right) + T5_i \\
\frac{\Delta t}{C6} \cdot \left(\frac{T5_i - T6_i}{R_{c1}} + \frac{T7_i - T6_i}{R_{c2}}\right) + T6_i \\
\frac{\Delta t}{C7} \cdot \left(\frac{T6_i - T7_i}{R_{c2}} + \frac{T8_i - T7_i}{R_{c3}}\right) + T7_i
\end{bmatrix}
$$

$$\left[\begin{array}{c}
\frac{\Delta t}{C8}\cdot\left(\frac{T7_i - T8_i}{R_{c3}} + \frac{T9_i - T8_i}{R_{c4}}\right) + T8_i \\
\frac{\Delta t}{C9}\cdot\left(\frac{T8_i - T9_i}{R_{c4}} + \frac{T10_i - T9_i}{R_b}\right) + T9_i \\
\frac{-\left(\frac{1}{R_b}\cdot T9_i + \frac{1}{R_{cav3_i}}\cdot T11_i\right)}{\left(\frac{-1}{R_b} - \frac{1}{R_{cav3_i}}\right)} \\
\frac{-\left(\frac{1}{R_{cav3_j}}\cdot T10_i + \frac{1}{R_{gb1}}\cdot T12_i\right)}{\left(\frac{-1}{R_{cav3_i}} - \frac{1}{R_{gb1}}\right)} \\
\frac{\Delta t}{C12}\cdot\left(\frac{T11_i - T12_i}{R_{gb1}} + \frac{T13_i - T12_i}{R_{gb1}}\right) + T12_i \\
\frac{-\left(\frac{1}{R_{gb1}}\cdot T12_i + \frac{1}{R_{i_i}}\cdot TR\right)}{\left(\frac{-1}{R_{gb1}} - \frac{1}{R_{i_i}}\right)}
\end{array}\right]$$

non-linear heat transfer and nodal temp.

Variation of nodal temperatures for seven days (T13 is room-side wall surface temperature).

max(T1) = −7.48 •degC

max(T2) = 10.577 •degC

max(T3) = 51.542 •degC

max(T4) = 74.722 •degC

max(T5) = 70.458 •degC

max(T6) = 63.471 •degC

max(T7) = 58.233 •degC

max(T8) = 54.363 •degC

max(T9) = 51.223 •degC

max(T10) = 49.744 •degC

max(T11) = 36.857 •degC

max(T12) = 34.477 •degC

max(T13) = 32.099 •degC

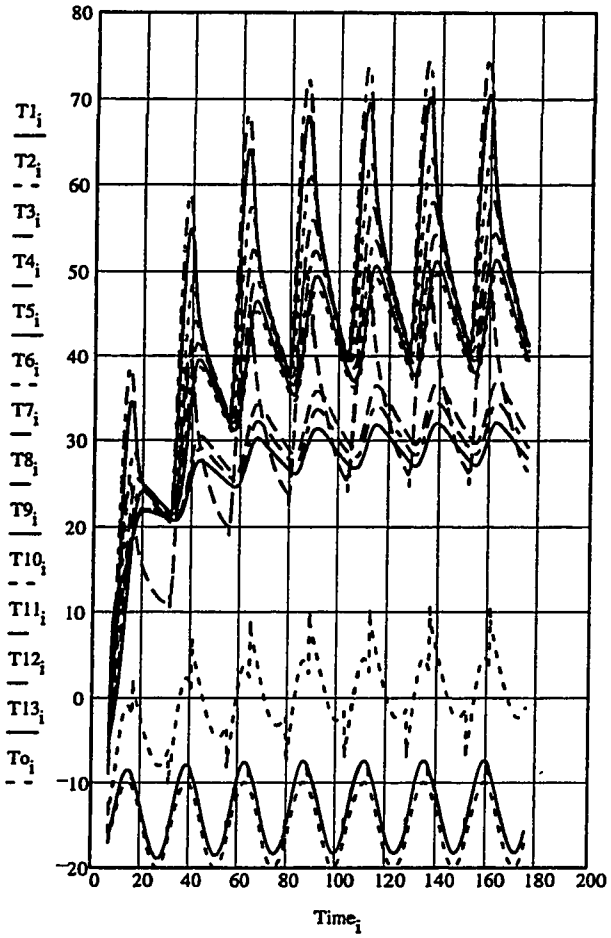

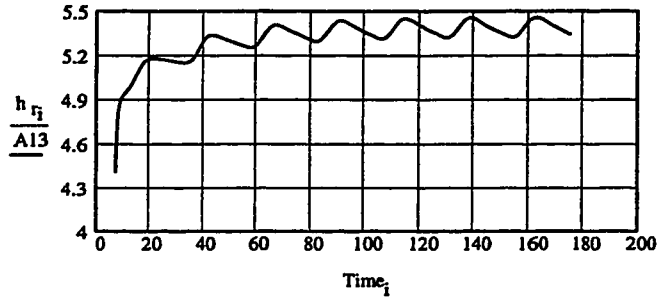

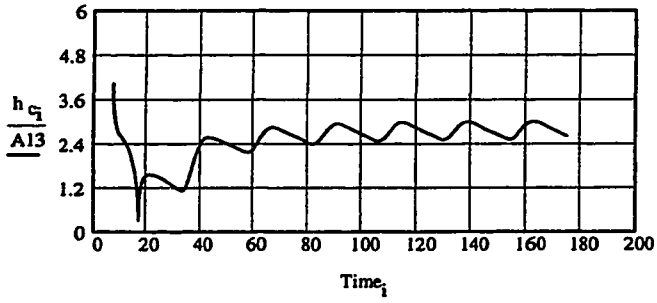

....where hr= heat transfer coefficient of the interior film due to radiation.
hc= heat transfer coefficient of the interior film due to convection.

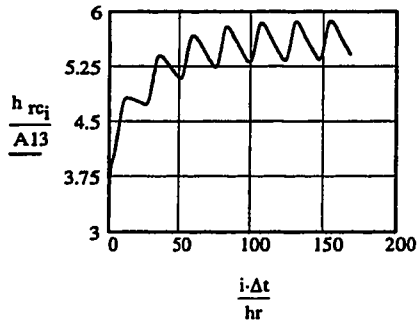

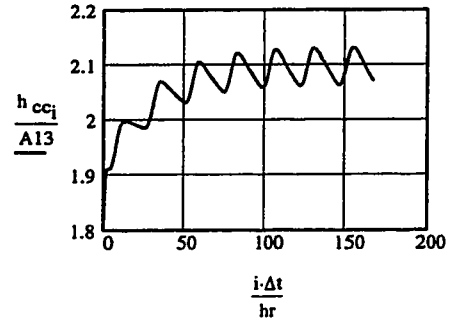

....where hrc= heat transfer coefficient of the third air gap due to radiation.
hc= heat transfer coefficient of the third air gap due to convection.

The heat transfer could be calculated for steady state case as:

$$Q_i := \left(TR - T13_i\right) \cdot \left(\frac{h_{r_i} + h_{c_i}}{A13}\right)$$

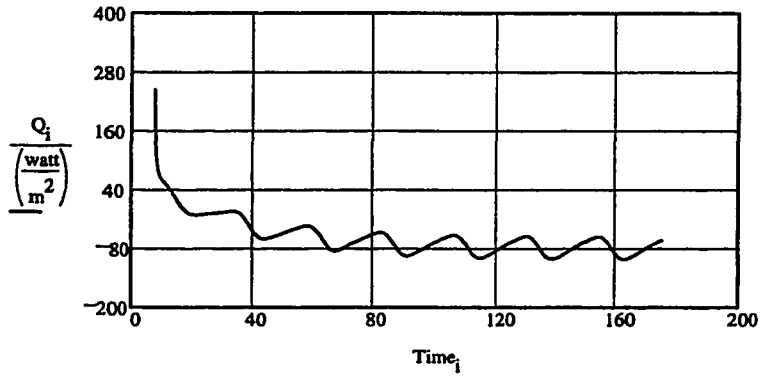

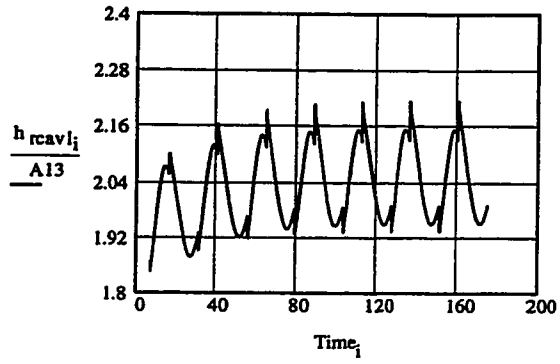

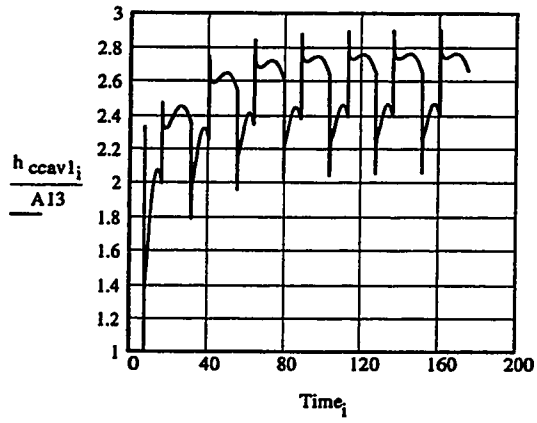

$$R_{exterior_i} := R_{cav1_i} + R_{cav2_i} + R_{ins} + Ro_i$$

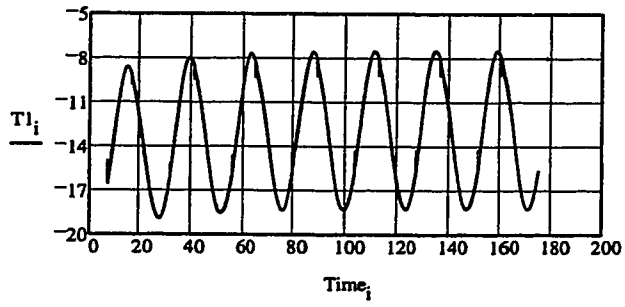

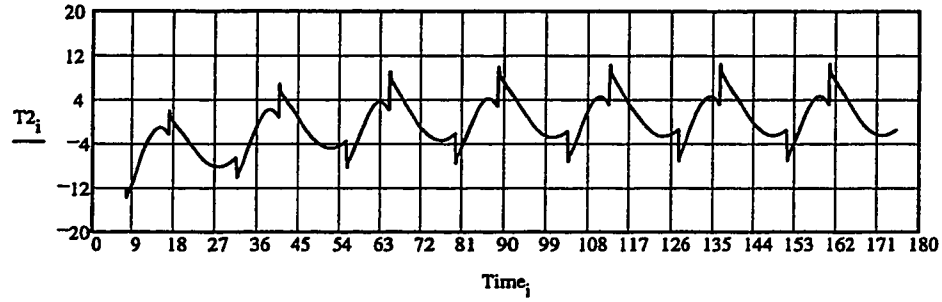
20
12
4
−4
−12
−20
T2i
0 9 18 27 36 45 54 63 72 81 90 99 108 117 126 135 144 153 162 171 180
Timei

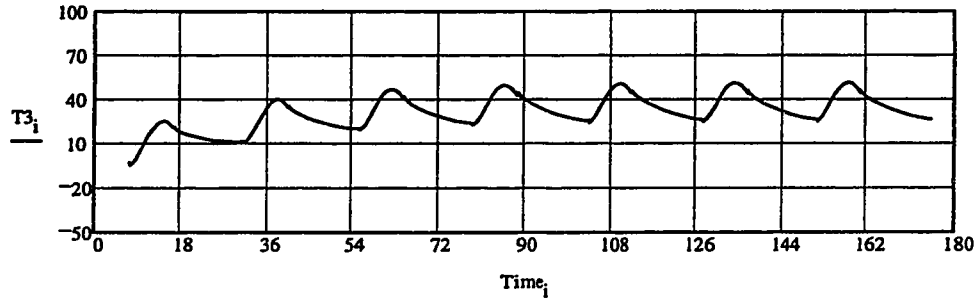
100
70
40
10
−20
−50
T3i
0 18 36 54 72 90 108 126 144 162 180
Timei

$$h_{cav3_i} := \frac{1}{R_{cav3_i} \cdot A13}$$

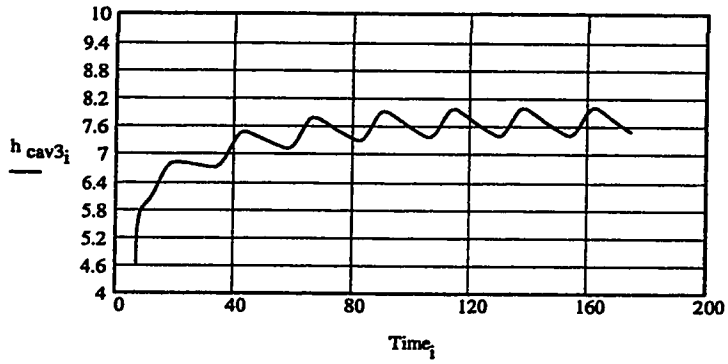

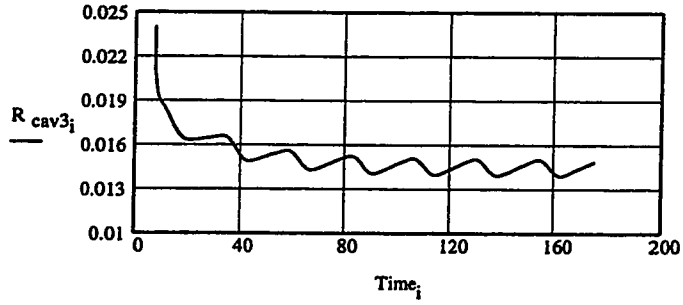

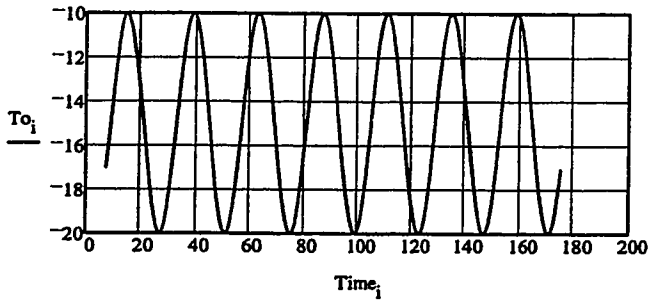

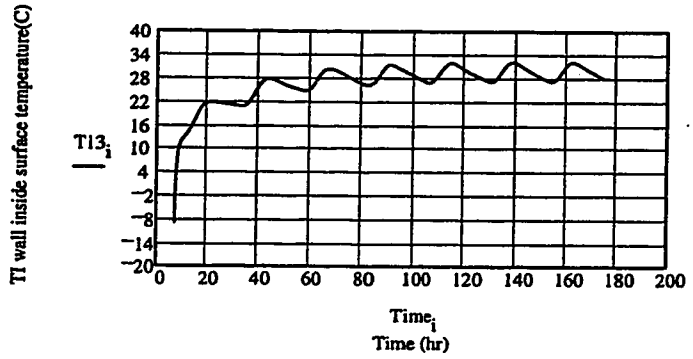
TI wall inside surface temperature(C)
T13i
40
34
28
22
16
10
4
−2
−8
−14
−20
0
20
40
60
80
100
120
140
160
180
200
Timei
Time (hr)